A Nonparametric Estimate of the Risk-Neutral Density and Its Applications

by

LIYUAN JIANG
B.S., Nankai University, Tianjin, P.R.China, 2010
M.S., University of Toledo, Toledo, OH, 2012

Thesis submitted in partial fulfillment of the requirements
for the degree of Doctor of Philosophy in Mathematics
in the Graduate College of the
University of Illinois at Chicago, 2017

Chicago, Illinois

Defense Committee:
Jie Yang, Chair and Advisor
Min Yang
Jing Wang
Cheng Ouyang
Fangfang Wang, University of Connecticut

To my dearest parents and my loved husband

Yubo Fan, Jiadong Jiang and Chunhui Jiang

ACKNOWLEDGMENTS

It would be several pages to thank my advisor, Professor Jie Yang, for his patience, guidance, support, encouragement over the years at the University of Illinois at Chicago. Working with Prof. Yang has always been a delightful and rewarding experience. His deep insights helped me at various stages of my research. I appreciate all his contributions of time, ideas and efforts to make my Ph.D. life stimulating. I also thank him for his helpful career advice and suggestions in general. Without his support and encouragement, I would certainly not be where I am today.

Very special thanks to Professor Fangfang Wang from University of Connecticut for serving on my thesis committee. Her insights, ideas, suggestions, guidance and remarkable knowledge of the topics discussed in the finance study group, were absolutely crucial for this work.

I would also like to thank Professors Min Yang, Cheng Ouyang and Jing Wang for serving on my committee and for their comments on the dissertation. I really appreciate their assistance and help.

I want to extend my grateful thanks to Professor Liming Feng from University of Illinois at Urbana-Champaign for his extremely help during data collection.

Also, my sincere thanks go to Professors Min Yang, Cheng Ouyang, Jing Wang, Hua Yun Chen from Division of Epidemiology and Biostatistics and Ryan Martin from North Carolina State University for their great guidance and assistance on my courses and my PhD study in the past years. I would especially like to thank Professors Min Yang, Cheng Ouyang and Jing

ACKNOWLEDGMENTS (Continued)

Wang. They are always willing to offer invaluable advice and tremendous help on both research as well as on my career that I'm so grateful for.

Some of the work in this dissertation would not be possible without the help of Keren Li, Shuang Zhou and Xianwei Bu, who have enhanced the depth and width of my knowledge and provided generous help and suggestions along with my study and research. I am also grateful to my friend, Yaru Shi, for her continuous support and encouragement in both my study and life for years. I need to express my gratitude to her who was always there when I need her and she is 'like family'.

Of course, I would like to thank the members of my department, Department of Mathematics, Statistics, and Computer Science. The faculty, stuff, and students really made my stay in UIC one I'll always remember.

Last but not the least, a warmest thank you to my loving parents and my husband for their priceless supports, sacrifices, encouragements and unconditional loves. They have been a constant source of strength and inspiration. Without their support, this work would not have been accomplished.

TABLE OF CONTENTS

LIST OF TABLES

LIST OF TABLES (Continued)

TABLE **PAGE**

LIST OF FIGURES

LIST OF ABBREVIATIONS

CBOE	Chicago Board Options Exchange
GH	Generalized Hyperbolic
ITM	In the Money
IUG	Implied Variance
LS	Least Squares
NIG	Normal Inverse Gaussian Distribution
NLS	First Order of Non-parametric Least Square
OP	Vanilla Option
OTC	Over the Counter
OTM	Out Of Money
RND	Risk-neutral Density
RUG	Realised Variance
VA	Variance Future with 12-month Expiration
VF	Variance Future
VS	Variance Swap
VT	Variance Future with 3-month Expiration
WLS	Weighted Least Square

SUMMARY

The risk-neutral density (RND) for a future payoff of an asset can be estimated from market option prices that expire on the same date. We propose a nonparametric approach to estimate the risk-neutral density using piece-wise constant functions with extended tails beyond traded strike prices. We reformulate the estimation problem into a double-constrained optimization problem to determine its parameters, which can be efficiently solved using numerical implementations in R. Our approach is very general and is able to recover the risk-neutral density very well with available market option prices. Our method provides accurate estimates for options with any strike, which further presents a practical way to reveal valuable insights and explore profitable investment opportunities in financial markets. We evaluate our method numerically using options on S&P 500 over twenty years. Our cross-validation study shows that our method performs much better than the cubic spline method proposed in the literature.

Pricing financial derivatives is a key application of the risk-neutral density. We apply our method in pricing variance swap (51), an over-the-counter financial contract that allows investors to hedge risks due to the volatility of financial products. We derive the theoretical price of a variance swap under the no-arbitrage assumption. Based on the vanilla option prices traded on the Chicago Board Options Exchange (CBOE), we estimate the moments of the risk-neutral density under a relatively general framework. Using our proposed nonparametric approach, we derive the moments from the estimated risk-neutral density function directly. In order to compare the fair prices based on our methods with the market prices of variance swaps, we reproduce the historical prices of variance swaps from the CBOE variance future prices. Our study shows that the proposed approach can capture the market prices of long-term variance swaps reasonably well.

CHAPTER 1

INTRODUCTION

A financial derivative is an asset whose value depends on the value of another asset. There are many kinds of derivatives in financial markets, such as various options with different underlying assets, equities and indices, futures and swaps, etc. The theoretical fair price of a derivative can be based on a risk-neutral density. In section 1, we review some preliminary knowledge about risk-neutral density as well as some commonly used methods for estimating a risk-neutral density. In section 2, we introduce a financial derivative, called variance swap, and reviews its pricing approaches in the literature. In the last section, we introduce the data sources used in our work and the corresponding time ranges.

1.1 Risk-neutral density

Risk-neutral density approach has been widely used in pricing derivatives in financial markets. It is essentially a probability measure which is also known as an equivalent martingale measure. The fair price of a derivative can be calculated as its expected discounted payoff under the risk-neutral measure assuming that there is no arbitrage in the market. Such a probability density is called "risk-neutral" since the risk (variance) of the future payoff is not under consideration when pricing. The first fundamental theorem of asset pricing (71) says a risk-neutral measure exists if and only if there is no arbitrage in the market. The future payoff of a derivative is discounted by a risk-free interest rate which stands for an investor's expectation of payoff for \$1 risk-free investment over a specified period. In the real world, such a rate may not exist since the market always carries certain risk. We use zero-coupon interest rate of the Treasure bills as the risk-free rate in our analysis.

The prices of derivatives contain much useful information about the dynamics of the underlying asset with the connection of its payoff and future price. They are often used to estimate the probability distribution of the future price of the asset, which is initially proposed by Breeden and Litzenberger (1978) (13). Different instruments can be used to recover risk-neutral densities. Among them, European options are the most common ones. European options refer to contracts that give the investors the right but not the obligation to trade assets at pre-agreed strike prices at the corresponding maturity date and can only be exercised at the maturity date. Among all the underlying assets which options written on, Standard & Poor's 500 Index is the most popular one which aggregates the value of stocks of the largest 500 companies traded on American stock exchanges and provides a credible view of American stock market for investors.

According to Bliss and Panigirtzoglou (2002) (11), the numerous methodologies toward recovering risk-neutral density functions can be classified into five groups, stochastic process method, implied binomial tree method, finite-difference method, implied volatility smoothing method and PDF approximation function method. As one of them, the stochastic process method uses a stochastic process, such as a geometric Brownian motion or jump-diffusion process, to describe the price dynamics of the underlying asset and then obtains an implicit characterization.

A stochastic process is defined as a collection of random variables with time indices and used to describe a random system evolving over time, such as random walks, martingales, etc. Martingale refers to a process that the conditional expectation of the future value equals to the present value. A geometric Brownian motion process is a continuous-time stochastic process that satisfies the stochastic differential equation:

$$dS_t = \mu S_t \, dt + \sigma S_t \, dW_t$$

where W_t is a standard Brownian motion which refers to a stochastic process that has 0 initial, independent Gaussian-distributed increments, and continuous paths. Here μ is the constant drift and σ is the constant volatility.

Different estimation approaches associated with various stochastic processes have been employed by Bates (1991) (7), Malz (1996) (58) and others. The stochastic process method doesn't rely on the market option prices. However, for general processes that contain jumps or other non-stationary volatilities, it is difficult to derive closed-form formula based on a stochastic process method.

Rather than specifying the process of the underlying asset, Rubinstein (1994) (65) and Jackwerth and Rubinstein (1996) (46) developed a non-parametric Bayesian method called "implied binomial tree method". This iterative approach focuses on constructing a binomial tree model on the evolution of the prices of the underlying asset.

One can also use the finite-difference method to approximate the risk-neutral density, as first proposed by Breeden and Litzenberger (1978) (13). It provides a general approach for estimating the function. Presented in Cox and Ross (1976) (28), the prices of call and put options are:

$$\begin{aligned} C_{t,T}(K) &= e^{-r(T-t)} \int_K^\infty f_Q(S_T)(S_T - K)dS_T \\ P_{t,T}(K) &= e^{-r(T-t)} \int_{-\infty}^K f_Q(S_T)(K - S_T)dS_T \end{aligned} \tag{1.1}$$

where $C_{t,T}(K)$ and $P_{t,T}(K)$ denote the prices of European call and put options with strike price K at time t that expire at T. Here r represents the risk-free rate and $f_Q(S_T)$ is the risk-neutral density for the underlying asset at the maturity date. Breeden and Litzenberger (1978) (13) showed that differentiating the expression for call option with respect to strike price K is given by

$$\frac{\partial C_{t,T}(K)}{\partial K} = -e^{-r(T-t)} \int_K^\infty f_Q(S_T)dS_T \tag{1.2}$$

and differentiating again with respect to K yields a result that is equal to the discounted risk-neutral density at future asset price

$$\frac{\partial^2 C_{t,T}(K)}{\partial K^2} = -e^{-r(T-t)} f_Q(S_T) \tag{1.3}$$

The derivation of the results only requires $C_{t,T}(K)$ to be twice differentiable. One drawback of this approach is the requirement of options across a wide range of strike prices. Unfortunately, there are limited options traded at a discrete level of strike prices, and therefore, the approach essentially needs to interpolate between observed strike prices and extrapolate outside the range.

As an alternative method, implied volatility smoothing method is to infer the risk-neutral density indirectly by estimating volatility smile instead. The plot of implied volatilities from options with same expirations across strike prices is like a smile. One can determine the implied volatility by converting option price under Black-Scholes model. A continuous smoothing approximation function can then be used to interpolate the implied volatility on strike prices. The derived volatilities are converted back to option prices based on Black-Scholes model again. A variety of functions can be used to estimate the implied volatility nonparametrically, Shimko (1993) (18) used a polynomial function, smoothing spline was employed in Campa et. al. (1997) (70), a three-dimensional kernel regression was suggested by Ait-Sahalia and Lo (1995) (1) and a natural spline was described in Robert and Nikolaos (2002) (11). This approach can eliminate much of non-linearity and result in more smoothness and accurate results but is lack of guarantee that the total cumulative probability is one, as reviewed by Bhupinder Bahra (1997) (5). Later, Seung (2014) (56) improved this method by adding power tails and chooses an optimum number of knots.

And the last but not the least is the PDF approximation function method which is further divided into parametric and nonparametric approaches. One can assume parametric statistical distribution families to infer the risk-neutral density and to recover the parameters by solving an optimization problem. When some parametric assumptions of the underlying asset dynamics are satisfied, this approach is more common to use. Jarrow and Rudd (1982) (47) applied this method by assuming lognormal distributions. A similar approach taken by Melick and Thomas (1997) (59), they considered a model proposed by Ritchey (1990) (63), which solved the parameters of a mixture of lognormal distributions. A three-parameter Burr distribution employed by Sherrick et al (1992) (69) where Burr family is a unimodal family of distributions that covers a broad range of shapes and the distributions are very similar to gamma distributions, lognormal distributions, the J-shaped beta distributions, etc. Other principal distributions used to estimate the risk-neutral density are, for example, Weibull distribution, Variance Gamma distribution, Normal Inverse Gaussian distribution.

Considering the limitation on the model-based assumptions for the parametric approach, the nonparametric procedure is more general and robust to estimate the risk-neutral density without restrictions on the price dynamics of the underlying asset or distribution families. The nonparametric method can be realized in the following three ways: the first one is by solving an optimization problem that minimizes the distance between the risk-neutral density and the prior density regarding squared errors with the knowledge of prior distribution. In Rubinstein 1994 (65), he specified the prior distribution as a lognormal distribution and solved the quadratic optimization problem for recovering the risk-neutral density. In a later paper written by Jackwerth and Rubstein (1997) (46), they minimized the distance regarding the roughness of estimated risk-neutral density. The second maximum entropy method is a Bayesian method proposed by Jaynes (1979 (49), 1982 (50)). Later, Kelly and Buchen (1995) (17) used the approach based on given information and that claimed that the resulted risk-neutral distribution was the only distribution that one could infer from market options. Entropy measures the amount of missing information. The last kernel estimation method, which dates back to Rosenblatt (1956) (64) and Parzen (1962) (61), was used by Ait-Sahalia and Lo (1995) (1) and others.

In our paper, we propose a piece-wise constant nonparametric approach to estimate the risk-neutral density from market option prices on S&P 500. Our contributions are twofold: firstly, our method can recover the risk-neutral density effectively with available options; and secondly, our method provides a practical way to explore profitable investment opportunities in financial markets by comparing the fair prices and the market prices. In addition, piece-wise constant functions are concise and easy to understand and implement. Our cross-validation study shows that our method performs much better than the cubic spline method proposed by Monteiro et. al. (2008) (60).

One key application of the risk-neutral density is to provide a fair price for any derivative with the same time to expiration based on the market options. In the next section, we briefly introduce another financial derivative called variance swap, and review the standard methods in the literature for valuing variance swap.

1.2 Variance swap

A variance swap is a financial product which allows investors to trade realized variance against current implied variance. Variance is the square of volatility. Volatility measures the price movements of the underlying asset. Realized volatility refers to the standard deviation of log returns over a specified period that has happened or will have occurred in the future. Implied volatility indicates the market expectation or assessment of the volatility. There are many advantages trading variance swaps. It offers an easier and straightforward way to hedge risks. More important, it provides the investors pure exposure to the variance of the underlying asset without directional risk. The transaction cost for trading variance swap is rather low since it is a forward contract and there is no charge to enter technically. It is also notable liquid across major equities, indices and stock markets, and growing across other markets. Historical evidence indicates selling variance systematically is profitable.

There are numerous methods in the literature for valuing variance swap. Following Song-Ping Zhu and Guang-Hua Lian (2010) (76), we classify the methods into two categories, analytical method and numerical method. The analytical method is further divided into a valuation by portfolio replication and stochastic volatility model. The portfolio replication replicates the variance swap by a portfolio of standard options when the prices of the underlying asset evolve continuously. One can approximate a discretely sampled variance by a continuously sampled variance, see examples in Carr and Madan (1998) (23) and Demeterfi et. al. (1999) (29). This replication method has a significant advantage that it doesn't rely on the volatility process. However, there are two drawbacks commented by Carr and Corso (2001) (21) that the replication strategy requires consecutive strikes and it may not be the case in the financial market. Moreover, the continuous sampling time of the variance swap assumes a continuous model, which is violated when the trading frequency is not high enough, yielding inaccurate results.

The stochastic volatility model method is also popular. GARCH model and jump-diffusion model are employed many times in evaluating variance swap as shown in Javaheri et. al. (2004) (48), Heston (2000) (44), and Howison et. al. (2004) (45). Elliott at al. 2007 (32) developed a model under Heston stochastic process for pricing variance swap. Before that, Swishchuk (2004) (73) used a similar approach to model variance swap under the same Heston model. The stochastic volatility model method also assumes a continuous sampling time of variance and introduces a significant systematic bias.

Despite the analytical success of the replication method and the stochastic volatility model method, numerical solution is more attractive and explicit in pricing derivatives. Due to this reason, the numerical method is another major approach for valuing variance swap, especially in cases where analytic solutions are not available. A fair amount of papers is devoted to this approach. Little and pants (2001) (57) applied a finite-difference method under a diffusion model for a discretely sampled variance swap, and their results were shown to be extremely accurate and robust. Similarly, Windcliff et. al. (2006) (75) adopted a partial-integral differential equation approach and extended it to handle other model assumptions that have no stochastic volatility involved. Brodie and Jain (2008) (15) studied the effects of jumps and discrete sampling time, resulting in a closed-form solution for pricing variance swap under a variety of models such as Heston model, jump-diffusion model, etc. Zhu and lian (2010) (76) further investigated the Heston two-factor stochastic volatility model and also derived a closed-form exact solution.

In the real world, the variance of the prices of the underlying asset varies with time. Any method assuming continuous models may result in systematic bias. Motivated to find an alternative way to price variance swap that is independent of the continuous time model assumption and also ends in a better estimate of the fair price, we propose a moment-based method under a general framework with only no-arbitrage assumption. In order to compare the fair prices based on our methods with the market prices of variance swaps, we further reproduce the historical prices of variance swaps by variance futures, which are future products similar to variance swaps in the sense that they both trade the difference of variance. Our study shows that the proposed approach can capture the market prices of long-term variance swaps reasonably well.

1.3 Data source and preparation

Our data contains standard European options written on S&P 500 indices from January 2nd, 1996 to August 31st, 2015. The expiration date of the options is on the third Saturday of the delivery month. Given the fact that no trading data is available on Saturday, we treat the third Friday instead as the expiration date. The continuously compounded zero-coupon interest rates cover dates from January 2nd, 1996 to August 31st, 2015. For variance futures, the trading dates are from December 10th, 2012 to August 31st, 2015, with start dates from December 21st, 2010 to July 30th, 2015 and expiration dates from January 18th, 2013 to January 1st, 2016. We download options and interest rates from Wharton Research Data Services, and variance futures from CBOE website. We use variance futures to replicate variance swaps in our analysis and the date coverages for variance swaps are entirely consistent with those for variance futures.

To prepare the options, we keep the options that satisfy all the three filters.

1. Positive bid prices.

2. Positive volumes.

3. Expiry more than seven days.

The first filter is intuitive to perform. Under the theoretical assumptions, options shouldn't have negative bid prices. We then drop options with zero volumes given that options with small trading volumes are less likely to indicate the market directions. Besides, options that have expiries within seven days are more fluctuate and easy to be overwhelmed by other influencing factors, and therefore more unstable and unpredictable.

There are 7385062 raw options in total, and after filter 1, there are 6760963 options. After filter 2, there are 1971929 options left, and after the last screen, there are 1844693 options for our analysis. The start dates of the rest options is from January 02, 1996 to December 30, 2015.

Bid-ask spread

In general, the ask price is always greater than the bid price to make a transaction happen. Two parties make a deal when the seller asks for an asking price but is willing to sell at a bid price. The buyer requests for a bid price but is going to pay at an asking price. Brokers take the difference between the asking and bid prices at settlement as the transaction cost. There is a column named "Volume" in the data that should provide us the information about transactions. However, there are a non-trivial amount of records have zero volume that indicates no agreements. After applying filter one, we keep all the options with positive bid prices and take the average price of the bid and ask prices to serve as the settlement price for each option. However, this is not applicable for options with zero volume. Besides the previously mentioned problem that such an option is insufficient to indicate the market direction, it is also far from stable because one could ask or bid for any price. Therefore, we perform an investigation on

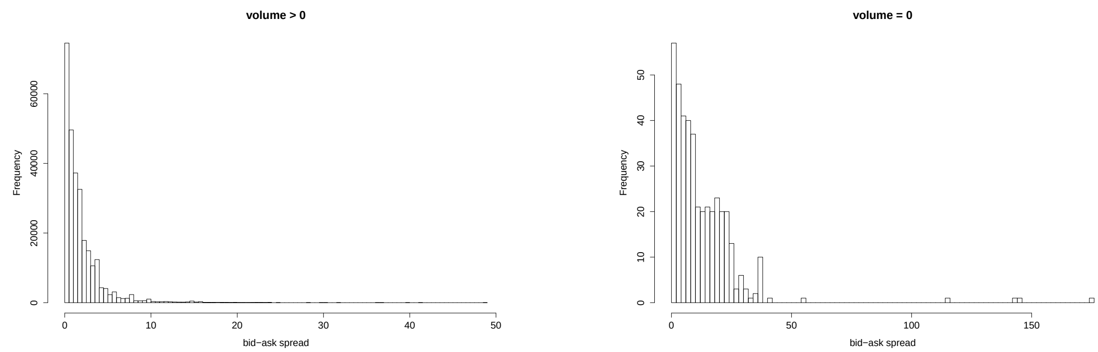

(a) data with volume 0 (b) data with volume greater than 0

Figure 1: Histogram for bid-ask spread of data.

options with zero volume and check if there is greater bid-ask spread. We are also aware that a transaction could still be manipulated by brokers to make an agreement even when the volume is nonzero. We ignore these cases in our analysis. As shown in Figure 1, the outcomes are consistent with our assertion that for those options with zero volumes, the bid-ask spreads are wider in general.

The remainder of the thesis is organized as follows. In Chapter 2, we first describe the non-negativity cubic spline approach in the literature. Then we present our piece-wise constant nonparametric approach to estimating risk-neutral density in details under different scenarios. A comparison between our method and the non-negativity cubic spline approach is conducted, establishing some evidence in favor of ours. Chapter 3 is devoted to the application of variance swap valuation from our proposed nonparametric approach. We summarize our work in Chapter 4.

CHAPTER 2

NONPARAMETRIC APPROACHES FOR ESTIMATING RISK-NEUTRAL DENSITY

We review a variety of nonparametric approaches for recovering the risk-neutral probability density function in the first chapter. Among them, the method proposed by Monteiro et. al. (2008) (60) is the most related one to our proposed approach. They addressed the recovering problem using a cubic spline method which ensures smoothness property for the estimated density and chose more knots than option strikes for more flexibility under the constraints of non-negativity of the density. In the first section, we review the details of their cubic spline method with the non-negativity conditions and explain how the optimization was implemented. We introduce our proposed nonparametric method in the second section. To extend the analysis, we further present the weighted least square method in section 2.3. We then describe the data manipulation for our analysis. In the last section, we provide the applications of our method in details. A comparison study between our approach and the cubic spline approach is also conducted at the end.

2.1 Nonparametric approaches in the literature

Following Monteiro et. al. (2008) (60), to formulate the cubic spline for our problem, we fix a current trading date t and an expiration date T, and let $[a, b]$ be the range of all available strike prices and $R_{t,T}$ be the annualized risk-free interest rate for the period $[t, T]$. Consider $n_s + 1$

equally spaced knots for the spline problem with $a = x_1 < x_2 < x_3 < ... < x_{n_s} < x_{n_s+1} = b$. For the cubic spline approach, there are four parameters for each interval between two adjacent knots, $(\alpha_s, \beta_s, \gamma_s, \delta_s)$, $s = 1, 2, \ldots, n_s$, with a total of $4n_s$ parameters. Let z denote the collection of all the parameters, and $p_z(x)$, $x \in [a, b]$ be the cubic spline functions over $[a, b]$.

According to Monteiro et. al. (2008) (60), the knots of cubic splines are not necessarily to be a subset of the available strikes with expiration T. Nevertheless, the closer the knots are to the strikes, the better the result of the optimization is. Moreover, the first and last knot points must be within a distance of 6% away from the range of available strikes. They further emphasized that the number of knots should not be too bigger than the number of strikes.

In their experiments with the market option prices, they first eliminate all the prices of the options that contain potential arbitrage opportunities by the following procedures:

1. Remove any price that is not in the bid-ask interval.
2. Regenerate all call option prices by the put-call parity based on available put option prices. If there is already a call option available with the same strike, whose price is different from the price generated from the corresponding put option, the price with a higher trading volume stays.
3. Check the monotonicity and strict convexity of the remaining call options after the above steps and remove any violated prices.

To ensure the non-negativity of the estimated risk-neutral density function for every single point in $[a, b]$, a corollary (Corollary 1 in Monteiro et. al. (2008) (60)) is considered in the paper.

However, the problem guaranteed non-negativity is much more complicated and computationally expensive to solve. Since the set with non-negative constraints everywhere is only a subset of the solutions from another optimization problem with the non-negativity property ensured only at the knots, that is,

$$f_s(x_s) \geq 0, \;\; s = 1, 2, \ldots, n_s \text{ and } f_{n_s}(x_{n_s+1}) \geq 0. \tag{2.1}$$

We only solve the latter optimization problem for comparison purpose. If our approach could perform better than the cubic spline method with constraints given in Equation (2.1), then our approaches are guaranteed to be better than the solution obtained from the original optimization problem as well.

Cubic spline approach, by definition, is continuous and is a good technique to yield appropriate smoothness for fitting a function given the nature that splines are piecewise polynomial functions. The additional knots in their method enables the model with more flexibility. Most of all, their method using spline functions are the first approach that guarantees positivity of the risk-neutral density estimation.

However, cubic spline requires more work than constant interpolation and through their studies, they generated "fake" call option prices using put-call parity to eliminate "artificial" arbitrage opportunities. In other words, they manually replaced "abnormal" options and resulted in much information loss from the market and these prices in their analysis may not reflect the true expectations from investors in the market.

2.2 Piece-wise constant nonparametric approach

In this section, we state our method in details. In our work, we assume the risk-neutral density for the log function of the future payoff $log(S_T)$ is piecewise constant across the range of the strike prices. We formulate the estimation problem into an optimization problem that can yield appropriate coefficients for the risk-neutral density. Denote the fair prices of the put and call options traded at time t with the expiration date T by $P_{t,T}(S_t, K)$ and $C_{t,T}(S_t, K)$, respectively, where S_t stands for current price of the underlying asset and K is the corresponding strike prices. Let $K_1 < K_2 < \ldots < K_q$ stand for the collection of all distinct strikes for put or call options traded in the market at time t with expiration T. Let $\mathcal{C}$ be the collection of indices for call options and $\mathcal{P}$ be the collection for put options. Then $\mathcal{C} \bigcup \mathcal{P} = \{1, 2, \ldots, q\}$. Let $m = |\mathcal{C}|$ be the number of call strikes, and $n = |\mathcal{P}|$ be the number of put strikes. Note that $m + n \geq q$.

Let $f_Q(y)$ denote the risk-neutral density function, where Q stands for the risk-neutral measure. According to the definition of the risk-neutral density, we have the fair price

$$\begin{aligned} P_i &\equiv P_{t,T}(S_t, K_i) \\ &= \mathbb{E}_Q e^{-R_{t,T}} (K_i - S_T)_+ \\ &= e^{-R_{t,T}} \int_{-\infty}^{logK_i} (K_i - e^y) f_Q(y) dy, \ i \in \mathcal{P}. \end{aligned} \tag{2.2}$$

$$
\begin{aligned}
C_{j'} &\equiv C_{t,T}(S_t, K_{j'}) \\
&= \mathbb{E}_Q e^{-R_{t,T}}(S_T - K_{j'})_+ \qquad (2.3) \\
&= e^{-R_{t,T}} \int_{logK_{j'}}^{\infty} (e^y - K_{j'}) f_Q(y) dy, \;\; j' \in \mathcal{C}.
\end{aligned}
$$

where $R_{t,T}$ stands for the risk-free interest rate from t to T. That is, \$1 at time t ends for sure with $e^{R_{t,T}}$ dollars at time T.

We extend the support of risk-neutral density function f_Q on both sides of available strike prices by multipliers c_1 and c_2 with $c_1 > 1, c_2 > 1$. Here c_1 and c_2 are two predetermined numbers. The knots for our method are $K_0 = (c_1)^{-1}K_1 < K_1 < K_2 < \ldots < K_q < c_2K_q = K_{q+1}$. The values of function f_Q which are constant for each interval are denoted as $a_1, a_2, \ldots, a_{q+1} \geq 0$. Based on the pricing mechanism for options, any option with strike price greater than c_2K_q or less than $(c_1)^{-1}K_1$ has almost no liquidity. Therefore, the density to fit is in the form of $f_Q(y) = a_l$ for $logK_{l-1} < y \leq logK_l$ where $l = 1, 2, \ldots, q+1$ and zero elsewhere. Later in the chapter, we show that our proposed density function can recover the risk-neutral density fairly well.

Based on the properties of the density function, we have $\int_{-\infty}^{+\infty} f_Q(y)dy = 1$. That is

$$
\sum_{l=1}^{q+1} a_l \; log\frac{K_l}{K_{l-1}} = 1 \qquad (2.4)
$$

In general, our optimized objective function is

$$\underset{a_1,\ldots,a_{q+1}}{\operatorname{argmin}}\{\sum_{j'\in\mathcal{C}}(C_{j'}-\tilde{C_{j'}})^2+\sum_{i\in\mathcal{P}}(P_i-\tilde{P_i}^2)\} \tag{2.5}$$

subject to $a_l \geq 0,\ l = 1, 2, \ldots, q+1$ and Equation (2.4). Note that $C_{j'}$ and P_i depend on f_Q and thus are functions of $a_1, a_2, \ldots, a_q, a_{q+1}$.

We then rewrite the call and put option prices in Equation (2.2) and Equation (2.3) in terms of $a_1, a_2, \ldots, a_q, a_{q+1}$ as follows

$$\begin{aligned} e^{R_{t,T}}P_i &= \int_{-\infty}^{logK_i}(K_i-e^y)f_Q(y)dy \\ &= \sum_{l=1}^{q+1}\int_{logK_{l-1}}^{logK_l}(K_i-e^y)a_l dy\cdot \mathbb{1}(K_i\geq K_l) \\ &= \sum_{l=1}^{q+1}a_l[(K_i log\frac{K_l}{K_{l-1}})-(K_l-K_{l-1})]\cdot\mathbb{1}(K_i\geq K_l),\ i\in\mathcal{P}. \end{aligned} \tag{2.6}$$

$$\begin{aligned} e^{R_{t,T}}C_{j'} &= \int_{logK_{j'}}^{\infty}(e^y-K_{j'})f_Q(y)dy \\ &= \sum_{l=1}^{q+1}\int_{logK_{l-1}}^{logK_l}(e^y-K_{j'})a_l dy\cdot\mathbb{1}(K_{j'}\leq K_{l-1}) \\ &= \sum_{l=1}^{q+1}a_l[(K_l-K_{l-1})-K_{j'}log\frac{K_l}{K_{l-1}}]\cdot\mathbb{1}(K_{j'}<K_l),\ j'\in\mathcal{C}. \end{aligned} \tag{2.7}$$

Let $X_{i,l}^{(p)} = [K_i log(K_l/K_{l-1}) - (K_l - K_{l-1})]\cdot\mathbb{1}(K_i \geq K_l)$, $l = 1, 2, \ldots, q+1$ be an entry of the design matrix for put options; and $X_{j',l}^{(c)} = [(K_l - K_{l-1}) - K_{j'}log(K_l/K_{l-1})]\cdot\mathbb{1}(K_{j'} < K_l)$, $l = 1, 2, \ldots, q+1$ for call options.

From Equation (2.4), a_{q+1} can be represented by $a_1, a_2, \ldots, a_q$, as

$$a_{q+1} = (1 - \sum_{l=1}^{q} a_l \frac{logK_l}{K_{l-1}})(logc_2)^{-1} \tag{2.8}$$

The fair price then can be written as a function of $a_1, a_2, \ldots, a_q$ only. We plug Equation (2.8) into Equation (2.6) and Equation (2.7) and have

$$\begin{aligned}
& e^{R_{t,T}} P_i = \sum_{l=1}^{q+1} a_l X_{i,l}^{(p)} \\
& = a_1 X_{i,1}^{(p)} + a_2 X_{i,2}^{(p)} + \ldots + a_q X_{i,q}^{(p)} \\
& \quad + (1 - a_1 log\frac{K_1}{K_0} - \ldots - a_q log\frac{K_q}{K_{q-1}})(logc_2)^{-1} X_{i,q+1}^{(p)} \\
& = a_1 [X_{i,1}^{(p)} - (log\frac{K_1}{K_0})(logc_2)^{-1} X_{i,q+1}^{(p)}] \\
& \quad + \ldots \\
& \quad + a_q [X_{i,q}^{(p)} - (log\frac{K_q}{K_{q-1}})(logc_2)^{-1} X_{i,q+1}^{(p)}] + \frac{1}{logc_2} X_{i,q+1}^{(p)} \\
& \triangleq a_1 X_{i,1}^{(P)} + a_2 X_{i,2}^{(P)} + \cdots + a_q X_{i,q}^{(P)} + X_{i,q+1}^{(P)}, \ i \in \mathcal{P}.
\end{aligned} \tag{2.9}$$

where $X^{(P)}_{i,l} = X^{(p)}_{i,l} - (logK_l/K_{l-1})(logc_2)^{-1}X^{(p)}_{i,q+1}$, $l = 1, 2, \ldots, q$ and $X^{(P)}_{i,q+1} = X^{(p)}_{i,q+1}/logc_2$.

Similarly for call options:

$$
\begin{aligned}
e^{R_{t,T}}C_{j'} &= \sum_{l=1}^{q+1} a_l X^{(c)}_{j',l} \\
&= a_1 X^{(c)}_{j',1} + a_2 X^{(c)}_{j',2} + \ldots + a_q X^{(c)}_{j',q} \\
&\quad + (1 - a_1 log\frac{K_1}{K_0} - \ldots - a_q log\frac{K_q}{K_{q-1}})(logc_2)^{-1}X^{(c)}_{j',q+1} \\
&= a_1[X^{(c)}_{j',1} - (log\frac{K_1}{K_0})(logc_2)^{-1}X^{(c)}_{j',q+1}] \\
&\quad + \ldots \\
&\quad + a_q[X^{(c)}_{j',q} - (log\frac{K_q}{K_{q-1}})(logc_2)^{-1}X^{(c)}_{j',q+1}] + \frac{1}{logc_2}X^{(c)}_{j',q+1} \\
&\triangleq a_1 X^{(C)}_{j',1} + a_2 X^{(C)}_{j',2} + \cdots + a_q X^{(C)}_{j',q} + X^{(C)}_{j',q+1}, \ j' \in \mathcal{C}.
\end{aligned}
\tag{2.10}
$$

where $X^{(C)}_{j',l} = X^{(c)}_{j',l} - (logK_l/K_{l-1})(logc_2)^{-1}X^{(c)}_{j',q+1}$, $l = 1, 2, \ldots, q$ and $X^{(C)}_{j',q+1} = X^{(c)}_{j',q+1}/logc_2$.

2.2.1 Numerical implementation algorithms adopted

In the optimization literature, there are many algorithms available for solving unconstrained optimization problems (Chong and Zak, 1996 (25); Kuang et. al., 2016 (54)). However, after combining the two constraints, non-negativity and unity integration, only limited methods could be used to solve our constrained optimization problem (Chong and Zak, 1996 (25)). In this part, we explain in details for some commonly used algorithms and choose the best fit for our study based on their empirical performances.

Many of the available algorithms rely on manipulations of matrices. We now state without proof some facts of matrix derivatives which are needed later in this part (Petersen and Pedersen, 2008 (62)).

$$\nabla_{\mathbf{x}}(\mathbf{a}^T\mathbf{x}) = \mathbf{a} \tag{2.11}$$

$$\nabla_{\mathbf{x}}(\mathbf{x}^T\mathbf{a}) = \mathbf{a} \tag{2.12}$$

$$\nabla_{\mathbf{x}}(\mathbf{x}^T\mathbf{A}\mathbf{x}) = (\mathbf{A} + \mathbf{A}^T)\mathbf{x} \tag{2.13}$$

Lawson-Hanson algorithm with q+1 parameters

We first consider the situation shown in Equation (2.6) and Equation (2.7). Lawson-Hanson algorithm with $q+1$ parameters has been used to solve this non-negative least square optimization problem (Lawson and Hanson, 1974 (55)). Given the design matrix $\mathbf{A}$ and the response vector $\mathbf{y}$, we solve the problem $\underset{\mathbf{x}}{\operatorname{argmin}} ||\mathbf{A}\mathbf{x} - \mathbf{y}||_2$ which subject to $\mathbf{x} \geq 0$ and $\mathbf{A}\mathbf{x} = \mathbf{y}$, where $||.||_2$ denotes the L^2-norm. For a vector $\mathbf{z} \in \mathbb{R}^n$, the L^2-norm $||\mathbf{z}||_2$ is given by $(\sum_{i=1}^{n} |z_i|^2)^{1/2}$.

For our problem, the design matrix $\mathbf{A} = (X_1, X_2, \ldots, X_q, X_{q+1})$ is an $(m+n)\times(q+1)$ matrix, where the l-th column X_l includes both $X_{i,l}^{(p)}$, $i \in \mathcal{P}$ and $X_{j',l}^{(c)}$, $j' \in \mathcal{C}$; $\mathbf{x} = (a_1, a_2, \ldots, a_q, a_{q+1})^T$ is a $(q+1)$-vector and $\mathbf{y}$ represents the $(m+n)$-vector including $\tilde{P}_i$, $i \in \mathcal{P}$ and $\tilde{C}_{j'}$, $j' \in \mathcal{C}$.

In R interface, the corresponding function is “nnls”. Due to the mechanism of the algorithm, the main problem when applying the Lawson-Hanson algorithm with $q+1$ parameters is that more than half of x’s are 0 because of the non-negativity restriction and it is also hard to include the unity constraint.

Algorithm 1 Lawson-Hanson algorithm ([Lawson and Hanson (1974) (55)])

1: Set $\mathcal{P} :=$ NULL, $\mathcal{Z} := \{1, 2, \ldots, q+1\}$, and $\mathbf{x} := \mathbf{0}$.
2: Compute the (q+1)-vector $\mathbf{w} := \mathbf{A}^T(\mathbf{y} - \mathbf{A}\mathbf{x})$.
3: If the set $\mathcal{Z}$ is empty or if $w_j \leq 0$ for all $j \in \mathcal{Z}$, go to Step 12.
4: Find an index $t \in \mathcal{Z}$ such that $w_t = \max\{w_j : j \in \mathcal{Z}\}$.
5: Move the index t from set $\mathcal{Z}$ to set $\mathcal{P}$.
6: Let $\mathbf{A}_{\mathcal{P}}$ be the $(p+1) \times (p+1)$ matrix defined by

$$\text{Column } j \text{ of } \mathbf{A}_{\mathcal{P}} := \begin{cases} \text{column } j \text{ of } \mathbf{A} & \text{if } j \in \mathcal{P} \\ \hfill 0 & \text{if } j \in \mathcal{Z} \end{cases}$$

Compute the (p+1)-vector $\mathbf{z}$ as a solution of the least square problem $\mathbf{A}_{\mathcal{P}}\mathbf{z} = \mathbf{y}$. Note that only the components $z_j, j \in \mathcal{P}$, are determined by the problem. Define $z_j := 0$ for $j \in \mathcal{Z}$.
7: If $z_j \geq 0$ for all $j \in \mathcal{P}$, set $\mathbf{x} := \mathbf{z}$ and go to Step 2.
8: Find an index $q \in \mathcal{P}$ such that $x_q/(x_q - z_q) = \min\{x_j/(x_j - z_j) : z_j \leq 0, j \in \mathcal{P}\}$.
9: Set $\alpha := x_q/(x_q - z_q)$.
10: Set $\mathbf{x} := \mathbf{x} + \alpha(\mathbf{z} - \mathbf{x})$.
11: Move all indices from set $\mathcal{P}$ to $\mathcal{Z}$ for those $x_j = 0$. Go to Step 6.
12: *End*: Completed.

Lawson-Hanson algorithm with q parameters

Considering the drawback from the Lawson-Hanson algorithm with $q+1$ parameters, we narrow the optimization problem to $a_1, a_2, \ldots, a_q$ and solve the problem under Equation (2.9) and Equation (2.10) where there are only q parameters. The unity constraint has been incorporated in the form. Here $\mathbf{A} = (X_1', X_2', \ldots, X_q')$ is an $(m+n) \times q$ matrix, where the l-th column X_l' includes both $X_{i,l}^{(P)}$, $i \in \mathcal{P}$ and $X_{j',l}^{(C)}$, $j' \in \mathcal{C}$; $\mathbf{x} = (a_1, a_2, \ldots, a_q)^T$ is a Q-vector and $\mathbf{y}$ represents the $(m+n)$-vector including $\tilde{P}_i$ and $X_{i,q+1}^{(P)}$, $i \in \mathcal{P}$; and $\tilde{C_{j'}}$ and $X_{j',q+1}^{(C)}$, $j' \in \mathcal{C}$.

Although the main problems of the previous algorithm have been solved, the lack of guarantee for the non-negativity of the last coefficient a_{q+1} is unsettled.

Quasi-Newton method with q+1 parameters

Given the drawbacks of the Lawson-Hanson algorithm, we apply an alternative penalty method called Quasi-Newton method, which optimizes the objective function using the function values and also the gradient values with a faster convergence rate (Broyden-Fletcher-Goldfarb-Shanno (16) (35) (38) (67)). It is also capable to minimize the objective function with linear inequality constraints.

In this case, the design matrix $\mathbf{A} = (X_1, X_2, \ldots, X_q, X_{q+1})$ is an $(m+n) \times (q+1)$ matrix, where the l-th column X_l includes both $X^{(p)}_{i,l}$, $i \in \mathcal{P}$ and $X^{(c)}_{j',l}$, $j' \in \mathcal{C}$; $\mathbf{x} = (a_1, a_2, \ldots, a_q, a_{q+1})^T$ is a $(q+1)$-vector and $\mathbf{y}$ represents the $(m+n)$-vector including $\tilde{P_i}$, $i \in \mathcal{P}$ and $\tilde{C_{j'}}$, $j' \in \mathcal{C}$. The feasible region in this scenario is $\mathbf{ux} - \mathbf{c} \geq 0$, where $\mathbf{u}^T = (\mathbf{I_{q+1}}, \mathbf{w})$ is $(q+1) \times (q+2)$, $\mathbf{I_{q+1}}$ is a $(q+1) \times (q+1)$ identity matrix, $\mathbf{w} = (-log(K_1/K_0), -log(K_2/K_1), \ldots, -log(K_{q+1}/K_q))^T$, $\mathbf{x} = (a_1, a_2, \ldots, a_{q+1})^T$ and $\mathbf{c} = (0, 0, \ldots, 0, -1)^T$. The illustration is shown in Algorithm 2.

Initial values are required before we implement the algorithm. To control for the sensitivity to different (t, T) combinations, uniform initial values are applied and modified accordingly. We start with initial values $1/(q+1)$, where q is the number of unique strike prices for each (t, T) pair. These initial values are considered to incorporate the effects of the contract duration and work well for most of the pairs, which are marked as general days. The rest special pairs fail to result in a feasible estimation of parameters because the general initials are too close to the boundary and the function doesn't work, and they need adjustments on the initials. All special pairs we have in this setup are shown in Table I. We summarize our options of initial values below.

Algorithm 2 Quasi-Newton method with q+1 parameters with BFGS update ([Broyden-Fletcher-Goldfarb-Shanno (16) (35) (38) (67)])

Initialize $\mathbf{x}^{(\mathbf{0})}$ either follow uniform $\frac{1}{q+1}$ for general dates or uniform 0.001 for special dates
$\mathbf{x}^{(\mathbf{0})} \in$ domain (F) $= \{\mathbf{ux} - \mathbf{c} \geq 0\}$, and an approximate Hessian matrix $\mathbf{H}_0$
For k = 1,2,... until convergence do
Compute Quasi-Newton direction $\Delta\mathbf{x} = -\mathbf{H}_{k-1}^{-1}\nabla F(\mathbf{x}^{(\mathbf{k-1})})$
Determine step size t (e.g. perform line search)
compute $\mathbf{x}^{(\mathbf{k})} = \mathbf{x}^{(\mathbf{k-1})} + t\Delta\mathbf{x}$
Update $\mathbf{H}_k = \mathbf{H}_{k-1} + \frac{\mathbf{y}\mathbf{y}^T}{\mathbf{y}^T\mathbf{s}} - \frac{\mathbf{H}_{k-1}\mathbf{s}\mathbf{s}^T\mathbf{H}_{k-1}}{\mathbf{s}^T\mathbf{H}_{k-1}\mathbf{s}}$
where $\mathbf{s} = \mathbf{x}^{(\mathbf{k})} - \mathbf{x}^{(\mathbf{k-1})}$, $\mathbf{y} = \nabla F(\mathbf{x}^{(\mathbf{k})}) - \nabla F(\mathbf{x}^{(\mathbf{k-1})})$
Inverse update $\mathbf{H}_k^{-1} = (\mathbf{I} - \frac{\mathbf{s}\mathbf{y}^T}{\mathbf{y}^T\mathbf{s}})\mathbf{H}_{k-1}^{-1}(\mathbf{I} - \frac{\mathbf{y}\mathbf{s}^T}{\mathbf{y}^T\mathbf{s}}) + \frac{\mathbf{s}\mathbf{s}^T}{\mathbf{y}^T\mathbf{s}}$
End for
Solution is $\mathbf{x}^* = (a_1^*, a_2^*, \ldots, a_{q+1}^*)$ and record $||\mathbf{A}\mathbf{x}^* - \mathbf{y}||_2 = -b$ as the least square.

TABLE I: Special dates

t	01/22/10	07/22/11	03/21/13	11/15/13	10/20/14
T	04/17/10	06/29/12	03/28/13	11/22/13	09/30/15
t	03/04/15	03/24/15	04/27/15	04/27/15	06/30/15
T	03/31/15	06/19/15	0515/15	03/31/16	07/10/15

1. For general dates, we set the initials for parameters to be $1/(q+1)$.

2. For special dates, we adjust the initials for the parameters to be all 0.001 such that they are not far from the general initials $1/(q+1)$.

In R interface, the corresponding function is "ConstrOptim" with option "BFGS". The main limitation using this algorithm compared with the Lawson-Hanson with $q+1$ parameters is that it can only handle inequality constraints. That causes a problem when we include the constraint $\sum_{l=1}^{q+1} a_l \ log(K_l/K_{l-1}) = 1$. In other words, the integration may not be even close to 1 for some solution sets. In addition, we have $q+2$ constraints here with the extra $a_{q+1} \geq 0$ for only $q+1$ parameters. That may give the function a narrower plane to optimize and often cause problems. Therefore, a minor inconsistency exists using the algorithm with all parameters considered.

Quasi-Newton method with q parameters

We improve the efficiency of the above Quasi-Newton method by considering only the first q parameters with constraints $a_1 \geq 0, \ldots, a_q \geq 0$ and $\sum_{l=1}^{q} a_l \ logK_l/K_{l-1} \leq 1$ as shown in Algorithm 3. This solves the issue in the previous approach that it can only handle inequality constraints. The feasible region in this scenario is $\mathbf{ux} \geq \mathbf{c}$, where $\mathbf{u}^T = (\mathbf{I_q}, \mathbf{w})$ is $q \times (q+1)$, $\mathbf{I_q}$ is a $q \times q$ identity matrix, $\mathbf{w} = (-log(K_1/K_0), -log(K_2/K_1), \ldots, -log(K_q/K_{q-1}))^T$, $\mathbf{x} = (a_1, a_2, \ldots, a_q)^T$ and $\mathbf{c} = (0, 0, \ldots, 0, -1)^T$. Here $\mathbf{A} = (X_1^{'}, X_2^{'}, \ldots, X_q^{'})$ is an $(m+n) \times q$ matrix, where the l-th column $X_l^{'}$ includes both $X_{i,l}^{(P)}$, $i \in \mathcal{P}$ and $X_{j',l}^{(C)}$, $j' \in \mathcal{C}$; $\mathbf{x} = (a_1, a_2, \ldots, a_q)^T$ is a q-vector and $\mathbf{y}$ represents the $(m+n)$-vector including $\tilde{P}_i$ and $X_{i,q+1}^{(P)}$, $i \in \mathcal{P}$; and $\tilde{C_{j'}}$ and $X_{j',q+1}^{(C)}$, $j' \in \mathcal{C}$.

The function to minimize is $f(\mathbf{x}) = (\mathbf{y} - \mathbf{Ax})^T(\mathbf{y} - \mathbf{Ax})$. The derivative of $f(\mathbf{x})$ with respect to $\mathbf{x}$ is given by

$$\begin{aligned}
\nabla_{\mathbf{x}} f(\mathbf{x}) &= \nabla_{\mathbf{x}}(\mathbf{y} - \mathbf{Ax})^T(\mathbf{y} - \mathbf{Ax}) \\
&= \nabla_{\mathbf{x}}(\mathbf{y}^T\mathbf{y} - \mathbf{y}^T\mathbf{Ax} - \mathbf{x}^T\mathbf{A}^T\mathbf{y} + \mathbf{x}^T\mathbf{A}^T\mathbf{Ax}) \qquad (2.14) \\
&= -2\mathbf{A}^T\mathbf{y} + 2\mathbf{A}^T\mathbf{Ax}
\end{aligned}$$

Note that we use Equation (2.11) to Equation (2.13) to derive Equation (2.14).

To best control for the sensitivity of the algorithm to initial values, we further consider two kinds of initials, uniform initials and random initials for the optimization problem:

1. Fixed initials:

   We set our initial parameter values for $a_1, \ldots, a_q$ to be a fixed value.

   Since $\sum_{l=1}^{q} a_l \;\; log(K_l/K_{l-1}) \leq 1$, that is, $(\max_{1\leq i\leq q} a_i) \sum_{l=1}^{q} log(K_l/K_{l-1}) \leq 1$, we have $\max_{1\leq i\leq q} a_i \leq (\sum_{l=1}^{q} log(K_l/K_{l-1}))^{-1} = (log(K_q/K_0))^{-1}$. To be more conservative, we set $a_1 = a_2 = \ldots = a_q = (2log(K_q/K_0))^{-1}$.

2. Random uniform initials:

   Besides the fixed initials, we add random initials that follow an uniform distribution. That is, $a_1, a_2, \ldots, a_q \sim unif(0, (log(K_q/K_0))^{-1})$.

In general, we solve the optimization problem using the fixed initial combined with three to five random uniform initials. The resulted parameters estimations are derived based on the initial value that minimizes the most of the objective function. This procedure guarantees our estimations are not so sensitive to the initial values.

We show four approaches to solve the optimization problem and in order to locate the one that works the best, we conduct a performance comparison on the randomly selected nine special pairs and six general pairs of dates mentioned in 2.2.1. The results from the Lawson-Hanson algorithm are excluded from the comparison table due to its high incapability to implement the non-negativity and unity constraints despite the fact that the prediction

Algorithm 3 Quasi-Newton method with q paramters

Initialize $\mathbf{x^{(0)}}$ either follow uniform initials or random initials (choose 3 random ones)
    $\mathbf{x^{(0)}} \in$ domain (F) $= \{\mathbf{ux} - \mathbf{c} \geq 0\}$
For k = 0,1,2,. . . until convergence do
    Evaluate $b = -F(\mathbf{x^{(k)}}) = -(\mathbf{y} - \mathbf{A}^T\mathbf{x^{(k)}})^T(\mathbf{y} - \mathbf{A}^T\mathbf{x^{(k)}})$
        with $\mathbf{J} = \nabla F(\mathbf{x^{(k)}}) = -2\mathbf{A}^T\mathbf{y} + 2\mathbf{A}^T\mathbf{A}\mathbf{x^{(k)}}$
    Solve $\mathbf{Js} = b$
    $\mathbf{x^{(k+1)}} = \mathbf{x^{(k)}} + \mathbf{s}$
End for
Record $||\mathbf{Ax}{-}\mathbf{y}||_2 = -b$ for each initial at convergence and choose the smallest one as selected one.
Solution is the corresponded $\mathbf{x}^* = (a_1^*, a_2^*, \ldots, a_q^*)$
    and $a^*_{(q+1)} = (1 - \sum_{l=1}^{q} a_l^* log(K_l/K_{l-1}))(log(c_2))^{-1}$.

errors are competitively small. We include the results from the Quasi-Newton method with $q + 1$ parameters in the comparison Table II, however, simulation studies show that it always results in a value much less than 1 when checking for the unity constraint. While, Quasi-Newton method with q parameters, in the other hand, provides a consistent nonnegative estimate for a_{q+1} in our studies despite the lack of guarantee in the theoretical way. Prediction errors are also calculated to support the best approach among Quasi-Newton methods in Table II. Here prediction error is calculated by root mean squared error (RMSE $= \sqrt{\frac{1}{n}\sum_{i=1}^{n}(P_i^{est} - P_i^{obs})^2}$).

From Table II, when the number of unique strikes in (t, T) is small, say 2 or 3, the Quasi-Newton methods are unstable based on the large dispersions. For those date pairs with a small number of unique strikes marked in the parenthesis in the table, errors from Quasi-Newton method with q parameters are relatively large. However, as mentioned earlier, Quasi-Newton with q+1 parameters has a serious drawback that the overall integration may not be 1.

TABLE II: Comparison between three approaches

			RMSE	
	t	T	Quasi-Newton with q+1	Quasi-Newton with q
Special	01/22/10	04/17/10	0.7895	0.7337
	07/22/11	06/29/12	1.1854e-11	(q=3)2.8737
	03/21/13	03/28/13	0.3460	0.2872
	11/15/13	11/22/13	1.0735	1.0291
	10/20/14	09/30/15	9.1205e-14	(q=2)1.9793e-21
	03/04/15	03/31/15	0.5757	0.5543
	03/24/15	06/19/15	2.4000	2.2890
	04/27/15	05/15/15	2.5932	2.5450
	04/27/15	03/31/16	5802.5240	(q=3)5601.8300
	06/30/15	07/10/15	3.4878	3.4285
General	05/08/96	05/18/96	159.8124	153.9730
	04/25/03	05/17/03	3.0660	3.0328
	08/19/10	11/20/10	0.3720	0.3705
	03/21/07	09/22/07	20.6366	20.5287
	12/01/10	06/18/11	0.5571	0.5543
	11/24/10	12/17/11	0.0518	0.05268

Additionally, the prediction errors from Quasi-Newton method with q parameters are smaller for the general pairs.

Note that all the prediction errors in the table are derived employing all options available to fit the density and reconciled from the fair option prices and the market prices. Therefore, combining all the advantages and disadvantages of the methods discussed above, Quasi-Newton method with q parameters is chosen for our study.

2.2.2 Estimation using out-of-the-money options

Inspired by the study of Ghysels and Wang (2014) (37), we employ out-of-the-money (OTM) options to fit the risk-neutral density and then find the fair prices for OTM and in-the-money (ITM) call and put options separately. OTM options refer to the options that have no intrinsic values. For call options, OTM is used to describe the situation when the strike price is higher than the current market price of the underlying asset, while for put options, OTM means the strike is lower than the current market price of the underlying asset. On the contrary, in-the-money means that the strike price is lower than the current market price of the underlying asset for call options or higher than the current price for put options, which does not necessarily indicate that the investors are sure to profit but are worthwhile to exercise options after considering the cost of trading options. In a real market, OTM options are more popular and have more liquidity than ITM options due to the following reasons. Firstly, OTM options are cheaper than ITM options. The deeper the options go ITM, the more they act similarly as"the underlying asset", the less volatile and more difficult they are to manage and hedge. Secondly, the more OTM options are traded, the closer the bid-ask spread is, which in returns, result in larger trading volume.

Let P_i^{obs}, $i = 1, 2, \ldots, n$ be the market price of n assets and P_i^{est}, $i = 1, 2, \ldots, n$ be our estimated/predicted prices. We use the absolute error (L_a) and the relative error (L_r) defined below to evaluate and compare prediction performance.

$$L_a = \sqrt{\frac{1}{n}\sum_{i=1}^{n}(P_i^{est} - P_i^{obs})^2}$$

$$L_r = \sqrt{\frac{1}{n}\sum_{i=1}^{n}(\frac{P_i^{est} - P_i^{obs}}{P_i^{obs}})^2}$$

Using OTM options to price OTM options

Let $K_1, K_2, \ldots, K_q$ be the distinct and increasing strike prices for all options traded for a pair of dates (t, T) and $K_1^o, K_2^o, K_3^o, \ldots, K_p^o$ be the distinct and increasing strike prices for OTM options only. For each fixed (t, T), we fit a risk-neutral density using all the available OTM call and put options, and then calculate the fair prices of both OTM options and ITM options based on the fitted density.

When we fit the density using OTM options, all the strikes of OTM call options are to the right of the strike which is equal to market price of the underlying asset and those of OTM put options are to the left. Assuming $K_p < S_T < K_{p+1}$, all OTM put options have strikes less than or equal to K_p and all OTM call options have strikes greater than or equal to K_{p+1}. The estimation of a_{p+1} for period K_p to K_{p+1} is unavailable and the corresponding row of design matrix X_{p+1} are all zeros. With the additional unity constraint, we solve all the density coefficients.

In terms of the tails of the risk-neutral density, we first start with combining the strike prices from OTM/ITM options together, and expanding the support for the density on both sides of available strike prices by predetermined numbers c_1 and c_2. There are two options on extending the support of the risk-neutral density.

1. Extend the support by $log(K_1/c_1)$ and $log(K_q \times c_2)$ which includes the information from ITM options as well
2. Extend the support by $log(K_1^o/c_1)$ and $log(K_p^o \times c_2)$ instead which excludes the information from ITM options

To determine which option is better to adopt, we testify the empirical results from both extensions using options with time to expirations within $7 \sim 14$ days. Based on the prediction errors of OTM-option fitting with selected Quasi-Newton method, the performance is fairly worse under the first option for support extension and it is not hard to understand considering that we are adding extra information extracted from ITM options when we fit the density for OTM options only. Therefore, the final strategy we adopted is the second option using the two strike prices on both sides of OTM options and extend the support by dividing and multiplying c_1 and c_2 on the two selected strikes. It turns out that the fair prices for OTM options are close to the market prices.

Using OTM options to price ITM options

It is intuitive to raise the question that, when we derive density using only OTM call and put options, the strike prices may not cover the same set of strikes of ITM options from the same date pair and that causes issue for pricing ITM options. As a solution, we carry forward the nearest density values for each additional strike knot from ITM options. We state a simple example to illustrate this idea. If all the strikes from a (t, T) pair is $K_1, K_2, \ldots, K_5$ and OTM option strikes cover only K_1, K_2 and K_5, and the estimated density value for the period K_2 to K_5 is a_2. To estimate the density values of the risk-neutral density for ITM options accordingly, we assign a_2 for periods K_2 to K_3, K_3 to K_4, and K_4 to K_5. Renaming a_2 to be b_2, b_3 and b_4 and we can calculate the fair prices for ITM options using the interpolated density function.

There are two similar considerations on extending the support of the risk-neutral density for ITM options:

1. Extend the support by $log(K_1/c_1)$ and $log(K_q \times c_2)$
2. Cut the support at $log(K_1)$ and $log(K_q)$ instead

We propose the first tail extension option using the two strikes on both sides of all the available options because the risk-neutral density for ITM options are interpolated from that of OTM options. An information abandon from OTM options on the support afterwards is not necessary. While, the other option is by considering the final selection of the support extended for the risk-neutral density of OTM options. When we extend the support of the density for OTM options using only the two strikes on both sides from OTM options, as we mentioned earlier, this set may not be the same set for the strikes of all options. Given the fact that we have employed the two strikes on both sides of all available option strikes instead of only ITM option strikes for the support extension of the density for ITM options, it actually can be regarded as a support extension is performed already. Therefore, the second option is stated to choose $log(K_1)$ and $log(K_q)$ as the support of the risk-neutral density. Based on the prediction errors from the fitted results for ITM options, applying the second option results in more desirable outcomes.

Numerical experiments

We use an example to illustrate the results using our best strategies. The start date of the options in this experiment is December, 10th, 2012 and the expiration date is December 21st, 2013, which was associated with a reasonable number of traded options. The error performances for pricing OTM options and ITM options using OTM options are shown in Figure 2.

Figure 2(a) and Figure 2(b) are the results from pricing OTM options using only OTM options. From Figure 2(a), when the log prices of options are positive, the absolute errors are larger for the options with higher prices if we ignore the three outliers. The absolute errors are unstable when option prices are cheaper, which are easier to be affected by external factors. Figure 2(b) further confirms the trend we observed from Figure 2(a). Although the absolute errors increase with the option prices, the absolute magnitude for absolute errors is no larger than 0.3. The actual deviations are small in the relative sense. Moreover, the mean of the relative errors is 0.038, that is, the fair prices are 3.8% far from the market prices in average.

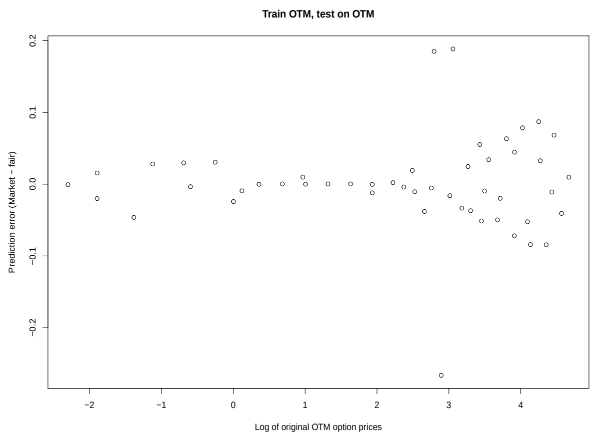

(a) absolute error from predicting OTM options

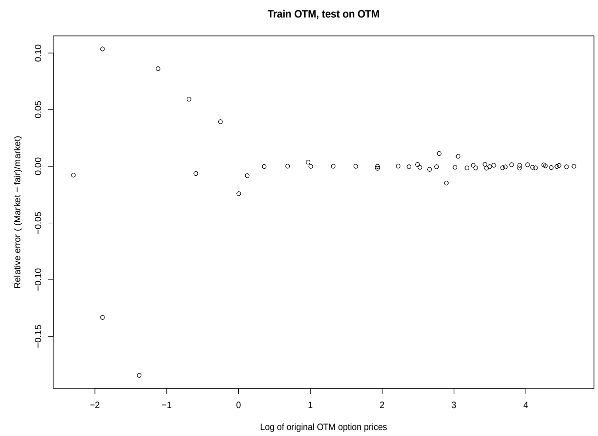

(b) relative error from predicting OTM options

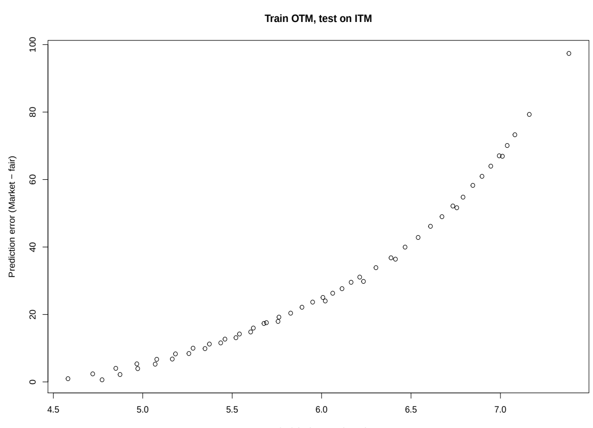

(c) absolute error from predicting ITM options

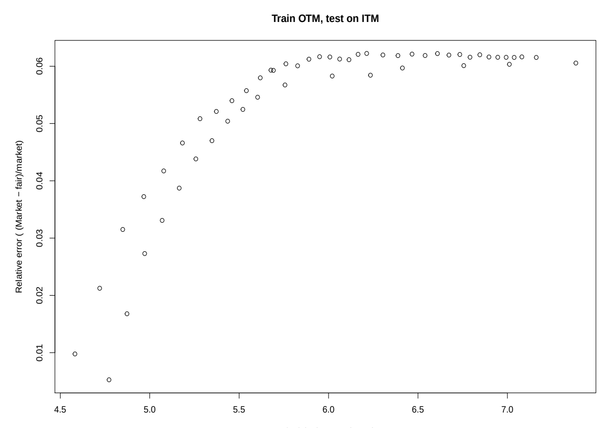

(d) relative error from predicting ITM options

Figure 2: Error results from the estimated risk-neutral density using only OTM options.

For ITM options, it is clear the absolute errors are increasing as the ITM options are more expensive from Figure 2(c). Two lines are corresponding to put and call options respectively. Although the magnitude of the errors is much larger than that of OTM options, the option prices are much higher as well. As seen from Figure 2(d), the relative errors are still small and the curves becomes flat after option prices hit certain values. The mean relative error is 0.044, which explains the fair prices are accurate compared to 5% level.

There are two core functions we implement through the studies:

1. Fair price prediction function: given a series of call options and put options with market prices and strike prices, and further provided the information of the new option on whether it is a call or put option (no need for the information whether it is an ITM/OTM option) and its strike price, we are able to output the fair price of the options.

2. Prediction evaluation function: given a series of call options and put options with their market prices and strike prices, and information of current market price of the underlying asset (used to identify ITM/OTM options), we are able to predict fair price for any option of the same (t, T) using OTM options and output the prediction errors for the whole option dataset.

After checking some random samples from options that have different time to expirations, the prediction errors are decreasing as the time to expiration gets longer. In order to get a better view of the error trend, we divide the time to expirations of all the options into more distinguished and informative expiry categories, as $7 \sim 14$ (about one or two weeks), $17 \sim 31$ (about one month), $81 \sim 94$ (about 3 months), $171 \sim 199$ (about 6 months), $337 \sim 393$ (about one year), $502 \sim 592$ (about one and a half years) and $670 \sim 790$ (about two years). We follow Ghysels and Wang (2014) (37) on the division of the first four categories, and based on their overall trends of the previous lasting periods: one week between $7 \sim 14$, two weeks between $17 \sim 31$, two weeks between $81 \sim 94$ and four weeks between $171 \sim 199$ for half year, we set four weeks each away from 365 days and get $337 \sim 393$. Similarly, for one and a half years, the center of the range is $365 + 364/2 = 547$ and the window is 45 days and we get $502 \sim 592$. The last one, with the window for two years to be 60 days and the center at $365 * 2 = 730$, we get $670 \sim 790$.

We divide all the options into the seven expiries and estimate their fair prices using our approach. Prediction error is calculated for each expiry and the results are shown in Table III. We extend the support of the risk-neutral density using $c_1 = c_2 = 2$, which is a reasonable choice to start.

As we indicate earlier, the error results for different expiries in Table III show an obvious decreasing trend at the beginning and a slightly increasing trend afterward in the relative errors indicating that as the time to expiration of options gets longer within three months, the predictions are more accurate. For options with even longer expirations, the prices are not as predictable compared to options with shorter expirations because of the less liquidity. But we don't get similar trend in absolute errors along with longer expiries. In addition, we have better predictions in OTM put options than ITM call options overall and it is easy to understand that as for put options, there is an upper limit for strike prices that is the market price of the underlying asset and therefore, put options are easier to estimate than call options.

TABLE III: Prediction errors using OTM options only ($c_1 = c_2 = 2$) across different numbers of days to expiration

Days	$7 \sim 14$	$17 \sim 31$	$81 \sim 94$	$171 \sim 199$	$337 \sim 393$	$502 \sim 592$	$670 \sim 790$
$L_r(OTM)^c$	0.1238	0.1152	0.0389	0.0646	0.0318	0.0545	0.0368
$L_a(OTM)^c$	0.0694	0.0830	0.1844	0.3579	1.0075	1.0560	1.0374
$L_r(ITM)^c$	0.0428	0.0282	0.1010	0.1932	0.3110	0.4265	0.3917
$L_a(ITM)^c$	3.0298	3.3180	9.7533	27.8996	53.8949	86.7297	89.0749
Days	$7 \sim 14$	$17 \sim 31$	$81 \sim 94$	$171 \sim 199$	$337 \sim 393$	$502 \sim 592$	$670 \sim 790$
$L_r(OTM)^p$	0.1266	0.0786	0.0419	0.0427	0.0462	0.0792	0.0792
$L_a(OTM)^p$	0.0891	0.0660	0.1098	0.1345	0.3228	0.4267	0.4487
$L_r(ITM)^p$	0.0352	0.0362	0.1268	0.1957	0.3693	0.4519	0.4806
$L_a(ITM)^p$	2.7418	3.1522	13.4135	25.9584	61.0158	116.4508	119.0193

From the predicted results under least square (LS) setup, the options with lower prices tend to have larger relative errors. To put more weights for such valued options, we incorporate option prices in our problem and solve the weighted least square problem using Quasi-Newton method with q parameters. More details are discussed in next section.

2.2.3 Support of risk-neutral density

For the choices of c_1 and c_2, initially, we proposed value 2 such that the density coverage extends from $log(K_1^o)$ and $log(K_q^o)$ to $log(K_1^o/2)$ and $log(2 \times K_q^o)$. From Figure 3(a) to Figure 3(d), we observe that OTM options are "predicted" vey well in terms of that all the blue triangles overlap most of red triangles, while there is still a large dispersion for ITM options. Since the ITM put options are the options with strikes above the market price of the underlying asset and their prices are more expensive for higher strikes, they are more related about the value choice of c_1 and similarly, ITM call options are more about c_2. Due to the large dispersions in ITM options, we come up with the three options for c_1 and c_2 below.

1. Option 1: $c_1 = c_2 = 25$. This option comes after we explore all the strikes we have in the data and the maximum of the ratio K_q/K_1 is 50. To be conservative, we choose half of the value that is 25.

2. Option 2: $c_1 = c_2 = (K_q/K_1)^{-1/d}$, where $d = 3, 4, 6$. The idea of this option is to extend the support of the risk-neutral density proportionally to the coverage of K_1 and K_q for each date pair.

3. Option 3: $c_1 = c_2 = D = T - t$. From Figure 3(a) to Figure 3(d), the dispersion gets larger as time to expiration gets longer. Therefore, we incorporate time effect and make the support of the density related to the calendar difference between trading date t and expiration date T.

For testing purpose, we select random samples consisting of 400 options from each expiry category and get the resulted Table IV to Table IX. Table IV saves the results under the same samples selected under initial values of $c_1 = c_2 = 2$ for comparison purposes. After comparing the prediction errors in the tables, we finally choose $c_1 = c_2 = 25$ which overall results in the most smallest prediction errors.

2.3 Weighted least square approach

From the results from OTM options fit in Figure 2, the performances of pricing ITM options are much better than those of OTM options with cheaper prices. Therefore, we introduce a

TABLE IV: Prediction errors using OTM options only ($c_1 = c_2 = 2$) across different numbers of days to expiration on random samples

Days	$7 \sim 14$	$17 \sim 31$	$81 \sim 94$	$171 \sim 199$	$337 \sim 393$	$502 \sim 592$	$670 \sim 790$
$L_r(OTM)^c$	0.1038	0.0923	0.0353	0.0268	0.0362	0.0545	0.0209
$L_a(OTM)^c$	0.0621	0.0807	0.2565	0.3460	1.5277	1.0206	1.1902
$L_r(ITM)^c$	0.0398	0.0346	0.1190	0.1721	0.2798	0.4683	0.3988
$L_a(ITM)^c$	4.3085	3.7492	11.8101	20.5624	47.8511	99.1927	86.0505
Days	$7 \sim 14$	$17 \sim 31$	$81 \sim 94$	$171 \sim 199$	$337 \sim 393$	$502 \sim 592$	$670 \sim 790$
$L_r(OTM)^p$	0.1006	0.0746	0.0353	0.0407	0.0356	0.0737	0.0936
$L_a(OTM)^p$	0.0711	0.0733	0.1013	0.1220	0.3683	0.3649	0.5370
$L_r(ITM)^p$	0.0468	0.0374	0.1170	0.1791	0.3932	0.4711	0.5369
$L_a(ITM)^p$	3.5978	3.2752	11.2022	21.6712	67.2936	163.7171	156.6169

TABLE V: Prediction errors using OTM options only ($c_1 = c_2 = 25$) across different numbers of days to expiration on random samples

Days	$7 \sim 14$	$17 \sim 31$	$81 \sim 94$	$171 \sim 199$	$337 \sim 393$	$502 \sim 592$	$670 \sim 790$
$L_r(OTM)^c$	0.1133	0.1123	0.0299	0.0376	0.0495	0.0353	0.0293
$L_a(OTM)^c$	0.0752	0.0940	0.2760	0.5491	1.2988	1.3148	1.5798
$L_r(ITM)^c$	0.0381	0.0332	0.1059	0.1832	0.3034	0.4056	0.3621
$L_a(ITM)^c$	4.3331	4.1401	10.3426	20.4578	52.8451	83.2963	67.9067
Days	$7 \sim 14$	$17 \sim 31$	$81 \sim 94$	$171 \sim 199$	$337 \sim 393$	$502 \sim 592$	$670 \sim 790$
$L_r(OTM)^p$	0.0945	0.0769	0.0396	0.0465	0.0419	0.0695	0.0591
$L_a(OTM)^p$	0.0561	0.0805	0.2111	0.2255	0.6349	0.5804	0.6653
$L_r(ITM)^p$	0.0422	0.0335	0.1075	0.1451	0.3277	0.4109	0.4210
$L_a(ITM)^p$	3.0744	3.0847	9.9002	17.0209	54.6001	80.4175	77.5613

TABLE VI: Prediction errors using OTM options only ($c_1 = c_2 = log(T - t)$) across different numbers of days to expiration on random samples

Days	$7 \sim 14$	$17 \sim 31$	$81 \sim 94$	$171 \sim 199$	$337 \sim 393$	$502 \sim 592$	$670 \sim 790$
$L_r(OTM)^c$	0.1112	0.1123	0.0297	0.0375	0.0497	0.0360	0.0295
$L_a(OTM)^c$	0.0704	0.0811	0.2792	0.5538	1.3311	1.3618	1.6156
$L_r(ITM)^c$	0.0836	0.0319	0.1057	0.1825	0.3024	0.4080	0.3663
$L_a(ITM)^c$	4.4863	3.8008	10.3880	20.2873	52.8986	84.2491	68.9093
Days	$7 \sim 14$	$17 \sim 31$	$81 \sim 94$	$171 \sim 199$	$337 \sim 393$	$502 \sim 592$	$670 \sim 790$
$L_r(OTM)^p$	0.0994	0.0750	0.0390	0.0478	0.0404	0.0657	0.0638
$L_a(OTM)^p$	0.0777	0.0750	0.2111	0.2323	0.6667	0.6213	0.7234
$L_r(ITM)^p$	0.0436	0.0387	0.1063	0.1411	0.3240	0.4102	0.4230
$L_a(ITM)^p$	3.3572	3.3735	9.7878	16.3755	54.2074	80.4826	79.0742

TABLE VII: Prediction errors using OTM options only ($c_1 = c_2 = (K_q/K_1)^{1/3}$) across different numbers of days to expiration on random samples

Days	$7 \sim 14$	$17 \sim 31$	$81 \sim 94$	$171 \sim 199$	$337 \sim 393$	$502 \sim 592$	$670 \sim 790$
$L_r(OTM)^c$	0.1046	0.0996	0.0426	0.1023	0.1529	0.2337	0.2102
$L_a(OTM)^c$	0.0584	0.0850	1.0362	2.0417	13.0792	16.7835	27.9646
$L_r(ITM)^c$	0.0952	0.0393	0.1694	0.2327	0.5010	0.5050	0.4303
$L_a(ITM)^c$	4.8199	4.5071	15.8765	34.1979	80.2804	103.0873	87.6817
Days	$7 \sim 14$	$17 \sim 31$	$81 \sim 94$	$171 \sim 199$	$337 \sim 393$	$502 \sim 592$	$670 \sim 790$
$L_r(OTM)^p$	0.1030	0.0763	0.0605	0.0690	0.1429	0.1923	0.2036
$L_a(OTM)^p$	0.0745	0.0785	0.9411	2.5309	7.7945	12.1792	13.8996
$L_r(ITM)^p$	0.0718	0.0584	0.2493	0.3690	0.5440	0.6503	0.6922
$L_a(ITM)^p$	4.1569	4.3017	20.9261	50.3718	90.1149	197.0478	143.2748

TABLE VIII: Prediction errors using OTM options only ($c_1 = c_2 = (K_q/K_1)^{1/4}$) across different numbers of days to expiration on random samples

Days	$7 \sim 14$	$17 \sim 31$	$81 \sim 94$	$171 \sim 199$	$337 \sim 393$	$502 \sim 592$	$670 \sim 790$
$L_r(OTM)^c$	0.1046	0.1084	0.0484	0.0930	0.1819	0.3180	0.2806
$L_a(OTM)^c$	0.0584	0.0844	1.1939	2.4008	14.6926	19.4472	30.5360
$L_r(ITM)^c$	0.0952	0.0476	0.1952	0.2645	0.5694	0.5593	0.4843
$L_a(ITM)^c$	4.8188	4.7278	18.4657	41.2385	88.9068	113.2197	94.1843
Days	$7 \sim 14$	$17 \sim 31$	$81 \sim 94$	$171 \sim 199$	$337 \sim 393$	$502 \sim 592$	$670 \sim 790$
$L_r(OTM)^p$	0.1030	0.0841	0.0763	0.0884	0.1710	0.2247	0.2309
$L_a(OTM)^p$	0.0745	0.0778	1.1246	2.8592	8.6809	13.7723	15.2062
$L_r(ITM)^p$	0.0718	0.0594	0.2838	0.4257	0.5816	0.7048	0.7458
$L_a(ITM)^p$	4.1569	4.1479	23.2385	57.6544	98.4602	251.9125	161.3962

TABLE IX: Prediction errors using OTM options only ($c_1 = c_2 = (K_q/K_1)^{1/6}$) across different numbers of days to expiration on random samples

Days	$7 \sim 14$	$17 \sim 31$	$81 \sim 94$	$171 \sim 199$	$337 \sim 393$	$502 \sim 592$	$670 \sim 790$
$L_r(OTM)^c$	0.11214	0.17477	0.05402	0.09095	0.18646	0.29904	0.27212
$L_a(OTM)^c$	0.07914	0.12204	1.55229	3.86591	13.41894	29.94325	31.82281
$L_r(ITM)^c$	0.06410	0.06706	0.29224	0.39968	0.70794	0.77012	0.54976
$L_a(ITM)^c$	4.69434	5.54487	26.85361	52.00493	118.67398	145.53461	129.04097
Days	$7 \sim 14$	$17 \sim 31$	$81 \sim 94$	$171 \sim 199$	$337 \sim 393$	$502 \sim 592$	$670 \sim 790$
$L_r(OTM)^p$	0.11828	0.10083	0.10468	0.13835	0.22255	0.27483	0.27900
$L_a(OTM)^p$	0.09178	0.13253	1.29180	3.07821	8.57532	15.04433	17.10664
$L_r(ITM)^p$	0.09055	0.08519	0.31122	0.41914	0.69427	0.78684	1.16228
$L_a(ITM)^p$	4.41297	4.90298	25.07219	52.09654	104.57145	371.04980	205.80759

weighted least square method (WLS) as an estimation technique and reformulate our problem by incorporating weight factors that are inversely proportional to option market prices. Weighted least squares are similar to least squares but more efficient in handling situations where the data points are various in quality. But it is not hard to imagine that there are sacrifices in absolute difference evaluation using weighted least square approach which is in favor of relative errors.

Denote z_d be the adjusted price of an option calculated from $\tilde{P}_i$, $i \in \mathcal{P}$ or $\tilde{C}_{j'}$, $j' \in \mathcal{C}$, where $d = 1, 2, \ldots, m+n$. Here $\mathbf{A} = (X_1', X_2', \ldots, X_q')$ is an $(m+n) \times q$ matrix, where the l-th column X_l' includes both $X_{i,l}^{(P)}$, $i \in \mathcal{P}$ and $X_{j',l}^{(C)}$, $j' \in \mathcal{C}$; $\mathbf{x} = (a_1, a_2, \ldots, a_q)^T$ is a q-vector and $\mathbf{y}$ represents the $(m+n)$-vector including $\tilde{P}_i$ and $X_{i,q+1}^{(P)}$, $i \in \mathcal{P}$; and $\tilde{C}_{j'}$ and $X_{j',q+1}^{(C)}$, $j' \in \mathcal{C}$. Let $\mathbf{W}$ be an $(m+n) \times (m+n)$ diagonal matrix with diagonal entries $1/z_d^2$, $d = 1, 2, \ldots, m+n$. The function to minimize is $f(\mathbf{x}) = (\mathbf{y} - \mathbf{A}\mathbf{x})^T \mathbf{W} (\mathbf{y} - \mathbf{A}\mathbf{x})$. The derivative of $f(\mathbf{x})$ with respect to $\mathbf{x}$ is

$$
\begin{aligned}
\nabla_{\mathbf{x}} f(\mathbf{x}) &= \nabla_{\mathbf{x}} (\mathbf{y} - \mathbf{A}\mathbf{x})^T \mathbf{W} (\mathbf{y} - \mathbf{A}\mathbf{x}) \\
&= \nabla_{\mathbf{x}} (\mathbf{y}^T \mathbf{W} \mathbf{y} - \mathbf{y}^T \mathbf{W} \mathbf{A} \mathbf{x} - \mathbf{x}^T \mathbf{A}^T \mathbf{W} \mathbf{y} + \mathbf{x}^T \mathbf{A}^T \mathbf{W} \mathbf{A} \mathbf{x}) \\
&= -2\mathbf{A}^T \mathbf{W} \mathbf{y} + 2\mathbf{A}^T \mathbf{W} \mathbf{A} \mathbf{x}
\end{aligned}
\tag{2.15}
$$

Same as before, we use Equation (2.11), Equation (2.12) and Equation (2.13) with $\mathbf{A} = \mathbf{A}^T \mathbf{W} \mathbf{A}$ in the derivation. Similar to algorithm 3, the pseudo code for weighted least square is as follows.

Algorithm 4 Weighted Least Squares using Quasi-Newton method with q paramters (WLS(q))

Initialize $\mathbf{x^{(0)}}$ either follow uniform initials or random initials (choose 3 random ones)
    $\mathbf{x^{(0)}} \in$ domain (F) $= \{\mathbf{ux} - \mathbf{c} \geq 0\}$
For k = 0,1,2,. . . until convergence do
    Evaluate $b = -F(\mathbf{x^{(k)}}) = -(\mathbf{y} - \mathbf{A}^T\mathbf{x^{(k)}})^T\mathbf{W}(\mathbf{y} - \mathbf{A}^T\mathbf{x^{(k)}})$
        with $\mathbf{J} = \nabla F(\mathbf{x^{(k)}}) = -2\mathbf{A}^T\mathbf{W}\mathbf{y} + 2\mathbf{A}^T\mathbf{W}\mathbf{A}\mathbf{x^{(k)}}$
    Solve $\mathbf{Js} = b$
    $\mathbf{x^{(k+1)}} = \mathbf{x^{(k)}} + \mathbf{s}$
End for
Record $(\mathbf{y} - \mathbf{A}^T\mathbf{x})^T\mathbf{W}(\mathbf{y} - \mathbf{A}^T\mathbf{x}) = -b$ for each initial at convergence
    and choose the smallest one as selected one.
Solution is the corresponded $\mathbf{x}^* = (a_1^*, a_2^*, \dots, a_q^*)$
    and $a_{(q+1)}^* = (1 - \sum_{l=1}^{q} a_l^* log(K_l/K_{l-1}))(log(c_2))^{-1}$.

We conduct similar experiments under WLS structure with support extension under $c_1 = c_2 = 2$ and illustrate the comparison results in Table X and Table XI.

After comparisons of the fair prices from fitting OTM options under LS and WLS, the prediction errors for OTM options are much smaller under WLS which evident that WLS is preferable in small prediction errors for OTM options. It is also obvious to discover that when the time to expiration gets longer, the trends for relative errors under WLS behave totally different for OTM call and put options. More specifically, the relative errors for OTM options under WLS are decreasing over time especially for call options, when the relative errors decrease at the first several expiries and increase a bit for the last two longer expiries for put options. In addition, under both setups, the relative prediction errors of ITM options are much larger compared to those of OTM options which stay below 0.08 across different expiries.

TABLE X: Prediction errors for put options under WLS and LS using OTM options only across different numbers of days to expiration

LS	$7 \sim 14$	$17 \sim 31$	$81 \sim 94$	$171 \sim 199$	$337 \sim 393$	$502 \sim 592$	$670 \sim 790$
$L_r(OTM)^p$	0.1266	0.0786	0.0419	0.0427	0.0462	0.0792	0.0792
$L_a(OTM)^p$	0.0891	0.0660	0.1098	0.1345	0.3228	0.4267	0.4487
$L_r(ITM)^p$	0.0352	0.0362	0.1268	0.1957	0.3693	0.4519	0.4806
$L_a(ITM)^p$	2.7418	3.1522	13.4135	25.9584	61.0158	116.4508	119.0193
WLS	$7 \sim 14$	$17 \sim 31$	$81 \sim 94$	$171 \sim 199$	$337 \sim 393$	$502 \sim 592$	$670 \sim 790$
$L_r(OTM)^p$	0.0770	0.0646	0.0345	0.0317	0.0232	0.0390	0.0405
$L_a(OTM)^p$	0.1083	0.0794	0.1277	0.1603	0.3645	0.5362	0.5407
$L_r(ITM)^p$	0.0318	0.0337	0.1280	0.1967	0.3677	0.4521	0.4797
$L_a(ITM)^p$	2.6852	3.0818	13.4794	26.0510	60.9564	116.6707	119.6271

TABLE XI: Prediction errors for call options under WLS and LS using OTM options only across different numbers of days to expiration

LS	$7 \sim 14$	$17 \sim 31$	$81 \sim 94$	$171 \sim 199$	$337 \sim 393$	$502 \sim 592$	$670 \sim 790$
$L_r(OTM)^c$	0.1238	0.1152	0.0389	0.0646	0.0318	0.0545	0.0368
$L_a(OTM)^c$	0.0694	0.0830	0.1844	0.3579	1.0075	1.0560	1.0374
$L_r(ITM)^c$	0.0428	0.0282	0.1010	0.1932	0.3110	0.4265	0.3917
$L_a(ITM)^c$	3.0298	3.3180	9.7533	27.8996	53.8949	86.7297	89.0749
WLS	$7 \sim 14$	$17 \sim 31$	$81 \sim 94$	$171 \sim 199$	$337 \sim 393$	$502 \sim 592$	$670 \sim 790$
$L_r(OTM)^c$	0.0757	0.0707	0.0247	0.0199	0.0187	0.0165	0.0124
$L_a(OTM)^c$	0.0948	0.1064	0.2322	0.4277	1.2143	1.3484	1.3381
$L_r(ITM)^c$	0.0439	0.0289	0.1021	0.1921	0.3096	0.4264	0.3910
$L_a(ITM)^c$	3.0941	3.3411	9.8543	27.8492	53.6843	86.7620	88.9238

2.4 Applications of risk-neutral density estimate

From the above comparisons between LS and WLS structures, the error results show different behaviors for OTM options and ITM options. That implies the inconsistency between OTM options and ITM options. In other words, this could be served as an evidence that the financial market is not consistent. The market pricing mechanism for options has a main type that the ask-bid pricing mechanism operated through the system of market makers. The more active the option, typically the tighter the bid/ask spread. Therefore, from the inconsistency of relative error trends, the ask-bid pricing mechanisms for OTM options and ITM options are different. We find an example of a series of options that have fair amount of strikes and at the same time, have resulted in relative "bad" errors (we define any relative errors that are greater than 0.05 to be "bad") across all expiries to illustrate how the predictions perform as time to expiration gets longer. After checking all options, there is no single start date of options that have bad errors across all expiries. We alternate to find options that have large relative errors for longer expiries and there are five start dates ("2002-06-27", "2002-07-01", "2002-07-02", "2008-12-19" and "2011-06-28") that have large errors starting from 3-month expiry and longer. Take the first start date "2002-06-27" as an example. The results from OTM fitting are shown in Figure 3.

From the Figure 3, the dispersions between the market prices and fair prices for ITM options get a bit larger as strikes increase. In other words, the higher the market prices of ITM options, the more chance that the market prices are overpriced. The fair prices of options get higher than the market prices as time to expiration gets longer. Therefore, in the following part, we use all options to fit the density in order to include the information from ITM options as well and it is shown to have better predictions for ITM options.

As an application of our method, we are able to recover all the prices for call and put options given any strike price K. We extend our method using all options fit. The more options are included, more implied information of market we have and more accurate our results are.

2.4.1 Estimation using all options

In this part, we expand the option pricing strategy on options that expire in different expiries and compare the results between the groups. We use all the options in a (t, T) pair instead of only OTM options to fit the density. We also conduct cross-validation experiments, to be more specific, the leave-one-out cross validation. That is, we use all the options except the one to be estimated to fit the density and predict the option price using the estimated density.

We choose $c_1 = c_2 = 25$ in OTM options fit. While for all-option fit, it turns out that the results from the same coefficients are far from desirable. To be more considerate, we choose 3, 5, 10 as alternative testing options. Together with the results from candidate values 2 and 25, the results are all shown in Table XII to Table XVI. We only show the results under LS for illustration purposes. Comparing the prediction errors in the tables, we finally choose $c_1 = c_2 = 2$ for the support of the risk-neutral density, which overall outputs the most smallest prediction errors for all-option fit no matter under LS or WLS structure.

Based on the results under the final selection of the support extension numbers, the predictions for ITM options are better under all-option fit than using only OTM options to fit the density. We can understand in the following way. When we estimate OTM options using OTM

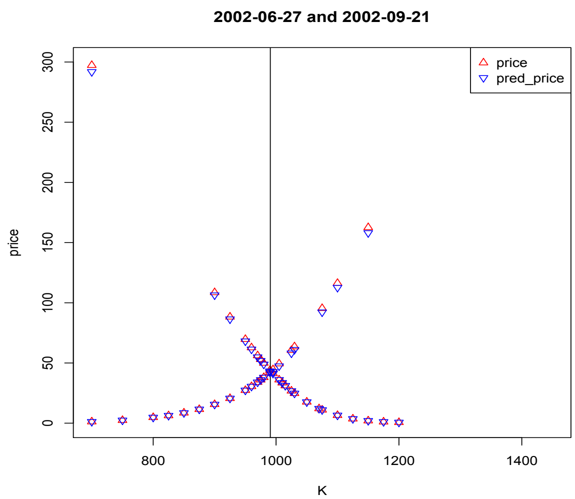

(a)

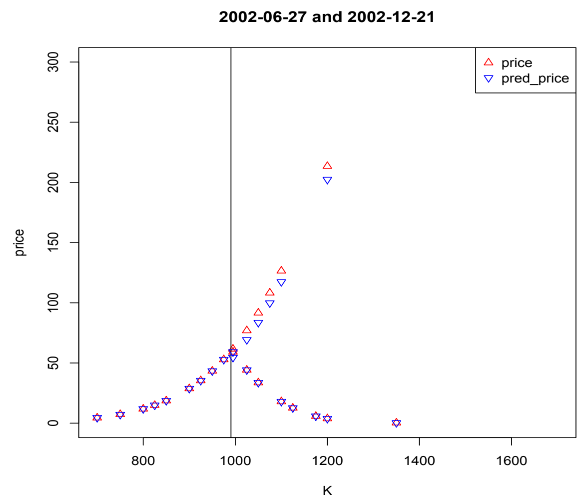

(b)

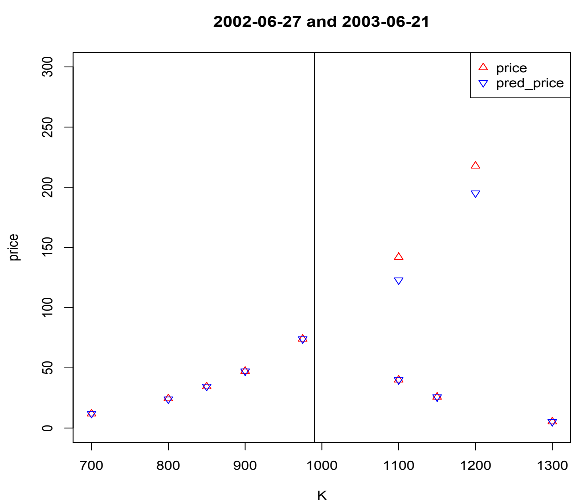

(c)

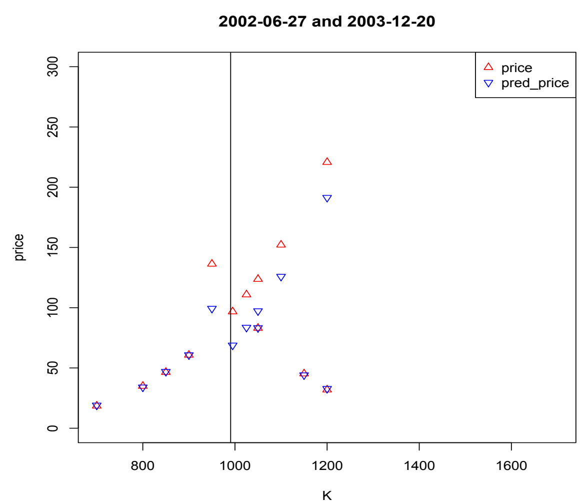

(d)

Figure 3: Example of trading day on 2002-06-27 comparing original prices and predicted prices across different expires using OTM-option fit under LS.

TABLE XII: Prediction errors using all options ($c_1 = c_2 = 2$) across different numbers of days to expiration

Days	$7 \sim 14$	$17 \sim 31$	$81 \sim 94$	$171 \sim 199$	$337 \sim 393$	$502 \sim 592$	$670 \sim 790$
$L_r(OTM)^p$	1.156	1.002	0.922	0.434	0.084	0.131	0.168
$L_a(OTM)^p$	0.406	0.474	0.617	3.313	2.400	3.200	5.009
$L_r(ITM)^p$	0.030	0.023	0.029	0.073	0.076	0.064	0.077
$L_a(ITM)^p$	1.633	1.824	3.308	5.158	8.464	15.729	10.06
Days	$7 \sim 14$	$17 \sim 31$	$81 \sim 94$	$171 \sim 199$	$337 \sim 393$	$502 \sim 592$	$670 \sim 790$
$L_r(OTM)^c$	2.764	2.006	1.256	0.519	0.691	0.176	0.177
$L_a(OTM)^c$	0.746	0.786	1.374	2.299	2.914	4.267	6.022
$L_r(ITM)^c$	0.027	0.014	0.012	0.041	0.028	0.037	0.047
$L_a(ITM)^c$	2.227	2.324	3.284	4.607	3.238	13.23	7.901

TABLE XIII: Prediction errors for put options using all options ($c_1 = c_2 = 3$) across different numbers of days to expiration

Days	$7 \sim 14$	$17 \sim 31$	$81 \sim 94$	$171 \sim 199$	$337 \sim 393$	$502 \sim 592$	$670 \sim 790$
$L_r(OTM)^p$	1.2363	1.0742	1.0469	0.5225	0.0998	0.1414	0.1879
$L_a(OTM)^p$	0.4151	0.4779	0.6399	6.0024	4.6917	6.3833	10.3420
$L_r(ITM)^p$	0.0297	0.0224	0.0435	0.1340	0.1483	0.1231	0.1613
$L_a(ITM)^p$	1.6041	1.7833	5.0110	9.5930	13.2879	16.0196	19.9915
Days	$7 \sim 14$	$17 \sim 31$	$81 \sim 94$	$171 \sim 199$	$337 \sim 393$	$502 \sim 592$	$670 \sim 790$
$L_r(OTM)^c$	2.8176	2.0826	1.3200	0.5376	0.6142	0.3121	0.1812
$L_a(OTM)^c$	0.7514	0.7995	1.6772	3.2090	4.1842	5.7418	7.8092
$L_r(ITM)^c$	0.0271	0.0136	0.0119	0.0574	0.0400	0.0486	0.0632
$L_a(ITM)^c$	2.2113	2.3071	3.2341	6.1779	5.2566	8.6651	10.5469

TABLE XIV: Prediction errors for put options using all options ($c_1 = c_2 = 5$) across different numbers of days to expiration

Days	$7 \sim 14$	$17 \sim 31$	$81 \sim 94$	$171 \sim 199$	$337 \sim 393$	$502 \sim 592$	$670 \sim 790$
$L_r(OTM)^p$	1.2671	1.1241	1.1530	0.5978	0.1227	0.1565	0.2167
$L_a(OTM)^p$	0.4159	0.4819	0.6552	9.0065	7.2336	10.0559	16.1629
$L_r(ITM)^p$	0.0291	0.0222	0.0620	0.2024	0.2293	0.1886	0.2534
$L_a(ITM)^p$	1.5772	1.7603	7.1750	14.6343	20.3607	21.3011	30.5641
Days	$7 \sim 14$	$17 \sim 31$	$81 \sim 94$	$171 \sim 199$	$337 \sim 393$	$502 \sim 592$	$670 \sim 790$
$L_r(OTM)^c$	2.8721	2.1205	1.3516	0.5478	0.9109	0.4944	0.1829
$L_a(OTM)^c$	0.7600	0.8034	1.7550	3.4632	4.7066	6.4902	8.0893
$L_r(ITM)^c$	0.0271	0.0135	0.0120	0.0610	0.0440	0.0541	0.0681
$L_a(ITM)^c$	2.2031	2.2947	3.1995	6.5523	5.4152	8.0756	11.4468

TABLE XV: Prediction errors for put options using all options ($c_1 = c_2 = 10$) across different numbers of days to expiration

Days	$7 \sim 14$	$17 \sim 31$	$81 \sim 94$	$171 \sim 199$	$337 \sim 393$	$502 \sim 592$	$670 \sim 790$
$L_r(OTM)^p$	1.156	1.002	0.922	0.434	0.084	0.131	0.168
$L_a(OTM)^p$	0.4107	0.4798	0.6587	12.0819	9.8675	13.8740	22.1820
$L_r(ITM)^p$	0.0279	0.0219	0.0816	0.2726	0.3127	0.2565	0.3477
$L_a(ITM)^p$	1.5595	1.7434	9.4794	19.8353	27.8990	28.6397	41.2097
Days	$7 \sim 14$	$17 \sim 31$	$81 \sim 94$	$171 \sim 199$	$337 \sim 393$	$502 \sim 592$	$670 \sim 790$
$L_r(OTM)^c$	2.9271	2.1293	1.3719	0.5519	0.9546	0.6387	0.1808
$L_a(OTM)^c$	0.7701	0.8056	1.5761	2.9582	4.1593	6.2396	6.9338
$L_r(ITM)^c$	0.0275	0.0136	0.0121	0.0511	0.0379	0.0483	0.0586
$L_a(ITM)^c$	2.2077	2.2929	3.1855	5.5744	5.0093	7.3338	10.0750

TABLE XVI: Prediction errors for put options using all options ($c_1 = c_2 = 25$) across different numbers of days to expiration

Days	$7 \sim 14$	$17 \sim 31$	$81 \sim 94$	$171 \sim 199$	$337 \sim 393$	$502 \sim 592$	$670 \sim 790$
$L_r(OTM)^p$	1.2169	1.0801	1.2237	0.7075	0.1731	0.1961	0.2886
$L_a(OTM)^p$	0.4014	0.4637	0.6510	14.6686	12.1104	17.1537	27.3416
$L_r(ITM)^p$	0.0265	0.0213	0.0985	0.3317	0.3831	0.3166	0.4278
$L_a(ITM)^p$	1.5536	1.7352	11.4666	24.2388	34.2975	35.2836	50.2617
Days	$7 \sim 14$	$17 \sim 31$	$81 \sim 94$	$171 \sim 199$	$337 \sim 393$	$502 \sim 592$	$670 \sim 790$
$L_r(OTM)^c$	2.9146	2.1238	1.3569	0.5542	0.9967	0.7447	0.1770
$L_a(OTM)^c$	0.7784	0.8120	1.2817	2.0270	3.0845	5.5750	4.9766
$L_r(ITM)^c$	0.0282	0.0139	0.0122	0.0334	0.0256	0.0360	0.0393
$L_a(ITM)^c$	2.2222	2.3182	3.2074	3.8660	4.0796	5.7753	7.2660

options only, there is no external noise and when we estimate ITM options using only OTM options, the results are highly affected by the difference between the two pricing mechanisms. While using all options to fit and price, things work in the opposite direction.

We also conduct a comparison of the performances under LS setup and WLS setup, with results shown in Table XVII and Table XVIII. From the results, the results under WLS setup are more preferable if we control our relative errors within 0.07. In terms of absolute errors, WLS is in good performance in predicting OTM options and the regular LS is good in ITM options.

In Figure 4, we use another example of options traded on March 18th, 2015 and expired on April 17th, 2015 to show the fitted performance under WLS.

TABLE XVII: Prediction errors for call options under LS and WLS using all options ($c_1 = c_2 = 2$) across different numbers of days to expiration

LS	$7 \sim 14$	$17 \sim 31$	$81 \sim 94$	$171 \sim 199$	$337 \sim 393$	$502 \sim 592$	$670 \sim 790$
$L_r(OTM)^c$	2.764	2.006	1.256	0.519	0.691	0.176	0.177
$L_a(OTM)^c$	0.746	0.786	1.374	2.299	2.914	4.267	6.022
$L_r(ITM)^c$	0.027	0.014	0.012	0.041	0.028	0.037	0.047
$L_a(ITM)^c$	2.227	2.324	3.284	4.607	3.238	13.23	7.901
WLS	$7 \sim 14$	$17 \sim 31$	$81 \sim 94$	$171 \sim 199$	$337 \sim 393$	$502 \sim 592$	$670 \sim 790$
$L_r(OTM)^c$	0.0751	0.0701	0.0241	0.0377	0.0367	0.0342	0.0440
$L_a(OTM)^c$	0.1063	0.1212	0.2460	2.7290	3.4660	3.5504	6.1585
$L_r(ITM)^c$	0.0212	0.0196	0.0155	0.0896	0.0445	0.0403	0.0537
$L_a(ITM)^c$	2.8701	3.0760	4.5941	10.4246	10.2022	15.3275	10.7337

TABLE XVIII: Prediction errors for put options under LS and WLS using all options ($c_1 = c_2 = 2$) across different numbers of days to expiration

LS	$7 \sim 14$	$17 \sim 31$	$81 \sim 94$	$171 \sim 199$	$337 \sim 393$	$502 \sim 592$	$670 \sim 790$
$L_r(OTM)^p$	1.156	1.002	0.922	0.434	0.084	0.131	0.168
$L_a(OTM)^p$	0.406	0.474	0.617	3.313	2.400	3.200	5.009
$L_r(ITM)^p$	0.030	0.023	0.029	0.073	0.076	0.064	0.077
$L_a(ITM)^p$	1.633	1.824	3.308	5.158	8.464	15.729	10.06
WLS	$7 \sim 14$	$17 \sim 31$	$81 \sim 94$	$171 \sim 199$	$337 \sim 393$	$502 \sim 592$	$670 \sim 790$
$L_r(OTM)^p$	0.0767	0.0644	0.0344	0.0468	0.0327	0.0444	0.0518
$L_a(OTM)^p$	0.1125	0.0878	0.1903	1.8165	2.0243	2.7545	5.1333
$L_r(ITM)^p$	0.0226	0.0202	0.0333	0.0623	0.0636	0.0701	0.0704
$L_a(ITM)^p$	2.2309	2.3946	4.6722	5.3686	8.7092	17.4991	11.9397

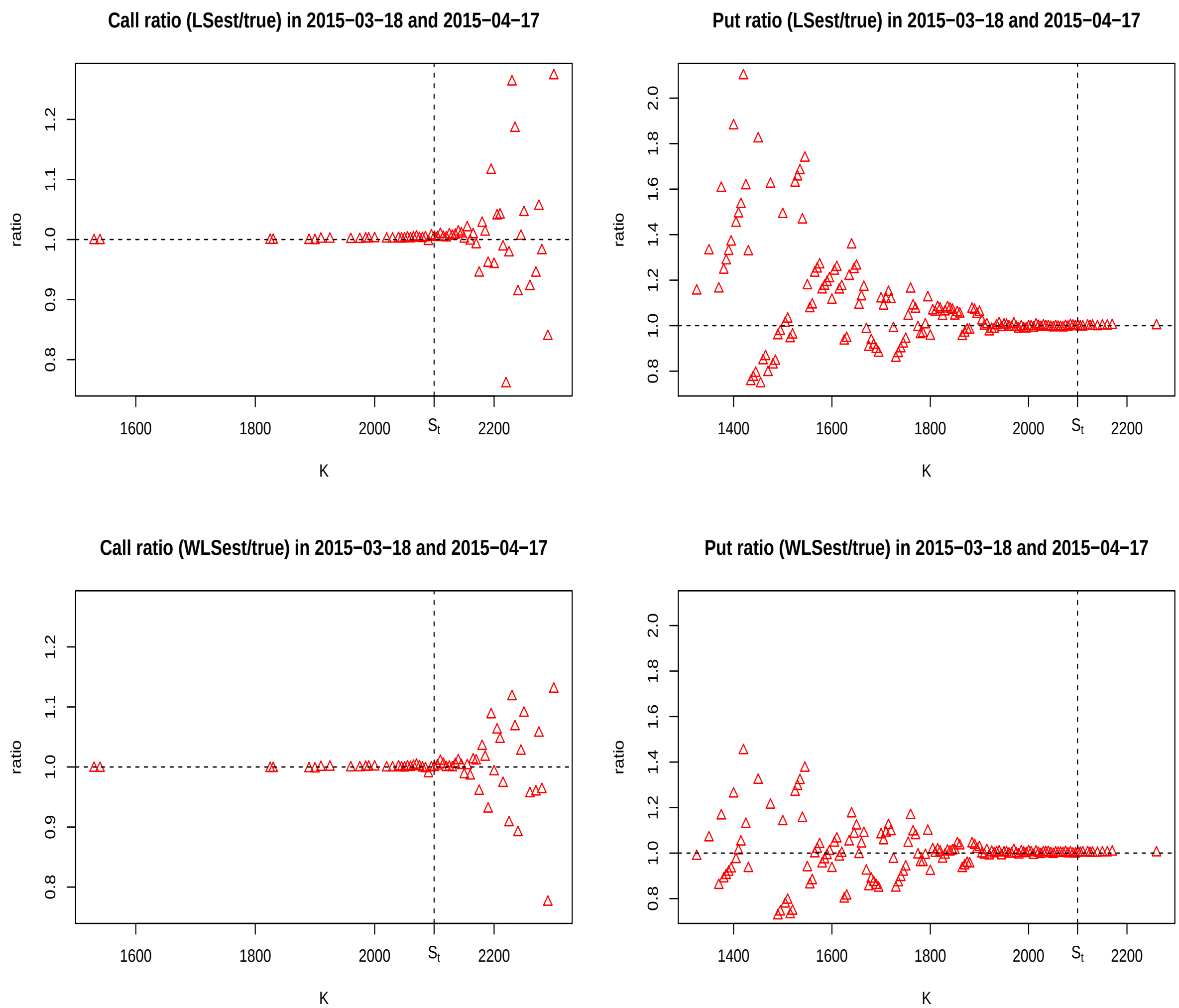

Figure 4: An example of ratio of fitted option prices and market prices under LS and WLS setup

There is an obvious scale decrease of the ratios of the fair prices over the market prices for both call and put options, suggesting the efficiency of reformulating the problem by incorporating the weight factor of option values.

More investigation on confidence bounds

We further calculate the error values for each (t, T) pair and derive summaries that enable us to get more informative plots. We investigate the confidence bounds for the absolute and relative errors from pricing call and put options in the seven different expiries under LS setup. For each plot, we mark medians and two boundary quantiles as references. For the choices of quantiles, if 97.5% and 2.5% quantiles are too spread, 90% and 10% are also appropriate; even 75% and 25% are reasonable. In our work, results of 75-25 confidence bounds are shown in Figure 5 and Figure 6. When looking at the absolute errors, the errors are all increasing when expiries get longer generally regardless of whether we are predicting OTM or ITM options and call or put options. These are not hard to understand. As expiries get longer, the affects from the market on options get weaker and the prices of options are more unstable. Also given the reason that the liquidity is small for options with longer time to expirations, the bid-ask spreads are wider and consequently, the estimation variations are more and more noticeable. For the relative ones, they are in the opposite trends due to the facts that the option prices are more expensive with longer expirations. Even though we have the same level of absolute errors, we are getting more accurate estimations compared to the market prices relatively.

We also investigate the points that have large relative errors under WLS using all-option fit since the relative errors under WLS are supposed to be constantly small, and also inspired by

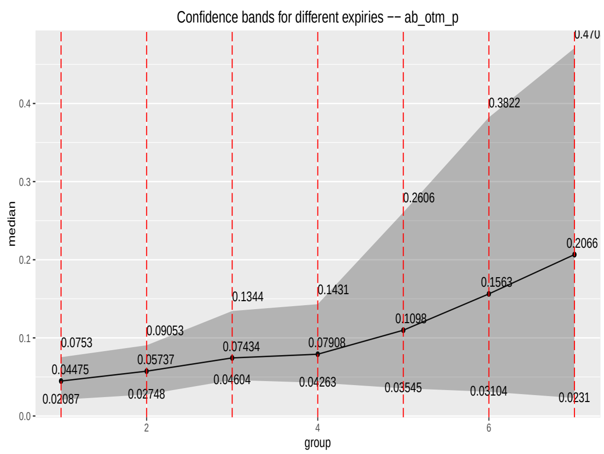

(a) Predicting OTM put options

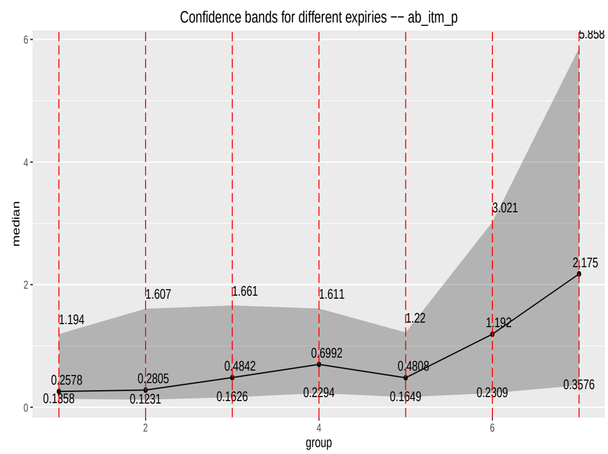

(b) Predicting ITM put options

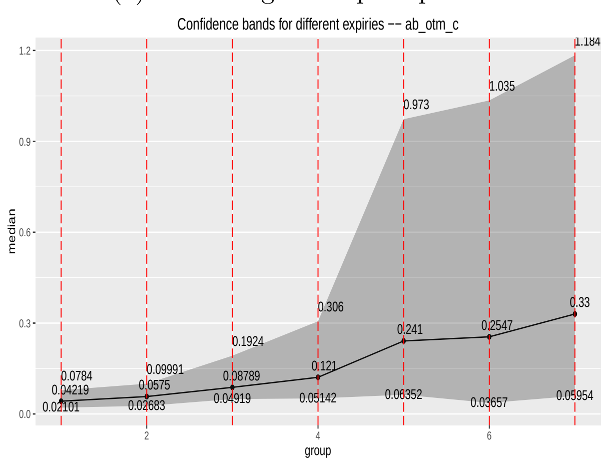

(c) Predicting OTM call options

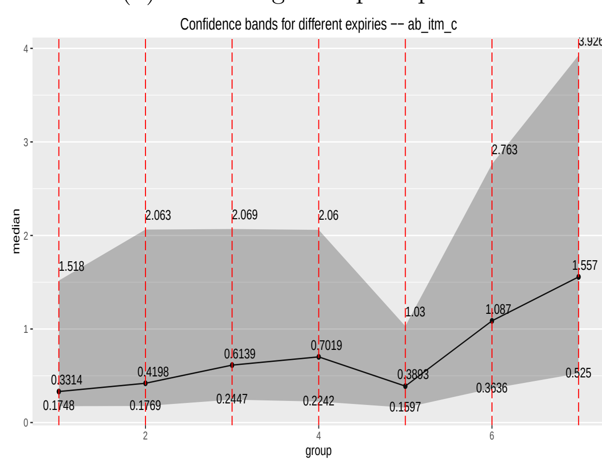

(d) Predicting ITM call options

Figure 5: Absolute prediction errors using all-option fit, group 1 to 7 are corresponding to 7 expiries: $7 \sim 14$, $17 \sim 31$, $81 \sim 94$, $171 \sim 199$, $337 \sim 393$, $502 \sim 592$ and $670 \sim 790$

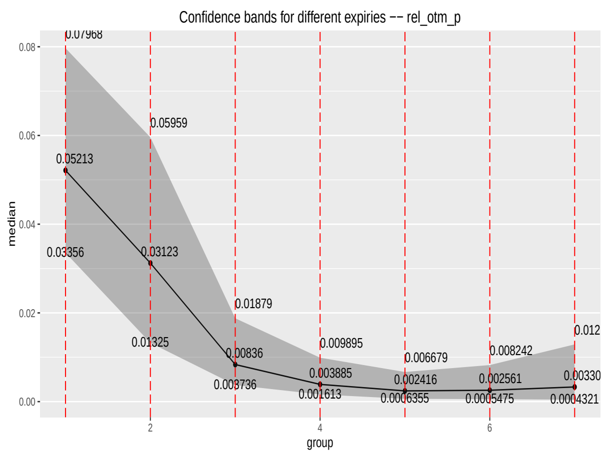

(a) Predicting OTM put options

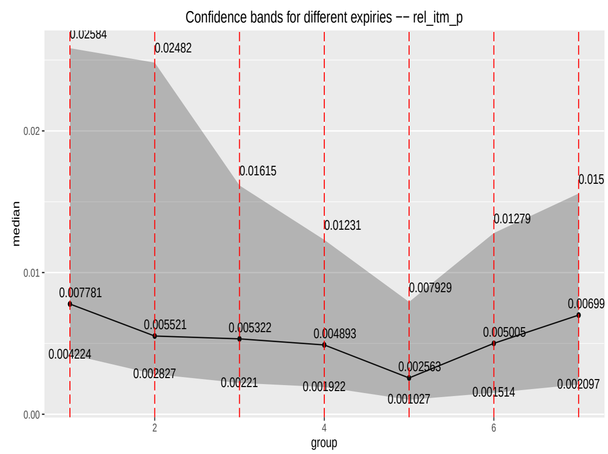

(b) Predicting ITM put options

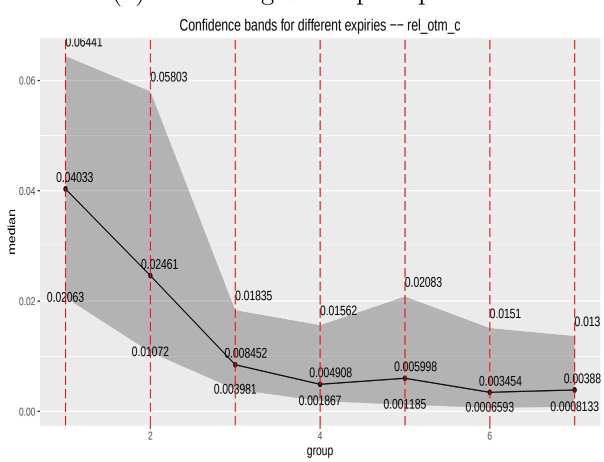

(c) Predicting OTM call options

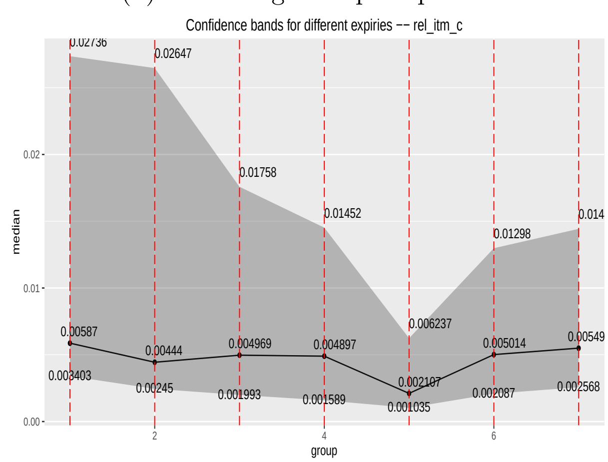

(d) Predicting ITM call options

Figure 6: Relative prediction errors using all-option fit, group 1 to 7 are corresponding to the seven expiries

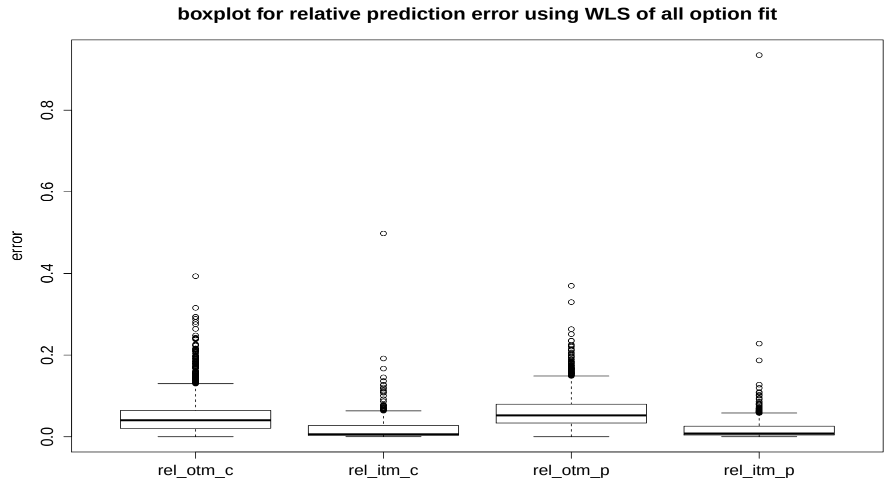

Figure 7: Box plot of relative error using all-option fit under WLS

our belief that the option prices are not consistent in the market. The resulted box plot for the four relative errors using all-option fit under WLS are exhibited and the axis range is manually cut to show the main part, as shown in Figure 7. After investigation,

1. For the relative error of OTM put options using WLS, there are two cases where the error rate is larger than 0.3. The two cases are 2014-12-10 to 2014-12-20 and 2014-12-12 to 2014-12-20.

   (a) 2014-12-10 to 2014-12-20: There are 142 unique strike prices and 194 options where among which there are 124 options with price lower than \$10. Also there are 37 OTM call options and 102 OTM put options. The range of strike prices is from 1400 to 3000 and the current price for the underlying asset is \$2026.14.

(b) 2014-12-12 to 2014-12-20: There are 148 unique strike prices and 204 options where among which there are 130 options with price lower than \$10. Also there are 38 OTM call options and 109 OTM put options. The range of strike prices is from 1400 to 2195 and the trading price for the underlying asset is \$2002.33.

2. For the relative error of ITM put options using WLS, there are two cases where the error rate is larger than 0.2. The two cases are 2002-05-10 to 2002-05-18 and 2007-12-21 to 2007-12-28.

   (a) 2002-05-10 to 2002-05-18: There are 19 unique strike prices and 29 options where among which there are 9 OTM call options and 6 OTM put options. The range of strike prices is from 900 to 1375 and the trading price for the underlying asset is \$1054.99.

   (b) 2007-12-21 to 2007-12-28: There are 2 unique strike prices and 2 options where among which there are 0 OTM call options and 0 OTM put options. The range of strike prices is from 1440 to 1485 and the trading price for the underlying asset is \$1484.46.

The dates where the fair prices are relatively further from the market prices are mainly focused on year 2002, 2007 and 2014. Those are the dates when the overall stock market was near the most values, see Figure 8. Therefore, it is reasonable to believe that the market prices were highly over or under estimated and that also explains why the predicted prices are relatively far from the market prices.

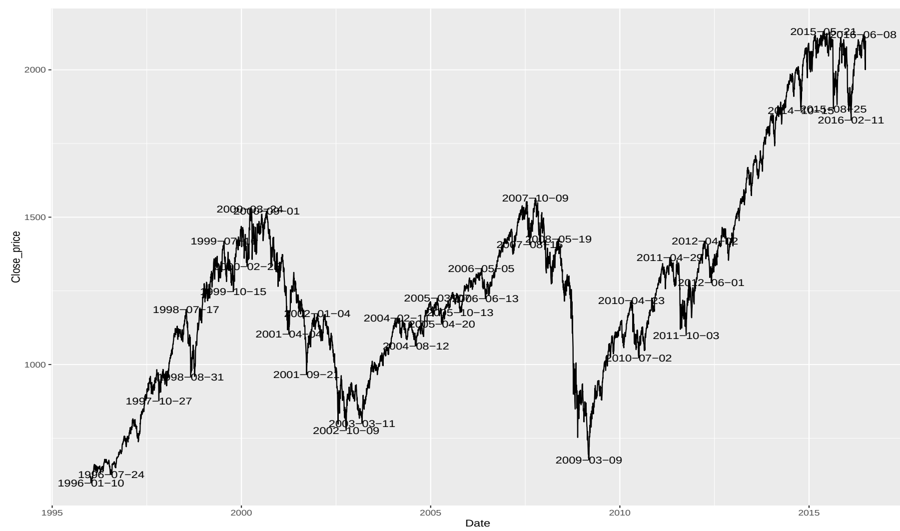

Figure 8: $S\&P500$ historical price trend

In summary, our method has very practical applications. Our approach can estimate the risk-neutral density given any option data set, and can predict the option fair price precisely for any strike price given a set of options traded on the same trading date and expiration date. The performance from leave-one-out cross validation study guarantees the accuracy of the method.

1. Reasonable RND estimation

   Our method results in an appropriate estimation of the risk-neutral density. We pick a certain day which has many options available for better illustration purpose and draw the estimated risk-neutral density function to visually review the shape of the density. Based on our results, the density plot derived from WLS setup is more clear in the shape. Shown in Figure 9 is an example of our fitted density of options traded on December 10th,

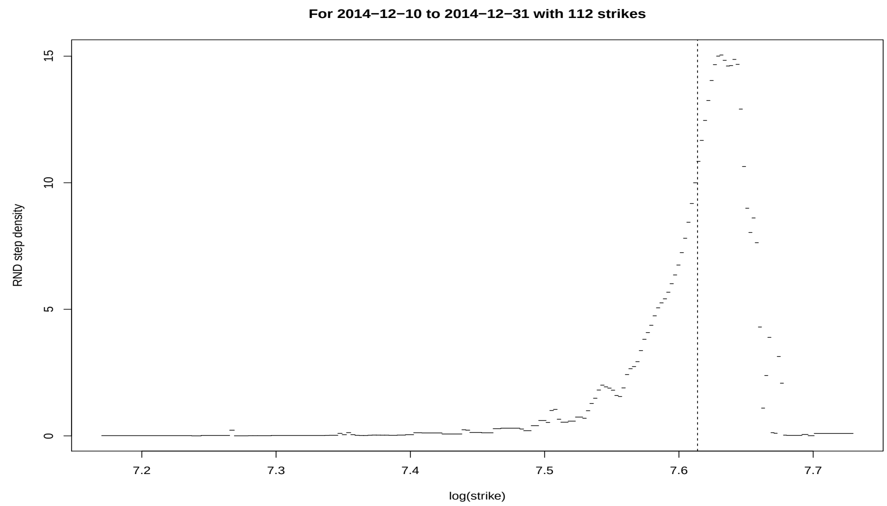

Figure 9: An example of fitted risk-neutral density plot.

2014 and expired on December 31st, 2014. The graph is very consistent with the common guess of RND shape.

2. Recover option prices

   Our method can further recover the fair option price for any strike price given a set of corresponding options. For any given series of option prices with their corresponding strike prices and information of put/call options, we could estimate the fair option price for any given strike prices reasonably well.

3. Unveil investment opportunities

   From an economic point of view, we are able to use the estimated density to price options and recognize some options on the markets that are under or above estimated. Although it is inadequate to claim the existence of the arbitrage opportunities as the lack of guarantee to earn and there is mature system in the market that is designed to catch such direct difference in the option prices, we can explore profitable investment opportunities for investors. An example is shown in Figure 10. We can look into those points where there is a dispersion between the market price (red triangle) and the fair price (blue triangle) for profitable investment opportunities. While in the statistical point of view, we utilize market options directly, options that have noises from different sources. As a result, the option pricing estimation process is noisy. By incorporating experiments on confidence bounds, we can have more confidence to make better strategy and improve the rate of returns.

We also conduct the leave-one-out cross validation study. Cross validation is powerful in checking the performance of a prediction method. We set aside one option each time and perform estimation for the RND and then predict the option price for the one outside the pool and compare how close is the fair price with the market value. Our example of options traded on April 14th, 2014 and expired on May 9th, 2014 gives a good sense how well our method performs even without incorporating weight factors in Figure 11.

2.4.2 Comparison with cubic spline methods

We conduct comparison between the cubic spline approach in the literature (Monteiro et. al. (2008) (60)) with our method. In contrast to the existing techniques, we allow better fitness without the smoothness assumption required by the cubic spline method in finding the optimized risk-neutral density. In the meanwhile, our approach, extracting information

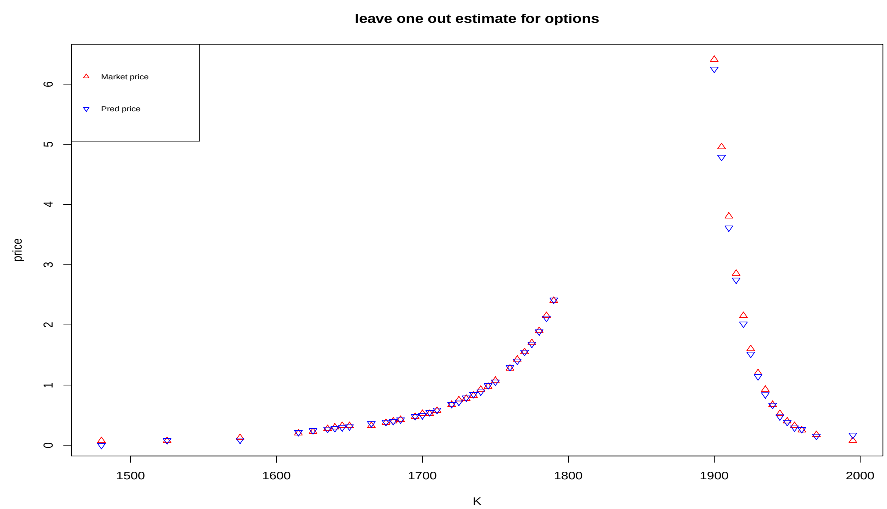

Figure 10: An example of leave-one-out cross validation performance of our approach under LS setup for unveil investment opportunities

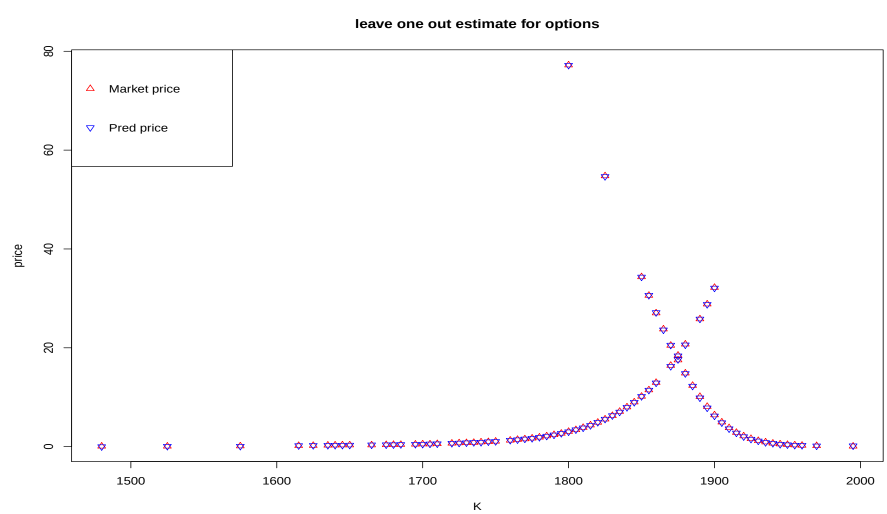

Figure 11: An example of leave-one-out cross validation performance of our approach under LS setup where t = 2014-04-14 and T = 2014-05-09

from the market prices of call and put options, acknowledges the existing market noise in the prices. The comparison test is also conducted with the European options on S&P 500. The rest of the section is organized as follows: In the first subsection, steps of preprocessing data in the cubic spline method are specified. Second subsection is devoted to a numerical comparison of our approach and the existing cubic spline approach using the market data. An example of options traded on April 29th, 2003 with expiration date on May, 17th, 2003 is used as an illustration for the performance on cross validation study. A comparison of fitted errors is also shown afterwards. We have 20 years in coverage and randomly select 10 pairs of (t, T) from each year. Then, we testify the results on these 200 pairs of (t, T) using all the options traded to compare the fitting performance of our approach with the cubic spline method. We conclude in the last subsection with a detailed discussion.

Our numerical implementations are based on "[R]: lsei(**a, b, c, d, e, f**)" from package "lsei", where **a** stands for design matrix; **b** for response vector; **c** for matrix of numeric coefficients on the left-hand sides of equality constraints; **d** for vector of numeric values on the right-hand sides of equality constraints; **e** for matrix of numeric coefficients on the left-hand sides of inequality constraints and **f** for vector of numeric values on the right-hand sides of inequality constraints. The reason why we alternative numerical implementation method is because the large amount of equality constraints imposed in the cubic spline method and *lsei* function is able to take all into consideration at the same time. In general, the optimization problem with constraints can be solved using previously mentioned Quasi-Newton method with syntax *ConstrOptim* in [R].

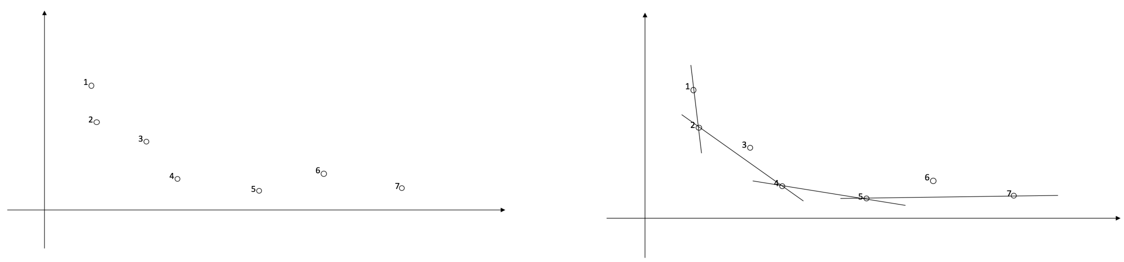

(a) 7 points given

(b) points left after testing strict convexity

Figure 12: Convex hull idea illustration.

We follow the same filter steps they did on the market options, the new data set consists of updated call options and original put options, which is ready for the optimization problem. When tested for strict convexity which is not stated in details in the paper, we employ the idea of convex hull to eliminate options that violate. The idea of convex hull is shown in Figure 12. Suppose we have 7 points shown in Figure 12(a), if we could detect a high density point set, the set contains the points retained for convexity. We then connect every two points and check if every other points are above the line, if so, add 1 on the index vector for the two points. Finally, we have a point set like what is shown in Figure 12(b). The 5 points on the boundary are the points that satisfy strict convexity. The index vector is (1, 2, 0, 2, 2, 0, 1). The points corresponding to 0 in the index vector are dropped for violation.

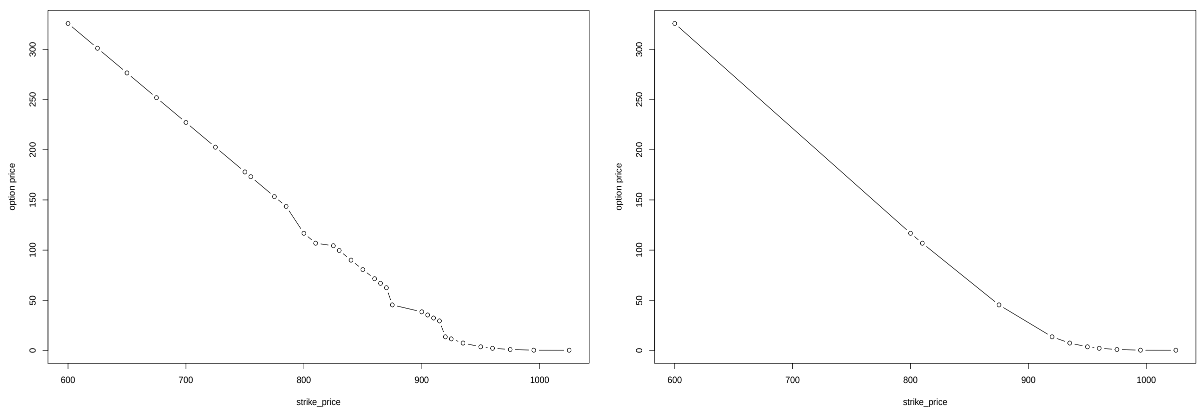

(a) all call options after monotonicity, before convexity

(b) all call options after monotonicity, after convexity

Figure 13: Strict convexity check.

Example on a specific date

We test the performance of the cubic spline approach with our method on options traded on April 29th, 2003 and expired on May 17th, 2003 for illustration and this is also the example used in the paper.

Figure 13 is the result after applying the convex hull in this example. After checking strict convexity, call options in Figure 13(b) are ready to be used in the optimization problem.

Before we solve the problem, we also check Figure 14 which shows more information about which option is actually used in RND estimation. The red triangle options are the ones we have in the raw data set. After updating call options following the above three steps, we have blue triangles left representing the options finally used in the optimization problem. The point

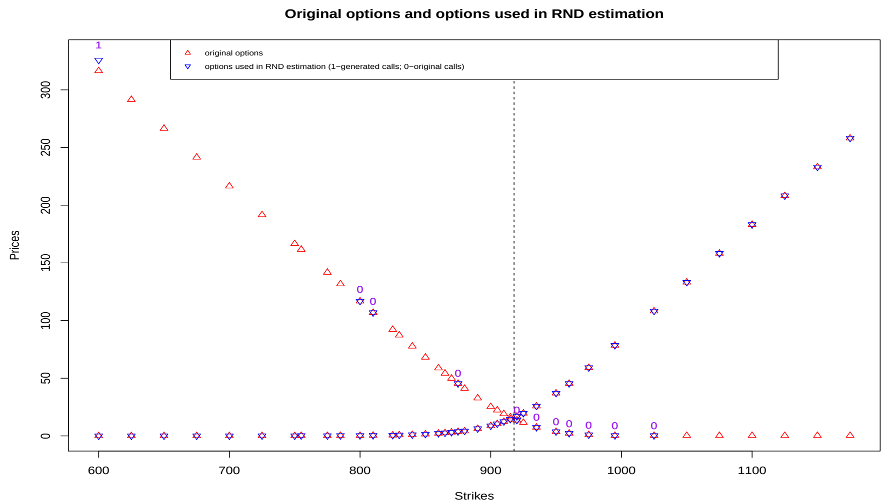

Figure 14: Call option used in RND fitting in cubic spline

with zero value on the side in the graph indicates the corresponding call options are used in RND estimation which are from the original raw data set. Those call options with value one indicate that the options are generated by the put-call parity. The vertical dotted line presents the current price of the underlying asset.

No matter whether we incorporate the trading volume as weights or not, the updating process for call options is the same. We solve the optimization problem under the ordinal least square and also weighted least square setup and the fitted results are shown in Figure 15. Again, the red triangles are the market prices for the options and blue triangles are the fair prices from the cubic spline method.

We further check the performance of the cubic spline method by cross validation study. Assuming one of the option is missing from the option data set and we use the rest of options

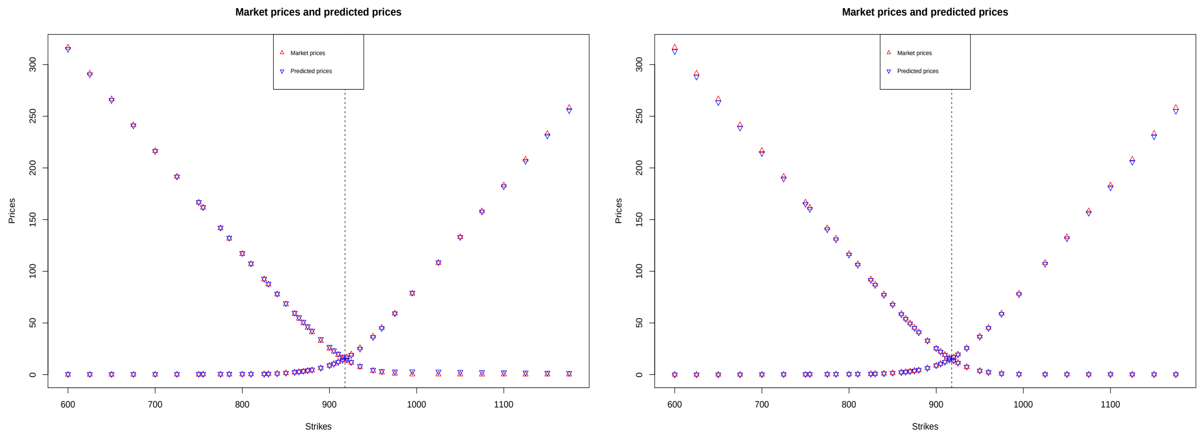

(a) No weight optimization

(b) Volume as weight optimization

Figure 15: Original option prices and fitted option prices from cubic spline approach.

TABLE XIX: Prediction errors for cubic spline and our approach from leave-one-out cross validation

Error	LS		WLS	
	cubic spline	our approach	cubic spline	our approach
L_r	6.0574	0.4786	4.7060	0.2033
L_a	1.1519	0.3034	1.0401	0.2952

to solve the optimization problem and estimate the parameters. The fair price of the missing option is derived then and the results are shown in Figure 16. We present the relative and absolute errors from the cubic spline and our approach in Table XIX.

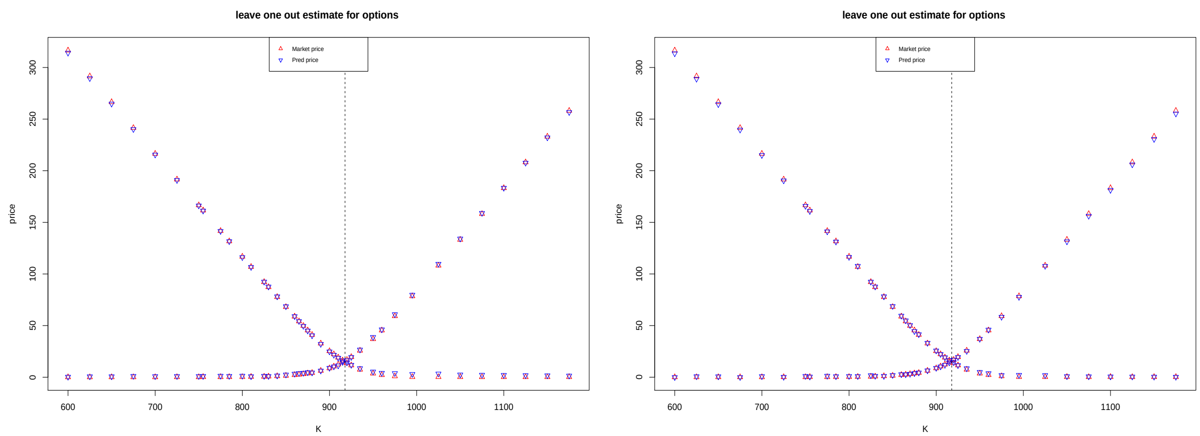

(a) No weight optimization

(b) Volume as weight optimization

Figure 16: Leave-one-out cross validation results from cubic spline approach.

Example on 200 random pairs of (t, T) for each expiry

To test performance for generosity, we select all the options from randomly selected 200 pairs of (t, T) from each expiry. Among the 200 pairs, their approach is not applicable for some pairs due to the following reasons.

1. When there are only one or two call options left after monotonicity, it is not enough to perform strict convexity test.

2. When there are no put options in a pair of (t, T), three-step filter and generation of call options is unavailable.

3. When we use updated call options to solve the problem and derive the estimation for parameters to further price other options, the strike prices of other options may exceed

the knots range for the cubic spline that based on only updated call option strike prices and there is a potential problem.

4. Sometimes, the number of options used in optimization problem is just too small.

For the reasons mentioned above, we could only get a portion of 200 pairs from each expiry available for the cubic spline approach. We retain the same set of options predicted using our method and compare the relative and absolute errors for each expiry. The results are in Table XX to Table XXIII.

TABLE XX: Prediction errors under LS across different numbers of days to expiration for the random samples - cubic spline

Days	$7 \sim 14$	$17 \sim 31$	$81 \sim 94$	$171 \sim 199$	$337 \sim 393$	$502 \sim 592$	$670 \sim 790$
$L_r(OTM)^p$	3.8327	2.9500	2.6389	16829.2549	1012.6762	90.2878	266.3112
$L_a(OTM)^p$	2.6838	1.3278	2.8206	195650.2875	21201.5085	3996.7152	24199.6961
$L_r(ITM)^p$	0.2162	0.0840	0.1916	984.9820	362.7766	214.3127	0.1726
$L_a(ITM)^p$	4.0392	2.6735	12.7982	92972.8596	112651.8417	41209.6607	24.6097
Days	$7 \sim 14$	$17 \sim 31$	$81 \sim 94$	$171 \sim 199$	$337 \sim 393$	$502 \sim 592$	$670 \sim 790$
$L_r(OTM)^c$	9.7180	5.4070	14.1011	35249.5239	2320.8766	42857.0170	3821.7437
$L_a(OTM)^c$	4.8243	3.5290	64.8064	244086.2498	178003.2008	516510.8951	21750.0136
$L_r(ITM)^c$	0.3703	0.1814	0.8891	1132.6060	1343.2508	1254.2174	147.3485
$L_a(ITM)^c$	7.3512	6.2559	35.8245	160963.1956	358948.7427	387661.7611	71957.5822

Discussion and Conclusion

From all the comparison results shown in the specific example and in the 200 random samples from each expiry, our approach is more stable and precise than the cubic spline with

TABLE XXI: Prediction errors under WLS across different numbers of days to expiration for the random samples - cubic spline

Days	$7 \sim 14$	$17 \sim 31$	$81 \sim 94$	$171 \sim 199$	$337 \sim 393$	$502 \sim 592$	$670 \sim 790$
$L_r(OTM)^p$	4.3636	3.0586	2.9058	16392.0113	1002.5010	90.2846	266.3731
$L_a(OTM)^p$	3.3993	1.7206	3.4074	190668.5547	21012.3756	3996.6323	24201.2311
$L_r(ITM)^p$	0.2677	0.1566	0.2006	952.0472	359.5709	298.3378	0.1482
$L_a(ITM)^p$	5.3896	4.8317	13.6291	89828.9872	111633.9924	57267.4141	21.8593
Days	$7 \sim 14$	$17 \sim 31$	$81 \sim 94$	$171 \sim 199$	$337 \sim 393$	$502 \sim 592$	$670 \sim 790$
$L_r(OTM)^c$	8.8340	2.5977	14.0896	35153.2759	2302.5577	61680.2524	3823.3592
$L_a(OTM)^c$	5.1684	2.7804	64.7542	231577.1938	176428.5863	882193.0322	21758.2561
$L_r(ITM)^c$	0.3388	0.1643	0.8858	1129.9532	1330.0822	2032.7718	147.4041
$L_a(ITM)^c$	7.7784	5.5999	35.7376	160585.4643	355420.4223	637677.2702	71984.7514

non-negativity knots. Eliminating and smoothing out the option prices as indicated by their approach, loses much information from the market. The market prices are the real market's forecast for the real volatility of stock, and using observed option prices in the market makes more sense. While in comparison, our approach utilize all the available options. All the resulted are derived from knots which are the trading strike prices. Our method by constructing constant functions between adjacent knots performs better than the cubic spline approach from the cross validation study.

TABLE XXII: Prediction errors under LS across different numbers of days to expiration for the random samples - Our approach(LS)

Days	$7 \sim 14$	$17 \sim 31$	$81 \sim 94$	$171 \sim 199$	$337 \sim 393$	$502 \sim 592$	$670 \sim 790$
$L_r(OTM)^p$	1.7967	1.1802	1.3613	0.3295	0.0332	0.0284	0.0619
$L_a(OTM)^p$	0.5681	0.5121	0.7318	0.7259	0.6243	1.2463	1.3791
$L_r(ITM)^p$	0.0507	0.0314	0.0283	0.0127	0.0129	0.0154	0.0292
$L_a(ITM)^p$	1.3306	1.1971	1.6070	1.0579	1.0643	1.6030	2.6901
Days	$7 \sim 14$	$17 \sim 31$	$81 \sim 94$	$171 \sim 199$	$337 \sim 393$	$502 \sim 592$	$670 \sim 790$
$L_r(OTM)^c$	3.1561	1.7677	0.3382	0.1153	0.0700	0.0381	0.0866
$L_a(OTM)^c$	1.0150	0.7498	0.9550	0.9019	1.4528	1.9220	1.5863
$L_r(ITM)^c$	0.0337	0.0172	0.0170	0.0087	0.0083	0.0137	0.0124
$L_a(ITM)^c$	3.0607	1.9650	3.0129	1.6332	0.9139	1.9206	2.1083

TABLE XXIII: Prediction errors under WLS across different numbers of days to expiration for the random samples - Our approach(LS)

Days	$7 \sim 14$	$17 \sim 31$	$81 \sim 94$	$171 \sim 199$	$337 \sim 393$	$502 \sim 592$	$670 \sim 790$
$L_r(OTM)^p$	0.0821	0.0576	0.0195	0.0142	0.0041	0.0133	0.0337
$L_a(OTM)^p$	0.1058	0.0928	0.2323	0.4836	0.5745	0.9600	0.9866
$L_r(ITM)^p$	0.0306	0.0260	0.0202	0.0136	0.0145	0.0188	0.0423
$L_a(ITM)^p$	1.4264	1.3410	1.6377	1.3798	2.4415	2.5551	3.8917
Days	$7 \sim 14$	$17 \sim 31$	$81 \sim 94$	$171 \sim 199$	$337 \sim 393$	$502 \sim 592$	$670 \sim 790$
$L_r(OTM)^c$	0.0730	0.0502	0.0158	0.0164	0.0174	0.0201	0.0147
$L_a(OTM)^c$	0.1021	0.1154	0.3746	0.6520	1.4593	2.3057	1.2442
$L_r(ITM)^c$	0.0315	0.0271	0.0213	0.0168	0.0097	0.0204	0.0234
$L_a(ITM)^c$	4.0856	2.8867	5.0610	4.7761	1.1971	3.3539	4.1070

CHAPTER 3

PRICING VARIANCE SWAP

In this chapter, we start with the introduction to variance swap, including its pricing formula. In Section 3.2, we present how data is processed and prepared for our analysis, and illustrate variance future and how we replicate variance swap using variance future. Section 3.3 is devoted to describe two methods for estimating moments of the risk-neutral density. We evualate the prediction performance by comparing the fair prices of variance swap from the two approaches with the market prices and conclude in the end.

3.1 Introduction to variance swap

In this section, we first introduce the payoff function and the pricing formula for variance swap. Based on the form of the formula, we then describe a theoretical approach for obtaining the first two moments of the risk-neutral distribution. At last, we describe how we estimate the first moment of the risk-neutral distribution from real data.

Payoff function

The payoff of a variance swap is defined as the variance notional N_{var} multiplies by the difference between annualised realised variance $\sigma^2_{realised}$ and variance strike σ^2_{strike}, which is given by (see, for example, https://en.wikipedia.org/wiki/Variance swap)

$$N_{var}(\sigma^2_{realised} - \sigma^2_{strike}) \tag{3.1}$$

Variance notional and variance strike are usually given before the sale of a variance swap contract. Variance notional is referred as the profit/loss of the variance swap due to one unit change of realised variance or strike variance. The annualised realised variance is defined as

$$\sigma^2_{realised} = \frac{A}{n} \sum_{i=1}^{n} R_i^2 \tag{3.2}$$

where A is the number of trading days per year, which on average is 252. Here n denotes the total number of trading days during the observational period and R_i represents the ith daily return. Denote $S_0, S_1, S_2, ..., S_n$ be the closing prices of the underlying asset in the observational period with $n+1$ trading days, and then $R_i = log(S_i/S_{i-1})$, for $i = 1, \ldots, n$.

Under the assumption of no arbitrage, let K be the strike price, and $\{S_t\}$, $t \in [0, T]$, where T is the expiration time, be the current price of the underlying asset. One can denote the corresponding daily log return $R_i = log(S_i/S_{i-1})$, for $i = 1, \ldots, T$. We express the market prices of European call options and put options written on the underlying asset at time t with expiration date $t+n$ (here $t+n \leq T$) as $C_{t,n;K}$ and $P_{t,n;K}$. We also denote r_t be the risk-free interest rate for period $[t, t+1]$, which is obtained from risk-free zero coupon bond, and $R_{t,T} = \sum_t^{T-1} r_t$ be the cumulative risk-free interest rate from t to T.

Assuming the stock price follows martingale, the fair price of a variance swap is the discounted expected payoff under the risk-neutral measure $\mathbb{Q}$. We denote the price of variance swap at time t with expiration T by $VS_{t,T}$, given by

$$\begin{aligned} VS_{t,T} &= \mathbb{E}_t^{\mathbb{Q}}\{e^{-R_{t,T}} \times \text{payoff}\} \\ &= \mathbb{E}_t^{\mathbb{Q}}\{e^{-R_{t,T}} N_{var}(\sigma^2_{realised} - \sigma^2_{strike})\} \\ &= e^{-R_{t,T}} N_{var}\{\mathbb{E}_t^{\mathbb{Q}}(\sigma^2_{realised}) - \sigma^2_{strike}\} \\ &= e^{-R_{t,T}} N_{var}\{\mathbb{E}_t^{\mathbb{Q}}(\frac{A}{T}\sum_{i=1}^{T} R_i^2) - \sigma^2_{strike}\} \end{aligned} \tag{3.3}$$

To proceed, we describe the assumptions required in our method and derive the corresponding pricing formula for variance swap in the next section.

3.2 Data preparation

In this section, we start with the details how we interpolate risk-free interest rates for our study, followed by the assumptions needed in our analysis. We then illustrate the replication strategy by variance future for variance swap valuation. We also present the full data preparation process afterwards.

3.2.1 Formula and interest rates

In Equation (3.3), N_{var} and σ^2_{strike} are known values. We begin with the estimation of the cumulative risk-free interest rate $R_{t,T} = \sum_t^{T-1} r_t$. In our data, for each calendar day, the cumulative risk-free interest rates are given in the discrete time points, shown in Figure 17. The days difference provided in the original data set may not cover the time to expirations of

date	days	rate
19960102	9	0.05763067
19960102	15	0.05745902
19960102	50	0.05673317
19960102	78	0.05608884
19960102	169	0.05473762

Figure 17: Illustration of original risk-free interest rates

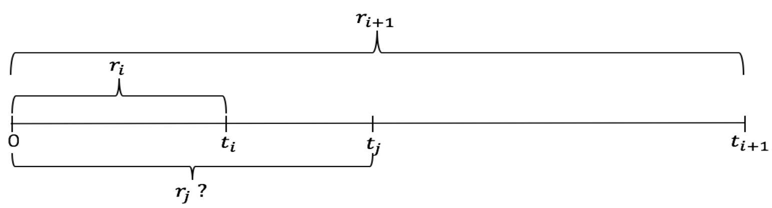

Figure 18: Illustration of interest rate interpolation

the available options. We, therefore, employ an interpolation method to derive the cumulative risk-free interest rates needed in the pricing formula for variance swap.

To interpolate a cumulative risk-free interest rate, we utilize the two adjacent cumulative interest rates. Denote $[0, t_i]$ be the shorter period of days to maturity, $[0, t_{i+1}]$ be the longer period of days to maturity. Let r_i denote the cumulative risk-free interest rate for period $[0, t_i]$, and r_{i+1} be the interest rate for $[0, t_{i+1}]$. Assume $t_j \in [t_i, t_{i+1}]$ and $r_{[i,i+1]}$ presents the unit risk-free interest rate in period $[t_i, t_{i+1}]$. The interpolation idea is shown in Figure 18.

To interpolate interest rate r_j, the first equation is:

$$
\begin{aligned}
& e^{r_i \times \frac{t_i}{365}} \; e^{r_{[i,i+1]} \times \frac{t_{i+1}-t_i}{365}} = e^{r_{i+1} \times \frac{t_{i+1}}{365}} \\
& r_{[i,i+1]} = \frac{r_{i+1}t_{i+1} - r_i t_i}{t_{i+1} - t_i}
\end{aligned}
\tag{3.4}
$$

The second equation to calculate annualized daily interest rate r_j is:

$$
\begin{aligned}
& e^{r_i \times \frac{t_i}{365}} \; e^{r_{[i,i+1]} \times \frac{t_j-t_i}{365}} = e^{r_j \times \frac{t_j}{365}} \\
& r_j = \frac{r_i t_i + r_{[i,i+1]}(t_j - t_i)}{t_j}
\end{aligned}
\tag{3.5}
$$

In the second equation, we use the fact that the unit risk-free interest rate within time period $[r_i, r_{i+1}]$ is the same as the unit rate in time period $[r_i, r_j]$. Combine Equation (3.4) and Equation (3.5), we get $r_j = \{r_i t_i + [(r_{i+1}t_{i+1} - r_i t_i)/(t_{i+1} - t_i)] \times (t_j - t_i)\}/t_j \; for \; t_j \in [t_i, t_{i+1}]$, where $i = 0, 1, 2, \ldots, n-1$. Here t_0 is the start date for an option and t_n is the longest expiration date for options with the same start date. This formula solves one of the unknown quantities we have in Equation (3.3).

We then estimate $\mathbb{E}_t^{\mathbb{Q}}(\frac{A}{T}\sum_{i=1}^{T} R_i^2)$. Note that $\mathbb{E}_t^{\mathbb{Q}}[\sum_{i=1}^{T} R_i^2] = \sum_{i=1}^{t} R_i^2 + \sum_{i=t+1}^{T} \mathbb{E}_t^{\mathbb{Q}}[R_i^2]$. The key part

$$\begin{aligned}\sum_{i=t+1}^{T} \mathbb{E}_t^{\mathbb{Q}}[R_i^2] &= \sum_{i=t+1}^{T} \mathbb{E}_t^{\mathbb{Q}}[log\frac{S_i}{S_{i-1}}]^2 = \sum_{i=t+1}^{T} [\mathbb{E}_t^{\mathbb{Q}}(logS_i)^2 + \mathbb{E}_t^{\mathbb{Q}}(logS_{i-1})^2 - 2\mathbb{E}_t^{\mathbb{Q}}(logS_i)(logS_{i-1})] \\ &= \sum_{i=t+1}^{T} \mathbb{E}_t^{\mathbb{Q}}(logS_i)^2 + \sum_{i=t+1}^{T} \mathbb{E}_t^{\mathbb{Q}}(logS_{i-1})^2 - 2\sum_{i=t+1}^{T} \mathbb{E}_t^{\mathbb{Q}}(logS_i)(logS_{i-1}) \\ &= \sum_{i=t+1}^{T} \mathbb{E}_t^{\mathbb{Q}}(logS_i)^2 + \sum_{i=t+1}^{T} \mathbb{E}_t^{\mathbb{Q}}(logS_{i-1})^2 - 2\sum_{i=t+1}^{T} \mathbb{E}_t^{\mathbb{Q}}[logS_{i-1} + log(\frac{S_i}{S_{i-1}})][logS_{i-1}] \\ &= \sum_{i=t+1}^{T} \mathbb{E}_t^{\mathbb{Q}}(logS_i)^2 + \sum_{i=t+1}^{T} \mathbb{E}_t^{\mathbb{Q}}(logS_{i-1})^2 - 2\sum_{i=t+1}^{T} \mathbb{E}_t^{\mathbb{Q}}(logS_{i-1})^2 \\ &\quad - 2\sum_{i=t+1}^{T} \mathbb{E}_t^{\mathbb{Q}}[logS_{i-1}][log(\frac{S_i}{S_{i-1}})] \\ &= \mathbb{E}_t^{\mathbb{Q}}[logS_T]^2 - [logS_t]^2 - 2\sum_{i=t+1}^{T} \mathbb{E}_t^{\mathbb{Q}}[logS_{i-1}][log(\frac{S_i}{S_{i-1}})]\end{aligned} \tag{3.6}$$

To proceed, there are two assumptions we adopt on the Stock Price Process in order to evaluate variance swaps

1. No arbitrage in the financial market to ensure existence of risk-neutral density
2. Increments of the process $logS_t$ are independent, that is:

$$logS_t \perp\!\!\!\perp log\frac{S_{t+1}}{S_t}$$

The first assumption is necessary when we estimate the fair price of any derivative in the financial market. Applying the independent assumption, we have

$$\begin{aligned}\text{Equation (3.6)} &= \mathbb{E}_t^{\mathbb{Q}}[logS_T]^2 - [logS_t]^2 - 2\sum_{i=t+1}^{T}\mathbb{E}_t^{\mathbb{Q}}[logS_{i-1}]\mathbb{E}_t^{\mathbb{Q}}[log(\frac{S_i}{S_{i-1}})] \\ &= \mathbb{E}_t^{\mathbb{Q}}[logS_T]^2 - [logS_t]^2 - 2\sum_{i=t+1}^{T}\mathbb{E}_t^{\mathbb{Q}}[logS_{i-1}][\mathbb{E}_t^{\mathbb{Q}}logS_i - \mathbb{E}_t^{\mathbb{Q}}logS_{i-1}] \qquad (3.7) \\ &= \mathbb{E}_t^{\mathbb{Q}}[logS_T]^2 - [logS_t]^2 - 2\sum_{i=t+1}^{T}[\mathbb{E}_t^{\mathbb{Q}}logS_{i-1}\mathbb{E}_t^{\mathbb{Q}}logS_i - (\mathbb{E}_t^{\mathbb{Q}}logS_{i-1})^2]\end{aligned}$$

Here $[logS_t]^2$ is the function of the current price of the underlying asset. In Section 3.3, we estimate all the first and second moments in Equation (3.7) for evaluating the fair price of variance swap.

3.2.2 Replicating by variance futures

In this part, we introduce variance future and how we replicate variance swap using variance future. Variance future is another financial contract that is an over-the-counter variance trade. As stated by Biscamp and Weithers (2007) (9), variance swap and variance future are essentially the same in the sense that they both trade the difference of variance, yet providing more advantages from trading contracts. So one can replicate variance swap by variance future. Variance future products with 12-month(with futures symbol VA) or 3-month(with futures symbol VT) expirations are traded on the CBOE Futures Exchange (see, for example, http://cfe.cboe.com/products/products_va.asp). We use VA in our analysis.

We downloaded variance future data from CBOE website. If variance futures and variance swap share the same expiration date, then at the start point of the observation period, there is no difference between trading a variance future and trading a variance swap with \$50 variance notional. Once we enter the the observation period, there is a ratio multiplier for variance notional taking account for the number of past trading days.

$$\text{Variance Notional of Future} = 50 \times \frac{N_e - M}{N_e - 1} \tag{3.8}$$

where M is the number of observed days to date. Here N_a is the actual number of trading days and N_e is the expected number of trading days in the observation period. They are the same for most of the time. An example of an exception was on June 11, 2004, most of US markets were closed to mourn for former president Ronald Reagan. When this happens, N_a would be one day less while N_e stays the same.

For variance futures, the final realised variance RUG is defined similarly to that of variance swap, by measuring the variance from the time of initial listing until expiration of the contract

$$RUG = 252 \times (\sum_{i=1}^{N_a - 1} R_i^2/(N_e - 1)) \times 100^2 \tag{3.9}$$

In the pricing formula Equation (3.3) for variance swap

$$\begin{aligned} VS_{t,T} &= e^{-R_{t,T}} N_{var} \{\mathbb{E}_t^{\mathbb{Q}}(\frac{A}{T} \sum_{i=1}^{T} R_i^2) - \sigma_{strike}^2\} \\ &= e^{-R_{t,T}} N_{var} \{\frac{A}{T}[\sum_{i=1}^{M-1} R_i^2 + \mathbb{E}_t^{\mathbb{Q}}(\sum_{i=M}^{N_e} R_i^2)] - \sigma_{strike}^2\} \end{aligned} \tag{3.10}$$

Where $\sum_{i=1}^{M-1} R_i^2 = \sum_{i=1}^{M-1}(log(S_i/S_{i-1}))^2$ is solved using previous market prices of the underlying asset. We employ the similar formulation of calculating RUG for IUG, which is the square of market implied volatility (implied volatility is represented by the settlement price in the data), by

$$IUG = \sum_{i=M}^{N_e} R_i^2 \times \frac{A}{N_e - M + 1} \times 100^2 \tag{3.11}$$

We then have

$$\mathbb{E}_t^{\mathbb{Q}}(\sum_{i=M}^{N_e} R_i^2) = IUG \times \frac{N_e - M + 1}{A} \times \frac{1}{100^2} \tag{3.12}$$

After plugging into the formula, we derive the historical prices of variance swaps from variance futures.

3.2.3 Data information and manipulation

In this part, we illustrate in details how we process and prepare the data for our study. Our data contains standard European options on the S&P 500 index, which are exercised on the third Saturday of the expiration month. Since there is no trade data on Saturday to calculate return, we treat the previous Friday to be the expiration date.

Option data we used in the first two chapters covers from 12/10/2012 to 08/31/2015. The continuously compounded risk-free interest rate we have is from 01/02/1996 to 08/31/2015. While for variance future, the trade date is from 12/10/2012 to 08/31/2015, start date from 12/21/2010 to 07/30/2015 and end date from 01/18/2013 to 01/01/2016. Option and interest rate data are downloaded from Wharton Research Data Services while variance future data are downloaded from CBOE website.

Since we are using variance future to replicate variance swap, the date ranges for variance swap are determined by those of variance future. We illustrate the data manipulation for variance future first.

Variance future preparation

(I) Download daily VF files

We batch record the addresses and download the 771 daily files corresponding to variance futures with 12-month expirations from CBOE website (see, for example, http://cfe.cboe.com/products/vacdata.aspx) for our analysis. Each file contains multiple daily variance contract data, with an example shown in Figure 19. The first row saves the expiration dates corresponded to the inception dates (same as start dates) that in the second row. The strikes for the contracts are listed in the third row. How we manipulate the excel files when we read them in [R] interface and get needed information are presented in details.

1. The sheet name of those files are either "VA contract" or simply "1". We take special care of the sheet names when we use "[R]: read.xlsx" to load the files.
2. The date formats for some of the files are in the form of "date" class like "2014-08-18" while for others are in the form of "character" class like "06/21/15". We reformat the all the dates into "date" class.
3. For the trading date of the contract, we extract the date contained in the name of each daily file and replicate it to the same length as the number of pairs of start and expiration

dates in the file. We reorder the dates with the start date, trading date and expiration date into a new file containing such information.

(II) Download VF files for each expiration date

The variance future files are saved in small files according to different expiration months. Similarly to what we did to the daily files, we also batch record and download the 46 12-month S&P 500 variance future files from CBOE website (see, for example, http://cfe.cboe.com/data/historicaldata.aspx#VA), as shown in Figure 20. How we process and summarize the information from the files is explained here.

1. The file names are in the similar form as of "CFE_G14_VA.csv", where "VA" stands for the 12-month variance futures and "14" represents the year of the expiration date for variance futures. Here "G" is the monthly code for variance futures with a full list of codes here: F (January), G (February), H (March), J (April), K (May), M (June), N (July), Q (August), U (September), V (October), X (November), Z (December) (see, for example, http://cfe.cboe.com/tradecfe/ticker_va.aspx). To be consistent with the market default rule, we use the third Friday of the expiration month to be the expiration date for the contract. Further, for the ease of calculation in the following stage, the dates in column "Futures" are all transferred to "year-month-day" format.

2. The columns we keep in the VF files are "Trade Date", "Futures" and "Settle".

	18-Jan-13	15-Feb-13	15-Mar-13	21-Jun-13	20-Sep-13	20-Dec-13	20-Jun-14	19-Dec-14
Inception Date (SPX option listing)	20-Aug-12	22-Oct-12	19-Mar-12	20-Jun-11	24-Sep-12	21-Dec-10	18-Jun-12	19-Dec-11
Realized Variance to date	51.128405	31.704805	140.482227	630.861121	41.290595	704.895141	87.939914	174.504976
Number of expected Prices (Ne)	106	81	251	507	251	758	507	758
Number of returns elapsed	92	48	199	387	68	511	136	260
Previous settlement value	777.2521	890.4297	732.6829	824.0314	817.2345	685.2698	804.0177	742.8556
Discount Factor	0.99992186	0.99980206	0.99968728	0.99934128	0.99901000	0.99866808	0.99799628	0.99667820
Initial Strike (K0)	396.41	353.44	484.88	587.58	561.69	707.56	655.87	721.46
ARVM	-0.023819	-0.010661	-0.028324	-0.018449	-0.01823	-0.033167	-0.021007	-0.027537
Fed Funds Rate	0.0017							

Figure 19: Example of variance future contract daily file.

Trade Date	Futures	Open	High	Low	Close	Settle	Change	Total Volume	EFP	Open Interest
10/21/13	G (Feb 14)	0	0	0	0	15.5	15.5	0	0	0
10/22/13	G (Feb 14)	0	0	0	0	15.65	0.15	0	0	0
10/23/13	G (Feb 14)	0	0	0	0	15.65	0	0	0	0
10/24/13	G (Feb 14)	0	0	0	0	15.4	-0.25	0	0	0
10/25/13	G (Feb 14)	0	0	0	0	15.4	0	0	0	0
10/28/13	G (Feb 14)	0	0	0	0	15.6	0.2	0	0	0
10/29/13	G (Feb 14)	0	0	0	0	15.65	0.05	0	0	0
10/30/13	G (Feb 14)	0	0	0	0	15.85	0.2	0	0	0
10/31/13	G (Feb 14)	0	0	0	0	15.95	0.1	0	0	0
11/1/13	G (Feb 14)	0	0	0	0	15.9	-0.05	0	0	0
11/4/13	G (Feb 14)	0	0	0	0	15.5	-0.4	0	0	0
11/5/13	G (Feb 14)	0	0	0	0	15.65	0.15	0	0	0
11/6/13	G (Feb 14)	0	0	0	0	15.4	-0.25	0	0	0
11/7/13	G (Feb 14)	0	0	0	0	15.8	0.4	0	0	0

Figure 20: Example of variance future contract file.

(III) Data cleaning and modification

After we download and extract the information needed from the variance future files, we clean the data for our study.

1. There are 9 records that have start date same with the expiration date. It is intuitive that the neighborhood of the error records should share the same start and expiration date information. We correct the records accordingly.
2. The trading dates of the variance futures we keep are no later than "2015-12-31". Any contract that have trading dates and expiration dates later than "2016-01-01" are deleted from the data.
3. There are 3 records that have start dates later than the trading dates, which are dropped directly.

(IV) Data integration

After we extract and clean the data from daily files and variance future files, we combine the information together in the order of start date, trading date, expiration date, settlement prices and strike prices. There are some issues in the process as mentioned below.

1. One of the expiration dates in VF file is "2014-04-18" which is a Friday. While in the daily files, there is no such end date and only "2014-04-17" is available. Be subject to VF files, we make adjustments accordingly for daily files.
2. We calculate M and N_e, which stands for the number of observed days to date $t - t_0$ and the expected trading days in the observation period $T - t_0$. When the end date is

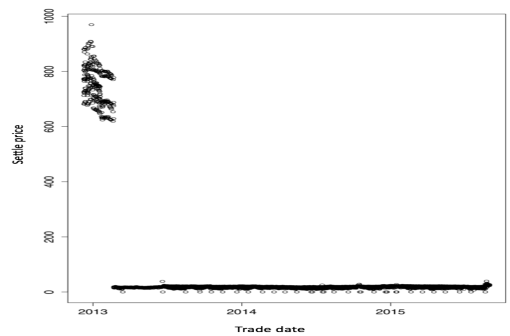

Figure 21: Check of settlement prices of variance futures.

"2014-04-18", it is not a trading day and therefore, no market price for underlying asset. We manually add this date and the market price of the underlying asset with values the same of the previous day.

3. The settlement price, which represents the market implied volatility, indicates the market's expectation for future prices. Evidenced from CBOE website (see, for example, http://cfe.cboe.com/Data/Settlement.aspx), the magnitude of settlement is around 20. However, there are some settlements in the file that are over 100. We check the settlement price in Figure 21, which explains some inconsistency. After further investigation, the values of settlement prices that are larger than 100 are divided by 32 as duotricemary notation for our analysis.

Prepare options

Options are used to estimate the moments of the risk-neutral density for pricing variance swaps. We compare the fair prices of variance swaps with the market historical prices from replicating variance futures. The options are filtered and those with the same starting dates for variance futures stay. The dates are from 2012-12-10 to 2015-08-31.

1. Options traded before 02/15/2015 are expired on the third Saturday of the expiration month, and those traded after 02/15/2015 are expired on the third Friday of the expiration month. As we mentioned earlier, there is no trading information from Saturday. We set the expiration dates for all the options be the third Friday of the expiration month.
2. There is no trading price available in the option data. We take the average of bid and offer prices as the trading price of the options.
3. There are in total of 686 trading dates in option data. For each of the trading dates, we locate how many expiration dates are corresponded. Afterwards, we calculate the calendar difference between every expiration date and trading date and save for our study.

To calculate the trading days between given start date and expiration date, we download a date set with S&P500 historical trading prices and simply count the difference of row numbers between the two dates. In this way, we accurately exclude all the holidays and non-trading days.

3.3 Estimating moments of the risk-neutral density

We present two methods to estimate the moments of the risk-neutral density for pricing variance swap, used in Equation (3.3). One is called moment-based method following Bakshi, Kapadia and Madan(2003). The other method is based on our proposed nonparametric approach to first estimate the risk-neutral density and calculate the moments accordingly. We start with the moment-based method.

3.3.1 Moment-based method

As was shown in Equation (3.3), the pricing formula of variance swap, the first and second moments are needed for evaluating the fair price. In this section, we illustrate how to estimate the available moments and further how to interpolate moments needed in the evaluation.

In traditional financial markets, the normal distribution is often used to model the risk-neutral density of log returns. Nowadays, people recognize that normal distribution performs bad in the sense that it doesn't possess semi-heavy tail or asymmetry in the actual risk-neutral density. We then introduce a more realistic modeling for the financial market based on generalized hyperbolic(GH) family of distributions. In the literature, Ghysels and Wang (2014) (37) used the GH family to model the risk-neutral density of conditional log return of the underlying asset. Following the approach of Bakshi, Kapadia and Madan (2003) (6), the risk-neutral moments can be written in terms of the volatility contract $V_{t,n}$, cubic contract $W_{t,n}$, and quartic contract $X_{t,n}$, which are estimated by portfolios of OTM call and put option prices respectively.

$$\begin{aligned} V_{t,n} &= \mathbb{E}_t^{\mathbb{Q}}(e^{-R_{t,n}} R_t^2(n)) \\ &= \int_{S_t}^{\infty} \frac{2(1 - ln(K/S_t))}{K^2} C_{t,n;K} dK \\ &\quad + \int_0^{S_t} \frac{2(1 - ln(K/S_t))}{K^2} P_{t,n;K} dK \end{aligned} \tag{3.13}$$

$$\begin{aligned} W_{t,n} &= \mathbb{E}_t^{\mathbb{Q}}(e^{-R_{t,n}} R_t^3(n)) \\ &= \int_{S_t}^{\infty} \frac{6ln(K/S_t) - 3(ln(K/S_t))^2}{K^2} C_{t,n;K} dK \\ &\quad + \int_0^{S_t} \frac{6ln(K/S_t) - 3(ln(K/S_t))^2}{K^2} P_{t,n;K} dK \end{aligned} \tag{3.14}$$

$$X_{t,n} = \mathbb{E}_t^{\mathbb{Q}}(e^{-R_{t,n}} R_t^4(n))$$
$$= \int_{S_t}^{\infty} \frac{12(ln(K/S_t))^2 - 4(ln(K/S_t))^3}{K^2} C_{t,n;K} dK \tag{3.15}$$
$$+ \int_0^{S_t} \frac{12(ln(K/S_t))^2 - 4(ln(K/S_t))^3}{K^2} P_{t,n;K} dK$$

Where $R_t(n) = log(S_{t+n}/S_t)$. Therefore, the conditional mean of $log(S_{t+n})$ is

$$\begin{aligned} Mean_{t,n} &= \mu_{t,n} + log(S_t) \\ Var(t,n) &= e^{R_{t,n}} V_{t,n} - \mu_{t,n}^2 \end{aligned} \tag{3.16}$$

Where $\mu_{t,n} = \mathbb{E}_t^{\mathbb{Q}} R_t(n) = \mathbb{E}_t^{\mathbb{Q}} log(S_{t+n}/S_t)$. By the martingale property, we have $\mathbb{E}_t^{\mathbb{Q}}(e^{-R_{t,n}} S_{t+n}) = S_t$, $t+n \in [t,T]$, where $R_{t,n}$ represents the cumulative risk-free interest rate for period $[t, t+n]$ and $e^{R_{t,n}}$ is a constant for fixed t and n. Here S_t is the current market price of the underlying asset. We rewrite the martingale property by $e^{R_{t,n}} = \mathbb{E}_t^{\mathbb{Q}}[S_{t+n}/S_t] = \mathbb{E}_t^{\mathbb{Q}}[S_{t+n}/S_t] = \mathbb{E}_t^{\mathbb{Q}} e^{R_t(n)}$. By Taylor Expansion for exponential function $e^x \approx 1 + x + x^2/2! + x^3/3! + x^4/4!$, we have

$$\mathbb{E}_t^{\mathbb{Q}} e^{R_t(n)} \approx \mathbb{E}_t^{\mathbb{Q}}[1 + R_t(n) + R_t^2(n)/2 + R_t^3(n)/6 + R_t^4(n)/24] \tag{3.17}$$

That is

$$\begin{aligned} e^{R_{t,n}} &= 1 + \mathbb{E}_t^{\mathbb{Q}} R_t(n) + \mathbb{E}_t^{\mathbb{Q}} R_t^2(n)/2 + \mathbb{E}_t^{\mathbb{Q}} R_t^3(n)/6 + \mathbb{E}_t^{\mathbb{Q}} R_t^4(n)/24 \\ &= 1 + \mu_{t,n} + e^{R_{t,n}} V_{t,n}/2 + e^{R_{t,n}} W_{t,n}/6 + e^{R_{t,n}} X_{t,n}/24 \end{aligned} \tag{3.18}$$

Move $\mu_{t,n}$ to the left and get

$$\mu_{t,n} = e^{R_{t,n}} - 1 - e^{R_{t,n}} V_{t,n}/2 - e^{R_{t,n}} W_{t,n}/6 - e^{R_{t,n}} X_{t,n}/24 \tag{3.19}$$

We then plug the Equation (3.19) into Equation (3.16) and calculate the moments.

3.3.2 Nonparametric approach

In the previous part, we calculate the moments for pricing variance swap using moment-based method. Next, we calculate the moments by our proposed nonparametric approach illustrated in Chapter 2. In Chapter 2, we first use OTM options to estimate the risk-neutral density. The main reason is to check the power of our prediction by using OTM options as a training data and ITM options as a testing data. The performance comparison is conducted by cross validation study. Another reason to start with OTM options comes from the moment-based method. We mentioned in previous part that following Bakshi, Kapadia and Madan (2003) (6), the three volatility contract, cubic contract and quartic contract are estimated by using OTM options. In this part, we instead, use all the available options to estimate the risk-neutral density and calculate moments, offering more information in the pricing process. Further, we estimate the risk-neutral densities from both least square and weighted least square structures.

Based on our nonparametric approach in estimating RND, we have the density of $log(S_T)$ in the form of $f_Q(x) = \sum_{i=1}^{q+1} a_i \mathbb{1}_{[logK_{i-1}, logK_i]}(x)$, where a_i is the piece-wise constant value on interval $[logK_{i-1}, logK_i]$, with q is the number of unique strikes for all the options in (t, T) and $K_0 = log(K_1/c_1)$ and $K_{q+1} = log(K_q \times c_2)$.

According to Equation (3.7), the key part of the payoff function of variance swaps is $\mathbb{E}_t^{\mathbb{Q}}[logS_T]^2 - [logS_t]^2 - 2\sum_{i=t+1}^{T}[\mathbb{E}_t^{\mathbb{Q}}logS_{i-1}\mathbb{E}_t^{\mathbb{Q}}logS_i - (\mathbb{E}_t^{\mathbb{Q}}logS_{i-1})^2]$. We calculate the first and second moments for evaluating the fair price of variance swap.

Since on each interval of the estimated risk-neutral density, it is a uniform distribution. Recall for $X \sim Unif(a, b)$, we have $f_X(x) = 1/(b-a)$ and $\mathbb{E}(X) = \int_a^b x1/(b-a)dx = 1/(b-a)x^2/2|_a^b = (b^2-a^2)/2(b-a)$. Therefore, for $X = log(S_T)$,

$$\begin{aligned}
\mathbb{E}_t^{\mathbb{Q}}(X) &= \int_{-\infty}^{\infty} xf(x)dx \\
&= \int_{logK_0}^{logK_{q+1}} x\sum_{i=1}^{q+1} a_i \mathbb{1}_{[logK_{i-1}, logK_i]}(x)dx \\
&= \sum_{i=1}^{q+1} a_i \int_{logK_{i-1}}^{logK_i} xdx \\
&= \sum_{i=1}^{q+1} a_i \frac{1}{2}[(logK_i)^2 - (logK_{i-1})^2]
\end{aligned} \tag{3.20}$$

$$\begin{aligned}
\mathbb{E}_t^{\mathbb{Q}}(X^2) &= \int_{-\infty}^{\infty} x^2 f(x)dx \\
&= \int_{logK_0}^{logK_{q+1}} x^2\sum_{i=1}^{q+1} a_i \mathbb{1}_{[logK_{i-1}, logK_i]}(x)dx \\
&= \sum_{i=1}^{q+1} a_i \int_{logK_{i-1}}^{logK_i} x^2dx \\
&= \sum_{i=1}^{q+1} a_i \frac{1}{3}[(logK_i)^3 - (logK_{i-1})^3]
\end{aligned} \tag{3.21}$$

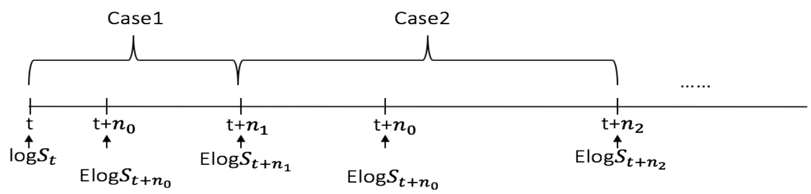

Figure 22: Illustration of mean interpolcation

We calculate the first and second moments at all available expiration dates for each start date t and the moments from both moment-based method and our nonparametric approach are pretty close. We then perform interpolations for mean and variance shown in next part.

Mean Imputation

We first illustrate the imputation idea used in calculating the first moment of the conditional log return. We have calculated means at all available expiration dates for each t . Imputation method is implemented to find all other mean values at each time point from trading date t to expiration date T. Denote all the expiration dates by $t + n_1, t + n_2, \ldots,$ as partially shown in Figure 22. The time point to be imputed is denoted by $t + n_0$. Since all the information at time t is available, $logS_t$ can be viewed as the expectation at time t, $\mathbb{E}_t^{\mathbb{Q}} logS_t$. Therefore, we separate into cases according to whether $t + n_0$ is in the interval $[t, t + n_1]$ or not. It is assumed that the log return is the same for each day.

1. **Case 1**: For $n_0 \in [0, n_1]$, , say, the mean value $\mathbb{E}_t^{\mathbb{Q}}(logS_{t+n_1})$ has been calculated.

$$\mathbb{E}_t^{\mathbb{Q}}(logS_{t+n_1}) - \mathbb{E}_t^{\mathbb{Q}}(logS_{t+n_0}) = \frac{(n_1 - n_0)[\mathbb{E}_t^{\mathbb{Q}}(logS_{t+n_1}) - logS_t]}{n_1} \tag{3.22}$$

   So:

$$\begin{aligned}\mathbb{E}_t^{\mathbb{Q}}(logS_{t+n_0}) &= \mathbb{E}_t^{\mathbb{Q}}(logS_{t+n_1}) - \frac{(n_1 - n_0)[\mathbb{E}_t^{\mathbb{Q}}(logS_{t+n_1}) - logS_t]}{n_1} \\ &= \frac{n_0\mathbb{E}_t^{\mathbb{Q}}(logS_{t+n_1}) + (n_1 - n_0)log(S_t)}{n_1}\end{aligned} \tag{3.23}$$

2. **Case 2**: For $n_0 \in [n_i, n_{i+1}]$, $i = 1, 2, \ldots$, say, the mean values $\mathbb{E}_t^{\mathbb{Q}}(logS_{t+n_i})$ and $\mathbb{E}_t^{\mathbb{Q}}(logS_{t+n_{i+1}})$ have already been calculated.

$$\begin{aligned}\mathbb{E}_t^{\mathbb{Q}}(logS_{t+n_0}) - logS_t &= \mathbb{E}_t^{\mathbb{Q}}(logS_{t+n_0}) - \mathbb{E}_t^{\mathbb{Q}}(logS_{t+n_i}) + \mathbb{E}_t^{\mathbb{Q}}(logS_{t+n_i}) - logS_t \\ &= \frac{(n_0 - n_i)[\mathbb{E}_t^{\mathbb{Q}}(logS_{t+n_{i+1}}) - \mathbb{E}_t^{\mathbb{Q}}(logS_{t+n_i})]}{n_{i+1} - n_i} + \mathbb{E}_t^{\mathbb{Q}}logS_{t+n_i} - logS_t\end{aligned} \tag{3.24}$$

   Cancelling out $logS_t$ on both sides, we have

$$\begin{aligned}\mathbb{E}_t^{\mathbb{Q}}(logS_{t+n_0}) &= \frac{(n_0 - n_i)[\mathbb{E}_t^{\mathbb{Q}}(logS_{t+n_{i+1}}) - \mathbb{E}_t^{\mathbb{Q}}(logS_{t+n_i})]}{n_{i+1} - n_i} + \mathbb{E}_t^{\mathbb{Q}}(logS_{t+n_i}) \\ &= \frac{(n_0 - n_i)\mathbb{E}_t^{\mathbb{Q}}(logS_{t+n_{i+1}}) + (n_{i+1} - n_0)\mathbb{E}_t^{\mathbb{Q}}(logS_{t+n_i})}{n_{i+1} - n_i}\end{aligned} \tag{3.25}$$

Variance Imputation

To calculate the variance at T of the log returns for pricing variance swaps, a similar interpolation is performed with the available variances of log returns for option data, which are traded at t and expired at time other than T. Based on the scatterplot of all available variances we have from the existing contracts, the trend of variances has a curved pattern. More specifically, it follows a quadratic curve. To implement the linear interpolation, a square-root transformation of variances is operated before interpolation. Then the interpolation is performed.

1. **Case 1**: For $n_0 \in [0, n_1]$, the values $\mathbb{V}_t^{\mathbb{Q}}(logS_{t+n_1})$ and $\sqrt{\mathbb{V}_t^{\mathbb{Q}}(logS_{t+n_1})}$ have been calculated.

$$\sqrt{\mathbb{V}_t^{\mathbb{Q}}(logS_{t+n_0})} = \frac{n_0\sqrt{\mathbb{V}_t^{\mathbb{Q}}(logS_{t+n_1})}}{n_1} \tag{3.26}$$

2. **Case 2**: For $n_0 \in [n_i, n_{i+1}]$, $i = 1, 2, \ldots$, the square-root values $\sqrt{\mathbb{V}_t^{\mathbb{Q}}(logS_{t+n_i})}$ and $\sqrt{\mathbb{V}_t^{\mathbb{Q}}(logS_{t+n_{i+1}})}$ have been calculated.

$$\begin{aligned}
\sqrt{\mathbb{V}_t^{\mathbb{Q}}(logS_{t+n_0})} &= \sqrt{\mathbb{V}_t^{\mathbb{Q}}(logS_{t+n_0})} - \sqrt{\mathbb{V}_t^{\mathbb{Q}}(logS_{t+n_i})} + \sqrt{\mathbb{V}_t^{\mathbb{Q}}(logS_{t+n_i})} \\
&= \frac{(n_0 - n_i)[\sqrt{\mathbb{V}_t^{\mathbb{Q}}(logS_{t+n_{i+1}})} - \sqrt{\mathbb{V}_t^{\mathbb{Q}}(logS_{t+n_i})}]}{n_{i+1} - n_i} + \sqrt{\mathbb{V}_t^{\mathbb{Q}}(logS_{t+n_i})} \\
&= \frac{(n_0 - n_i)\sqrt{\mathbb{V}_t^{\mathbb{Q}}(logS_{t+n_{i+1}})} + (n_{i+1} - n_0)\sqrt{\mathbb{V}_t^{\mathbb{Q}}(logS_{t+n_i})}}{n_{i+1} - n_i}
\end{aligned} \tag{3.27}$$

Any variance can be derived from the squared of interpolated square-root variance. After we have all the mean values and variance values at each time point, the second moment values are derived by $\mathbb{E}_t^{\mathbb{Q}}(logS_{t+n_0})^2 = [\mathbb{E}_t^{\mathbb{Q}}(logS_{t+n_0})]^2 + \mathbb{V}_t^{\mathbb{Q}}(logS_{t+n_0})$. Everything in the pricing formula (3.3) has been figured out. As we mentioned earlier, the estimated results for moments from moment-based method and our nonparametric approach are similar. We compare and calibrate our results in the next section using moments from our nonparametric approach for illustration.

3.4 Calibration results and comparisons

We now have all the moments of log returns needed for evaluating variance swap from options. We also have the market historical prices replicated from variance futures to calibrate. In addition, since the variance swaps to evaluate have already been exercised and the most important part in the price formula Equation (3.3) is the summation of log returns, we can evaluate the log returns by directly adding up the ratios of adjacent observed market prices of the underlying asset within the period to further check our results. That is, to estimate the realized variance part of the price formula $\mathbb{E}_t^{\mathbb{Q}}(\sigma^2_{realised})$ for variance swap, we have three ways to derive the quantity.

1. Method 1 (OP): Moment-based method or our nonparametric approach: use option data to calculate the moments, as our fair prices of variance swaps
2. Method 2 (VF): Calibration method: use CBOE traded variance future to replicate the historical market prices of variance swaps
3. Method 3 (True): Use the true observed market prices of the underlying asset of S&P 500 to calculate the "True" realized variance of corresponding period by taking summation of squares of log returns to provide further reference

It is clearer to use ratios to present the results. There are three ratio quantities that of interest: OP/True, VF/True, and OP/VF. We plot those quantities with x axis to be the remaining calendar days of each contract, see Figure 23(a), Figure 23(b) and Figure 23(c).

Comparison results

For the ratio OP/True, with respect to the remaining calendar days in the contract in Figure 23(a), our results indicates that our method using options performs well when the remaining days of the contract are more than 365 days. A reasonable guess for this phenomenon is that long-term option data are more reasonable and stable, which are less likely to be affected by the external factors or noises. However, there is an apparent exponential curve when the remaining days of the contract is greater than 365. The market also follows the same trend when we look at the ratio graph of VF and True in Figure 23(b). That indicates that neither options and variance futures can perfectly represent the expectation of the trend in the financial markets. Given the results that both ratios of OP/True and VF/True have a similar exponential trends, we compare the ratio of OP/VF across the remaining calendar days in the contract. As shown in Figure 23(c), the ratio is close to 1 when the remaining calendar days in the contract are over one year but less than two years, and it is increasing in an exponential curve as the remaining calendar days get even longer. Figure 23(d) is another view of the relation between OP and VF. The conclusion is consistent with Figure 23(c).

We further evaluated the pricing performance with respect to the end dates of the contracts. It turns out that the pricing method using options performs well when end dates of the contracts are in the last four months of 2015, which are also the last four months available in our data. The results are presented in Figure 24. In Figure 24(a), we compare OP with True. They are relatively close to each other and the over trend is an exponential curve. To calibrate our results from OP, we check Figure 24(b), which demonstrates a similar graph with Figure 24(a) and proves the good performance of our OP method. To demonstrate a more informative comparison, we plot the two ratios OP/True and VF/True across the remaining days of the contracts, that are in the last four months of 2015, in the same window and differentiate them by different colors, shown in Figure 24(c). The green dots represent the ratio OP/True and the red dots for VF/True. They are following almost the same trend, especially when the contracts have remaining calendar days within two years or so. One possible explanation could be that the options expired in the near future contain more information needed to price a variance swap and it is more accurate as an indication of the market expectation.

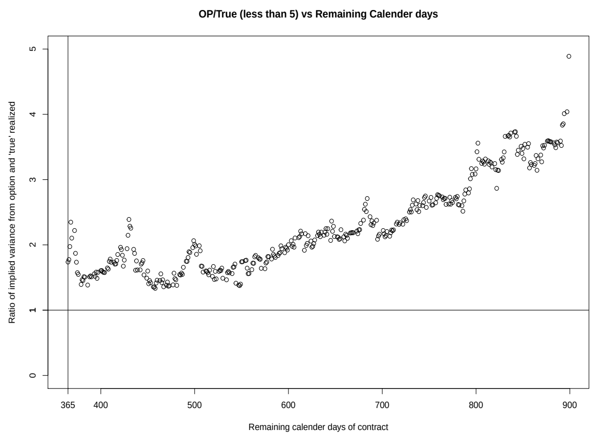

(a) The ratio of OP/True shows an exponential curve when time to expiration is more than 365.

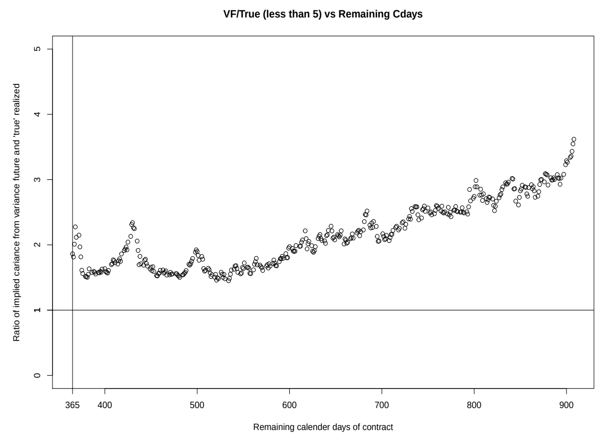

(b) The ratio of VF/True also shows an exponential curve when time to expiration is more than 365.

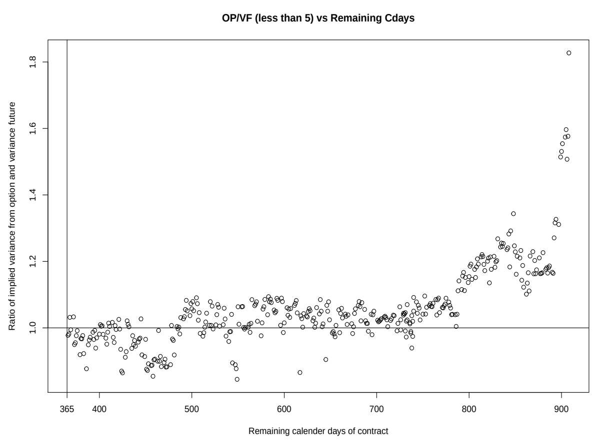

(c) The ratio of OP/VF is about 1 when time to expiration is more than 365. There is an exponential curve.

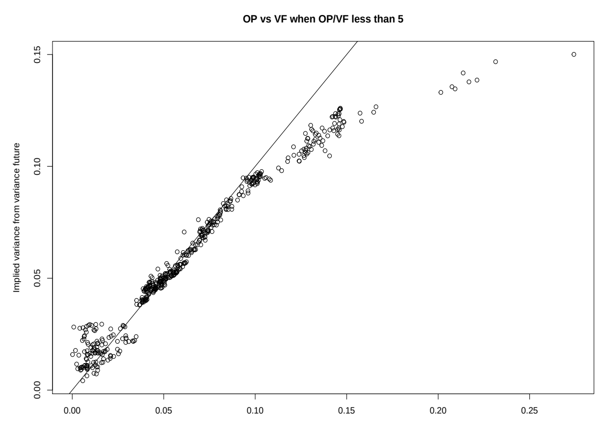

(d) Most of points are around the y=x line and there is an exponential curve.

Figure 23: Comparison of VS estimation based on OP, VF and True with respect to the remaining calendar days in the contract

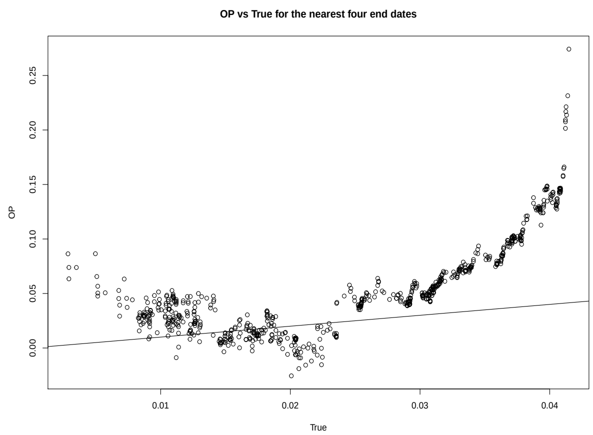

(a) OP generates a little bit larger implied variance than the true one but they are close to each other.

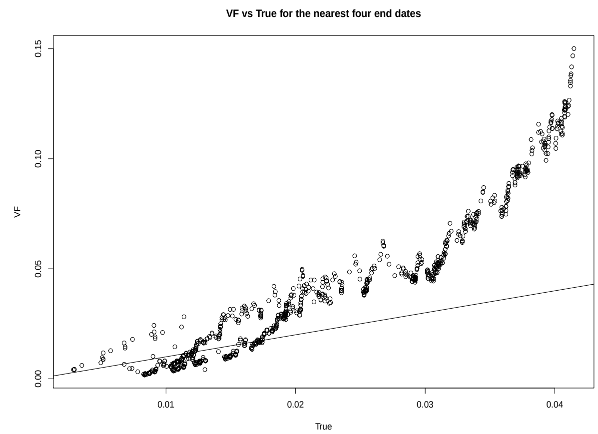

(b) The market implied variances (VF) compared to true one also behaves greater than the true one and follows an exponential curve.

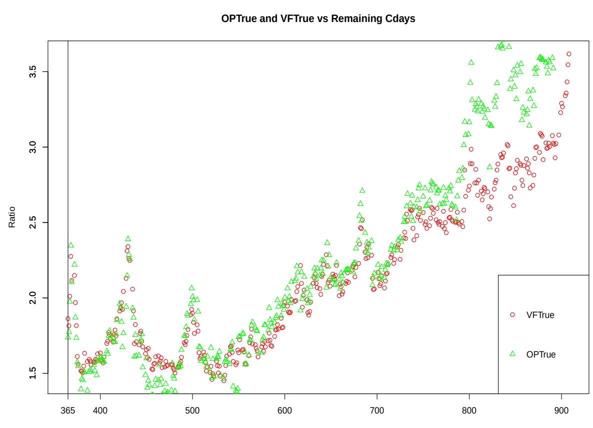

(c) The results from OP and VF are pretty consistent when the remaining days of the contract is more than 365.

Figure 24: Comparison of VS estimation based on OP, VF and True on the nearest four end dates

CHAPTER 4

CONCLUSION

The risk-neutral probability distribution for a future payoff of an asset can be estimated from market option prices that expire on the same date. In our work, we propose a nonparametric approach for estimating the risk-neutral density for an underlying asset from the corresponding options and investigate the empirical performance of our method.

Our proposed piece-wise constant nonparametric method in Chapter 2 is a highly efficient method for estimating the risk-neutral density in the sense that it provides a simpler form to implement. Under our approach, the risk-neutral density can be recovered effectively with available options. To guarantee a better estimate, we followed two alternatives after we reformulated the estimation problem into an optimization problem with constraints. In the first one, we employed the ordinal least square structure. In the second one, we incorporated the weights that are inversely proportional to option prices. In the examples tested, we observed that the weighted lease square structure is more in favor of the relative mean squared errors than the absolute mean squared errors which are favored by the regular least squares.

We also investigated the estimation performances employing only OTM options and all options available. We started from OTM-option fit by using OTM options as training data and tested for prediction accuracy for both OTM and ITM options. The results confirmed our assertions that the OTM and ITM options have different pricing mechanisms. We extended our work from using only OTM options to estimate the risk-neutral density to all the available options. The purpose of this to incorporate more information known for us for better pricing variance swap. The empirical performance of our approach compared to the non-negativity cubic spline approach in the literature shows that our method performs much better.

By comparing the fair prices from our method with the market prices, we can further provide a practical way to explore profitable investment opportunities in financial markets.

Risk-neutral density approach has been widely used in pricing derivatives in financial markets. In Chapter 3, using our nonparametric approach to derive moments for pricing variance swap, we can capture the market prices of long-term variance swaps reasonable well.

As part of future work, we plan to consider more complicated tail densities and study the performance under least square and weighted least square structures. We will examine different weights for different purposes. Another topic of our future research is to investigate short-term variance swaps based on more information given from CBOE researchers for its uncertainty in the data. It would be interesting to apply time series tools as well in the analysis.

CITED LITERATURE

1. Ait-Sahalia, Y. and Lo, A. W.: Nonparametric estimation of state-price densities implicit in financial asset prices. Journal of Finance, 53(2):499–547, April 1998.

2. Ait-Sahalia, Y. and Lo, A. W.: Nonparametric risk management and implied risk aversion. Journal of Econometrics, 94:9–51, 2000a.

3. Allen, P., Einchcomb, S., and Granger, N.: Variance swaps. J.P. Morgan Securities Ltd., November 2006. London.

4. Andersen, T. G., Bollerslev, T., Diebold, F. X., and Ebens, H.: The distribution of realised stock return volatility. Journal of Financial Economics, 61:43–76, 2001a.

5. Bahra, B.: Implied risk-neutral probability density functions from option prices: Theory and application. Bank of England, 1997. Working Paper.

6. Bakshi, G., Kapadia, N., and Madan, D.: Stock return characteristics, skew laws, and the differential pricing of individual equity options. The Review of Financial Studies, 16:101–143, 2003.

7. Bates, D. S.: The crash of 87: Was it expected? the evidence from options markets. Journal of Finance, 46(3):1009–1044, July 1991.

8. Bernard, C. and Cui, Z.: Prices and asymptotics for discrete variance swaps. Appl. Math. Financ., 21:140–173, 2013.

9. Biscamp, L. and Weithers, T.: Variance swaps and CBOE S&P 500 variance futures. Chicago Trading Company, LLC, 2007. Unpublished working paper.

10. Black, F. and Scholes, M.: The pricing of options and corporate liabilities. J. Political Econ., 81(3):637–654, 1973.

11. Bliss, R. R. and Panigirtzoglou, N.: Testing the stability of implied probability density functions. Journal of Banking & Finance, 26(2–3):381–422, March 2002.

12. Bossu, S., Strasser, E., and Guichard, R.: Just What You Need to Know about Variance Swaps. J.P. Morgan and Chase Co., 2005. Working Paper.

13. Breeden, D. T. and H.Litzenberger, R.: Prices of state-contingent claims implicit in option prices. The Journal of Business, 51(4):621–651, October 1978.

14. Brigo, D. and Mercurio, F.: Interest rate models-theory and practice: with smile, inflation and credit. Springer, 2006.

15. Broadie, M. and Jain, A.: The effect of jumps and discrete sampling on volatility and variance swaps. Int. J. Theor. Appl. Financ., 11:761–797, 2008.

16. Broyden, C. G.: The convergence of a class of double-rank minimization algorithms. Journal of the Institute of Mathematics and Its Applications, 6:76–90, 1970.

17. Buchen, P. W. and Kelly, M.: The Maximum Entropy Distribution of an Asset Inferred from Option Prices, April 2009.

18. Campa, J. M., Chang, P. H. K., and Reider, R. L.: Bounds of probability. Economic Policy, 6(4):33–37, April 1993.

19. Cao, J., Lian, G., and Roslan, T. R. N.: Pricing variance swaps under stochastic volatility and stochastic interest rate. Applied Mathematics and Computation, 277:72–81, March 2016.

20. Carr, P., Lee, R., and Wu, L.: Variance swaps on time-changed lévy processes. Finance Stoch, 16:335–355, 2012.

21. Carr, P. and Corso, A.: Commodity covariance contracting. Energy and Power Risk Management, pages 42–45, 2001.

22. Carr, P. and Lee, R.: Volatility derivatives. The Annual Review of Financial Economics, 1:319–339, 2009.

23. Carr, P. and Madan, D.: Towards a theory of volatility trading. Risk Book, R. Jarrow ed., pages 417–427, 1998.

24. Chiarella, C. and Kang, B.: The evaluation of american compound option prices under stochastic volatility and stochastic interest rates. J. Comput. Financ., 14:1–21, 2011.

25. Chong, E. K. P. and Zak, S. H.: An introduction to optimization. John Wiley & Sons, Inc, 1996.

26. Conrad, J., Dittmar, R. F., and Ghysels, E.: Ex ante skewness and ex- pected stock returns. Journal of Finance, 68:85–124, 2013.

27. Cox, J., Jr, J. I., and Ross, S.: A theory of the term structure of interest rates. Econometrica, 53:385–407, 1985.

28. Cox, J. C. and Ross, S. A.: The valuation of options for alternative stochastic processes. Journal of Financial Economics, 3(1–2):145–166, 1976.

29. Demeter, K., Derman, E., Kamal, M., and Zou, J.: Morethan you ever wanted to know about volatility swaps. Goldman Sachs Quantitative Strategies Research Notes, pages –, 1999.

30. Demeterfi, K., Derman, E., Kamal, M., and Zou, J.: A guide to volatility and variance swaps. Journal of Derivatives, 6:9–32, 1999.

31. Dennis, P. and Mayhew, S.: Risk-neutral skewness: Evidence from stock options. Journal of Financial and Quantitative Analysis, 37:471–493, 2002.

32. Elliott, R. J., Kuen, S. T., and Chan, L.: Pricing volatility swaps under heston's stochastic volatility model with regime switching. Applied Mathematical Finance, 14(1):41–62, 2007.

33. Elliott, R. J. and Lian, G.: Pricing variance and volatility swaps in a stochastic volatility model with regime switching: Discrete observations case. Quant. Financ., 13:687–698, 2012.

34. Elliott, R. J. and Siu, T.: On markov-modulated exponential-affine bond price formulae. Appl. Math. Financ., 16:1–15, 2009.

35. Fletcher, R.: A new approach to variable metric algorithms. Computer Journal, 13(3):317–322, 1970.

36. Fouque, J., Papanicolaou, G., Sircar, R., and Solna, K.: Multiscale stochastic volatility asymptotics. Multiscale Model. Simul., 2:22–42, 2003.

37. Ghysels, E. and Wang, F.: Moment-implied densities: Properties and applications. Journal of Business & Economic Statistics, 32(1):88–111, January 2014.

38. Goldfarb, D.: A family of variable metric updates derived by variational means. Mathematics of Computation, 24(109):23–26, 1970.

39. Goldfarb, D. and Idnani, A.: A numerically stable dual method for solving strictly convex quadratic programs. Mathematical Programming, 27:1–33, 1983.

40. Grunbichler, A. and Longstaff, F.: Valuing futures and options on volatility. J. Bank. Financ., 20:985–1001, 1996.

41. Grzelak, L. and Oosterlee, C.: On the heston model with stochastic interest rates. SIAM J. Financ. Math., 2:255–286, 2011.

42. Gulisashvili, A. and Stein, E.: Asymptotic behavior of distribution densities with stochastic volatility. Math. Financ., 20:447–477, 2011.

43. Heston, S. L.: A closed-form solution for options with stochastic volatility, with applications to bond and currency options. Review of Financial Studies, 6:327–343, 1993.

44. Heston, S. L. and Nandi, S.: Derivatives on volatility: Some simple solutions based on observables. Federal Reserve Bank of Atlanta WP, pages 2000–2020, November 2000.

45. Howison, S., Rafailidis, A., and Rasmussen, H.: On the pricing and hedging of volatility derivatives. Applied Mathematical Finance, 11(5):317–346, 2004.

46. Jackwerth, J. C. and Rubinstein, M.: Recovering probability distributions from option prices. Journal of Finance, 51(5):1611–1631, 1996.

47. Jarrow, R. and Rudd, A.: Approximate option valuation for arbitrary stochastic process. Journal of Financial Economics, 10(3):347–369, November 1982.

48. Javaheri, A., Wilmott, P., and Haug, E. G.: Garch and volatility swaps. Quantitative Finance, 4(5):589–595, 2004.

49. Jaynes, E. T.: Where do we stand on maximum entropy? The Maximum Entropy Formalism, Raphael D. Levine and Myron Tribus (eds.), M. I. T. Press, page 15, 1979. Cambridge, MA.

50. Jaynes, E. T.: On the rationale of maximum-entropy methods. Proceedings of the IEEE, 70(9):939–952, October 1982.

51. Jiang, L., Li, K., Wang, F., and Yang, J.: Pricing Variance Swap by Estimating Risk Neutral Density. Joint Statistical Meetings, Unpublished abstract, August 2016.

52. Kim, B. and Kim, J.: Default risk in interest rate derivatives with stochastic volatility. Quant. Financ., 11:1837–1845, 2011.

53. Kim, J., Yoon, J., and Yu, S.: Multiscale stochastic volatility with the hull-white rate of interest. J. Futures Mark., 34(9):819–837, 2014.

54. Kuang, P., Zhao, Q.-M., and Xie, Z.-Y.: Algorithms for solving unconstrained optimization problems. IEEE Xplore, pages 819–837, June 2016.

55. Lawson, C. L. and Hanson, R. J.: Solving least square problems. Prentice-Hall, Englewood Cliffs, NJ, 1974.

56. Lee, S. H.: Estimation of risk-neutral measures using quartic b-spline cumulative distribution functions with power tails. Quantitative Finance, 14(10):1857–1879, 2014.

57. Little, T. D. and Pant, V.: A finite difference method for the valuation of variance swaps. The Journal of Computational Finance, 5:81–101, 2001.

58. Malz, A. M.: Using option prices to estimate realignment probabilities in the european monetary system: the case of sterling-mark. Journal of International Money and Finance, 15(5):717–748, 1996.

59. Melick, W. R. and Thomas, C. P.: Recovering an asset's implied pdf from option prices: An application to crude oil during the gulf crisis. Journal of Financial and Quantitative Analysis, 32(1):91–115, March 1997.

60. Monteiro, A. M., Tutuncu, R. H., and Vicente, L. N.: Recovering risk-neutral probability density functions from options prices using cubic splines. European Journal of Operational Research, 187(2):525–542, June 2008.

61. Parzen, E.: On estimation of a probability density function and mode. Annals of Mathematical Statistics, 33:1065–1076, 1962.

62. Petersen, K. B. and Pedersen, M. S.: The matrix cookbook. [online] Available: http://www2.imm.dtu.dk/pubdb/p.php?3274, February 2008.

63. Ritchey, R. J.: Call option valuation for discrete normal mixtures. Journal of Financial Research, 13(4):285–296, 1990.

64. Rosenblatt, M.: Remarks on some nonparametric estimates of a density function. Annals of Mathematical Statistics, 27:832–837, 1956.

65. Rubinstein, M.: Implied binomial trees. Journal of Finance, 49(3):771–818, July 1994.

66. Schwert, G. W.: Why does stock market volatility change over time? Journal of Finance, 44:1115–1153, 1989.

67. Shanno, D. F.: Conditioning of quasi-newton methods for function minimization. Mathematics of Computation, 24(111):647–656, 1970.

68. Shen, Y. and Siu, T.: Pricing variance swaps under a stochastic interest rate and volatility model with regime-switching. Oper. Res. Lett., 41:180–187, 2013.

69. Sherrick, B. J., Irwin, S. H., and Forster, D. L.: Option-based evidence of the nonstationarity of expected s&p 500 futures price distributions. Journal of Futures Markets, 12(3):275–290, 1992.

70. Shimko, D. C.: Erm bandwidths for emu and after: Evidence from foreign exchange options. Risk, 24:55–89, 1997.

71. Shreve, S. E.: Stochastic calculus for finance II: Continuous−time models. Springer, 2008.

72. Stein, E. and Stein, J.: Stock price distributions with stochastic volatility: An analytic approach. Rev. Financ. Stud., 4:727–752, 1991.

73. Swishchuk, A.: Modeling of variance and volatility swaps for financial markets with stochastic volatilities. Wilmott Magazine, Tech.Art(2):64–72, September 2004.

74. Wang, Z., Wang, L., Szolnoki, A., and Perc, M.: Evolutionary games on multilayer networks: A colloquium. Eur. Phys. J. B, 88:1–15, 2015.

75. Windcliff, H. A., Forsyth, P. A., and Vetzal, K. R.: Pricing methods and hedging strategies for volatility derivatives. Journal of Banking & Finance, 30(2):409–431, 2006.

76. Zhu, S.-P. and Lian, G.-H.: A closed-form exact solution for pricing variance swaps with stochastic volatility. Mathematical Finance, 21(2):233–256, October 2010.

77. Zhu, S. P. and Lian, G.: On the valuation of variance swaps with stochastic volatility. Applied Mathematics and Computation, 219(4):1654–1669, November 2012.

VITA

LIYUAN JIANG

CONTACT

1228 Science and Engineering Offices (M/C 249)

851 S. Morgan Street, Chicago, IL 60607

ljiang26@uic.edu

EDUCATION

1. PH.D in Mathematics (Statistics), University of Illinois at Chicago. May 2017
2. M.S. in Mathematics (Statistics), University of Toledo. May 2012
3. B.S. in Mathematics (Statistics), Nankai University, China. June 2010

EXPERIENCE

1. **Statistical Consultant**, University of Illinois at Chicago Aug 2014 - May 2017

   Chicago, IL, USA

2. **Predictive Analytic Intern**, CNA Financial Corporation June 2016 - Aug 2016

   Chicago, IL, USA

3. **Teaching Assistant**, University of Illinois at Chicago — Aug 2012 - May 2017

   Chicago, IL, USA

4. **Teaching Assistant**, University of Toledo — Aug 2010 - May 2012

   Toledo, OH, USA

Award

Outstanding Consulting Award, MSCS, UIC — 2015 - 2016

Presentations

Joint Statistical Meeting, Chicago, IL — Aug 2016

Title: Pricing Variance Swap by Estimating Risk Neutral Density